AD

USAAVLABS TECHNICAL REPORT 64-68B

HEAVY-LIFT TIP TURBOJET ROTOR SYSTEM
VOLUME II
PARAMETRIC DESIGN STUDY

October 1965

U. S. ARMY AVIATION MATERIEL LABORATORIES
FORT EUSTIS, VIRGINIA

CONTRACT DA 44-177-AMC-25(T)
HILLER AIRCRAFT COMPANY, INC.
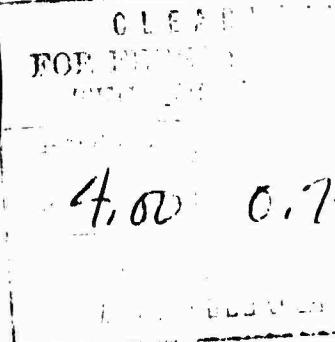
Task 1M121401D14412
Contract DA 44-177-AMC-25(T)
USAAVLABS Technical Report 64-68B
October 1965

HEAVY-LIFT TIP TURBOJET ROTOR SYSTEM

VOLUME II

PARAMETRIC DESIGN STUDY

Hiller Engineering Report No. 64-42

Prepared by

Hiller Aircraft Company, Inc.
Subsidiary of Fairchild Hiller Corporation
Palo Alto, California

For

U. S. ARMY AVIATION MATERIEL LABORATORIES
FORT EUSTIS, VIRGINIA

(U. S. Army Transportation Research Command when report prepared)

CONTENTS

CONTENTS (CONTINUED)

ILLUSTRATIONS

ILLUSTRATIONS (CONTINUED)

SYMBOLS

A_b	Total actual blade area, $bcR\xi$
A_I	Total compressor inlet area, $\left(\dfrac{F_R}{3,190} + .522\,n\right)$
A_π	Equivalent flat plate area $(C_D = 1.0)$
$A_{\pi E.L.}$	Value of A_π at which particular design would be power limited
a_I'	Slope of C_L of nacelle versus yaw angle ϕ where C_L is based on engine compressor inlet area
AR_b	Blade aspect ratio (R/chord)
B	Tip loss factor, .97
b	Number of blades
c	Blade chord, feet
C_{L_r}	Mean blade lift coefficient
$C_{L_{r_o}}$	Design (sea level) mean rotor lift coefficient
E	Modulus of elasticity
F_N	Net thrust (gross engine thrust less engine ram drag)
F_R	Engine total rated thrust $(\pounds_F \times W_G)$
$F.L.$	Fixed losses = 100 horsepower
g	Gravitational units $(32.2\ ft/sec^2)$
ihp	Induced horsepower
I	Moment of inertia
K_u	Inflow correction factor
$K_{F.T.}$	Ratio of fuel tank weight to fuel weight
K_μ	Profile power correction factor for forward speed
$\pounds_F$	Rated thrust loading (F_R/W_G)
m	Rotor blade mass per unit length

$MRTHP_{700}$ — Military rated thrust horsepower at sea level and 700 feet per second (see Equation 44)

$MRTW_{f700}$ — Fuel flow at military rated thrust and 700 feet per second

n — Load factor $= \dfrac{V_T^2}{R(32.2)}$

n_e — Number of engines

O-U — Over-under (refers to mounting of engines at blade tip)

php — Parasite drag horsepower

R — Rotor radius from rotor centerline to centerline of outboard engine (see Figure 1)

$R_{F_{avail}}$ — Fuel weight to gross weight ratio available

$R_{F_{req}}$ — Fuel weight to gross weight ratio required

$R_{u_{avail}}$ — Fuel weight available plus payload to gross weight ratio

$R_{u_{req}}$ — Fuel weight required plus payload to gross weight ratio

Rhp — Rotor profile horsepower (total)

Rhp_b — Contribution of blade to rotor profile horsepower

Rhp_N — Contribution of nacelle to rotor profile horsepower

S-S — Side-by-side (refers to mounting of engines at blade tip)

S — Single (refers to mounting of engine at blade tip)

U_1 — Induced velocity due to disk loading (forward flight)

U_b — Blade profile induced velocity.

U_{N_1} — Induced velocity due to nacelle lift

U_{N_2} — Induced velocity due to nacelle side load

U_D — Induced velocity due to fuselage drag

U_A — Induced velocity due to rotor ram drag

U_H — Induced velocity due to disk loading (hover)

V	Helicopter airspeed, feet per second
V_{max}	Design maximum velocity, miles per hour
V_T	Tip speed at centerline of outboard engine
V_{TH}	Hover tip speed
V_{TV}	Cruise tip speed
w	Disk loading $= (W_G / \pi R^2)$ or blade weight per unit length
W_B	Blade weight
W_{BO}	Body group weight
W_C	Helicopter component weight
W_{EC}	Engine component weight
W_{EL}	Electrical group weight
W_{EN}	Engine weight
W_F	Total fuel weight
W_f	Fuel flow rate, pounds per hour
W_{FU}	Furnishings weight
W_G	Gross weight
$W_{G_{sol}}$	Design gross weight that exactly meets the mission requirements (solution gross weight)
W_I	Instrument weight
W_{LG}	Landing gear weight
W_{LU}	Lubrication system weight
W_{PL}	Payload weight
W_{PY}	Pylon weight
W_{RO}	Rotor group weight (Equations (73) or (93))
W_{STA}	Stabilizer weight
W_{TR}	Tail rotor weight

α	Angle of attack about pitch axis of blade or nacelle
γ_e	Ratio of engine nacelle centerline to rotor radius (R''/R) (see Figure 1)
Δt	Time required for a given portion of mission
ΔW	Helicopter weight change
ΔW_F	Fuel weight change
ΔW_{PL}	Payload weight change
δ_{o_b}	Coefficient of drag of blade at $\alpha = 0$, referred to A_b ($= 0.00900$)
δ_{2_b}	Coefficient of drag of blade for use with $C_{L_r}^2$, referred to A_b ($= 0.00927$)
δ_{m_b}	Coefficient of drag of blade at given C_{L_r}
$\delta_{m_b \rho}$	Coefficient of drag of blade at 6,000-foot pressure altitude and 95 degrees Fahrenheit
δ_{o_I}	Nacelle coefficient of drag at $\alpha = 0$, referred to A_I
δ_{2_I}	Nacelle coefficient of drag for use with $C_{L_{r_o}}^2$
δ_{m_I}	Nacelle coefficient of drag in hover at a given C_{L_r}, $= \delta_{o_I} + \delta_{2_I} C_{L_r}^2$
$\delta_{m_I \rho}$	Nacelle drag coefficient at 6,000-foot pressure altitude and 95 degrees Fahrenheit
δ_{2_I}	Nacelle coefficient of drag for use with engine compressor inlet area and ϕ^2
ϵ	Rotor blade twist; negative sign indicates twist direction same as for a propeller with same rotational direction as rotor, washout
η	Overall efficiency factor $= .97$
μ	Advance ratio (V/V_{T_V})
ζ	Ratio of blade radius to rotor radius, (R'/R) (see Figure 1)
ρ	Density of atmosphere, slugs/cubic foot - or material density

ρ_0 Density of standard sea level atmosphere, .002378 slugs per cubic foot

σ Solidity $(A_b/g_\pi R^2)$

ϕ Nacelle yaw angle, radians

ψ Rotor blade azimuth angle

Ω Rotor angular velocity, radians/second
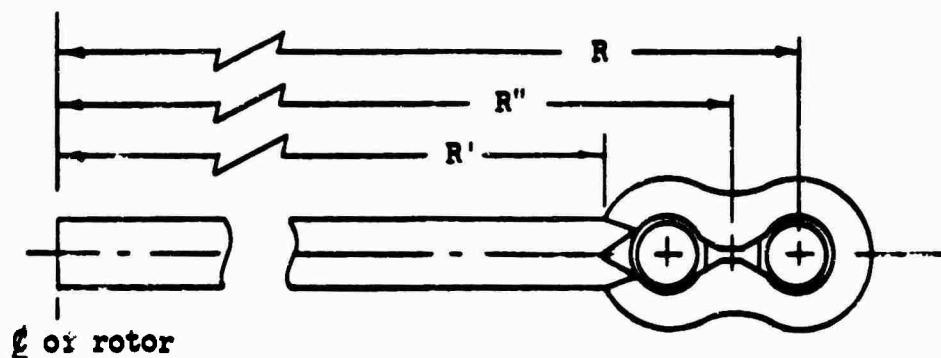
Figure 1. Rear View of Side-by-Side
Engine Arrangement.

1.0 SUMMARY

1.1 Initial Objectives

1.1.1 Introduction

The initial objectives of this study were to determine the optimum design parameters of a heavy-lift helicopter powered by turbojet engines installed at the rotor blade tips. The design parameters and configuration that yield minimum gross weight consistent with the mission requirements and performance specifications within the design limitations are considered optimum.

These optimum design parameters were found for each configuration considered by determining the minimum gross weight required to meet the fuel requirements of the mission which is set forth in Section 1.1.2 for each combination of the design parameters in Section 1.2. Meeting the hover requirement in the performance specification was ensured by selecting required power using a generalized method of engine size determination. A study was also performed to determine the solutions which would not meet the forward speed requirements. These studies showed that within the load factor limitations set forth in Section 1.1.4, no limitations would occur below a design mean lift coefficient of 0.50. This upper value is consistent with current helicopter practice.

1.1.2 Mission Requirements

a) Payload (outbound only) .... 12 tons
b) Radius .... 50 nautical miles
c) Cruising speed:
   1) Outbound .... 60 knots
   2) Inbound .... 100 knots
d) Atmospheric condition .... Sea level standard
e) Hovering time (out-of-ground effect):
   1) At takeoff .... 3 minutes
   2) At destination (with payload) .... 2 minutes
f) Fuel reserve .... 10% of initial fuel

1.1.3 Performance Specifications

a) Hover capability (OGE):
   1) Altitude .... 6,000 feet
   2) Temperature .... +95° Fahrenheit
b) Design maximum speed .... 125 miles per hour

1.1.4 Design Objectives and Limitations

a) Rotor tip environment 235g
b) Tip speed .... 650 to 750 feet per second

1

c) Gross weight .... 60,000 to 80,000 pounds
d) Design mean lift coefficient at sea
   level, $C_{L_{T_o}}$ .... .30 to .60
e) Engine thrust, weight and fuel
   consumption based on .... CAE 357-1 turbojet

1.2 Design Parameters

The variable design parameters used with each set of configuration parameters (see Section 1.3) are as follows:

a) Chord "c", ... 6.0, 6.5, 7.0, 7.5 feet
b) Hover tip speed, V_{T_H} .... 550, 600, 650, 700, 743, 750 feet per second

c) Centrifugal force field at centerline of outboard engine in gravity units, g. Values determined as outlined in Section 4.1.2.

1.3 Configuration Parameters Used

The following is a grouping of the configuration parameters used in the parametric design study.

a) Number of blades - 2, 3 and 4 (see Table 1 for values of tip loss factor, "B", used for each number of blades)

b) Engine arrangement (see Table 1 for engine arrangement parameters used at each blade tip):

   1) Over-under mounting, two per blade.
   2) Side-by-side mounting, two per blade.
   3) Single mounting, one per blade.

c) Fuselage and load configuration:

   1) Internal load, retractable landing gear (transport).
      Equivalent drag area:
         Outbound - 50 ft^2
         Inbound - 50 ft^2

   2) External load, fixed landing gear (crane).
      Equivalent drag area:
         Outbound - 200 ft^2
         Inbound - 100 ft^2

The parameters used for the crane fuselage are shown in Table 1. The internal load, retractable landing gear configuration, used the four-blade, eight-engine, over-under parameters which are shown in Table 1.

2

1.4 Optimum Configurations and Design Parameters

1.4.1 Generalized Engines

The generalized engines are based on the Continental (CAE) Model 357-1 version of the J69-T-29 engine. Specifically, the generalized engines have the same basic design as the CAE Model 357-1. The thrust variation with inlet area is given by Equation (28). The weight variation with thrust is shown in Figure 24, and the specific fuel consumption is the same as the CAE Model 357-1 engine.

The results of the parametric study with the generalized engines indicate that the machine with the lowest gross weight is obtained with the minimum permissible number of blades and the minimum number of engines per blade. The study also indicates that a configuration with a transport fuselage had a higher gross weight than a like configuration which utilized a crane-type fuselage.

The two-blade rotor configuration is not considered appropriate because of control power considerations. The results of the parametric analysis indicate that the optimum configuration for the prescribed mission (see Section 1.1.2) is a helicopter with the following characteristics:

a) Three blades
b) A single engine per blade
c) A crane-type fuselage

The optimum design parameters for the several configurations are presented in Table 2. Table 2 is composed of three parts:

a) Table 2a lists the optimum design parameters for all configurations; these parameters fall within the limitations set forth in Section 1.1.4.

b) Table 2b lists the optimum design parameters for the same configurations and conditions as Table 2a except that the hover tip speed is optimum for the configuration. (This optimum hover tip speed is less than the 650-foot-per-second minimum set forth in Section 1.1.4 for all but the two-blade configuration.)

c) Table 2c lists the optimum design parameters at 125 miles per hour with the 235g limit removed.

The optimum configuration within the limitations set forth in Section 1.1.4, "Design Objectives and Limitations," has its minimum gross weight at the following values of the design parameters and engine description:

3

Design gross weight, W_G .... 63,200 pounds
Hover tip speed at centerline of engine, V_{T_H} .... 650 feet per second
Chord length, c .... 6.91 feet
Main rotor radius, R (from centerline of rotor
to centerline of engine shaft) .... 55.83 feet
Rotor tip environment 235g
Design mean lift coefficient, $C_{L_{r_o}}$ .... .376
Cruise tip speed, V_{T_V} .... 642 feet per second
Number of main rotor blades, b 3
Number of engines, n_e 3
Engine arrangement .... one engine at tip of
each blade
Solidity, σ .... .1162
Total engine rated thrust .... 10,868 pounds
Rated thrust per engine .... 3,623 pounds
Weight per engine .... 735 pounds
Net thrust, F_N, available per engine at sea
level, standard atmosphere and 598 f.p.s. ...... 3,304 pounds
Net thrust, F_N, available per engine at 6,000
feet, 95°F. standard hot day .... 2,270 pounds
MRT s.f.c. at 598 f.p.s. and sea level standard
atmosphere .... $1.260 \frac{lb/hr.}{lb. \ thrust}$
75% NRP s.f.c. at 598 f.p.s. and sea level
standard atmosphere .... $1.416 \frac{lb/hr.}{lb. \ thrust}$

Maximum engine diameter .... 31.9 inches
Maximum nacelle diameter .... 37.9 inches
Engine length .... 60.6 inches
Nacelle length .... 86.2 inches
Empty weight .... 27,826 pounds
Fuel weight .... 10,774 pounds
Payload .... 24,000 pounds
Crew and oil .... 600 pounds

The minimum gross weight for the optimum configuration from Table 2b
occurs at the following values of the design parameters and engine
description:

Design gross weight, W_G .... 59,800 pounds
Hover tip speed at centerline of engine, V_{T_H} .... 598 feet per second
Chord length, c .... 6.82 feet
Rotor radius to center of engine shaft, R .... 47.3 feet
Rotor tip environment 235g
Design mean lift coefficient, $C_{L_{r_o}}$ 0.50
Cruise tip speed, V_{T_V} .... 598 feet per second

4

```
Number of blades, b ............................    3
Number of engines, n_e ........................    3
Engine arrangement ............................    one engine at tip
                                                   of each blade
Solidity, σ ...................................    .138
Total engine rated thrust .....................    12,148 pounds
Rated thrust per engine .......................    4,049 pounds
Weight per engine .............................    815 pounds
Thrust at 598 f.p.s., sea level, standard .....    3,670 pounds
Thrust at 598 f.p.s., 6,000 feet, 95°F. .......    2,510 pounds

MRT s.f.c. at 598 f.p.s., sea level,
standard ......................................    1.260 $\frac{lb/hr.}{lb.\ thrust}$

75% NRP s.f.c. at 598 f.p.s., sea level,
standard ......................................    1.416 $\frac{lb/hr.}{lb/\ thrust}$

Maximum engine diameter .......................    33.16 inches
Maximum nacelle diameter ......................    39.4  inches
Engine length .................................    63.0  inches
Nacelle length ................................    89.6  inches
Empty weight ..................................    24,007 pounds
Fuel weight ...................................    11,193 pounds
Payload .......................................    24,000 pounds
Crew and oil ..................................    600 pounds
```

An empty weight breakdown for these two conditions, 650 feet per second
and 598 feet per second hover tip speed, is given in Table 3.

1.4.2 CAE 357-1 Version of the J69-T-29 Engine

The description, performance, and installation of the CAE 357-1 engine
is presented in the tip turbojet design layout report, Volume III. This
version of the heavy-lift helicopter is designated as Model 1108.

An over-under engine installation arrangement was used for the Model
1108 because of the anticipated difficulties associated with unequal in-
let air distribution between side-by-side engine inlets at higher ad-
vance ratios and because of structural difficulties. At that time it
was realized that the nacelle drag effect would be increased by using
the over-under arrangement.

A supplementary parametric study indicated that while lower gross
weights may be achieved with hover tip speeds lower than the minimum
specified by Section 1.1.4, the rated thrust required increases as tip
speed decreases below the minimum of 650 feet per second. This reduc-
tion in gross weight with decreasing tip speed is shown in Figure 3.

Prior to the completion of the rotor design studies, the rotor group weight was not well defined; therefore, it was decided that for this configuration (Model 1108), rotor group weight would be determined by design layout. This rotor was selected from the standpoint of attaining the minimum blade weight and providing adequate clearance for the internal engine service lines without penalizing excessively the hover thrust capability at 6,000 feet, 95°F.

The final preliminary design analysis of the rotor group indicated a weight which is approximately 1,800 pounds heavier than originally considered. The current 1,700-pound rated thrust of the CAE 357-1 engine was thus marginal to provide HOGE capability at 6,000 feet, 95°F. Therefore, to provide hover capability, it was considered appropriate on the Model 1108 to consider meeting the mission requirements on six of the engines in cruise flight and with the cruise tip speed reduced to an optimum of 540 feet per second. This realized an 800-pound fuel weight reduction (see Section 2.7). An additional 600 pounds was removed from other components where savings could be achieved over the statistical estimates (see Table 3 for final weight breakdown of this configuration compared to estimates used in generalized engine study). The major differences between the final weight conditions and the generalized weight conditions for the study are that the generalized helicopters were considered to be fitted with two auxiliary power units, while the hardware engine versions were considered to have only one, and that three crew members were included instead of two. The following is a list of the design parameters for the Model 1108 with over-under engine mountings:

Design gross weight, W_G .... 72,104 pounds
Hover tip speed at centerline of engine, V_{T_H} ..... 650 feet per second
Chord length, c .... 6.5 feet
Rotor radius to centerline of engine shafts, R ... 55.83 feet
Rotor tip environment 235g
Design mean lift coefficient .... .329
Cruise tip speed .... 592 feet per second
Optimum tip speed .... 540 feet per second
Number of main rotor blades, b 4
Number of engines, n_e 8
Engine arrangement .... one over the other at each blade tip
Solidity, σ .... .148
Total engine rated thrust .... 13,600 pounds
Rated thrust per engine .... 1,700 pounds
Weight per engine .... 365 pounds
Thrust at 650 f.p.s. and sea level standard atmosphere .... 1,550 pounds
Thrust at 650 f.p.s. and 6,000 feet, 95°F. standard hot day atmosphere .... 1,057 pounds

MRT s.f.c. at 592 f.p.s. and sea level standard
atmosphere .... $1.256 \frac{\text{lb/hr.}}{\text{lb. thrust}}$

75% NRT s.f.c. at 592 f.p.s. and sea level
standard atmosphere .... $1.414 \frac{\text{lb/hr.}}{\text{lb. thrust}}$

Maximum engine diameter .... 25.25 inches
Maximum nacelle height .... 57.00 inches
Maximum nacelle width .... 30.0 inches
Engine length .... 47.97 inches
Nacelle length .... 68.3 inches
Empty weight .... 34,700 pounds
Fuel weight .... 12,924 pounds
Payload .... 24,000 pounds
Crew and oil .... 480 pounds

A three-blade, six-engine (over-under) crane configuration can be con-
sidered by using the optimum tip speed during cruise and using the same
component weight basis as was used for the four-blade, over-under ver-
sion. A three-blade crane configuration will meet the mission and
hover requirements with an 11.4-percent growth in the CAE engine thrust.
This solution occurs at the following values of the design parameters
and engine description:

Design gross weight, W_G .... 64,250 pounds
Hover tip speed at centerline of outboard
engine, V_{T_H} .... 650 feet per second
Chord length, c .... 6.5 feet
Rotor radius to centerline of outboard
engine, R .... 55.83 feet
Rotor tip environment 235g
Design mean lift coefficient, $C_{L_{ro}}$ .... .405
Cruise tip speed, V_{T_V} .... 639 feet per second
Optimum tip speed .... 590 feet per second
Number of blades, b 3
Number of engines, n_e 6
Engine arrangement .... over-under at each
                                               tip
Solidity, σ .... .111
Total engine rated thrust, F_R .... 11,400 pounds
Rated thrust per engine, F_R/n_e .... 1,900 pounds
Net thrust, F_N, available per engine at sea
level standard atmosphere and 650 f.p.s. ..... 1,730 pounds

Net thrust, F_N, available per engine at
6,000 feet, 95°F., standard hot day, and
650 f.p.s. .... 1,195 pounds

7

MRT s.f.c. at 590 f.p.s. and sea level standard
atmosphere .... $1.356 \frac{lb/hr.}{lb.\ thrust}$

75% NRP s.f.c. at 590 f.p.s. and sea level
standard atmosphere .... $1.414 \frac{lb/hr}{lb.\ thrust}$

Maximum engine diameter .... 30.00 inches
Maximum nacelle height .... 25.25 inches
Maximum nacelle width .... 57.00 inches
Engine length .... 47.97 inches
Nacelle length .... 68.3 inches
Empty weight .... 28,114 pounds
Fuel weight .... 11,676 pounds
Payload .... 24,000 pounds
Crew and oil .... 460 pounds

The weight breakdowns for the above four-blade and three-blade versions
with the proposed hardware engine are given in Table 3.

TABLE 1 INPUTS FOR VARIOUS TIP TURBOJET CONFIGURATIONS									
b	n_e	Engine Arrangement	δ_{o_I}	δ_{2_I}	δ'_{2_I}	ξ	γ	B	a'_I
4	8	O-U	.282	.10	5.0	.980	1.00	.967	4.50
3	6	O-U	.282	.10	5.0	.980	1.00	.956	4.50
4	8	S-S	.279	.15	3.25	.94	.96	.967	2.25
3	6	S-S	.279	.15	3.25	.94	.96	.956	2.25
4	4	S	.264	.12	3.85	.96	1.00	.967	4.00
3	3	S	.264	.12	3.85	.96	1.00	.956	4.00
2	2	S	.264	.12	3.85	.93	1.00	.930	4.00

TABLE 2a
OPTIMUM DESIGN PARAMETERS

Condition	Configuration	W_G	n	V_{TH}	C	$C_{L_{To}}$	V_{TV}	R	P_R	P_R/n_e
n = 235, Hover tip speed = 650 f.p.s. (minimum allowed by Sect.1.1.3) Chord is optimum for min. gross wt.	2 blades, S, Crane	56,800	235	652	7.50	.500	V_{TH}	55.83	9415	4708
	3 blades, S, "	63,200	235	650	6.91	.376	642	55.83	10868	3623
	3 blades, S-S, "	65,300	235	650	7.01	.382	641	55.83	12000	2000
	3 blades, O-U, "	66,280	235	650	7.01	.388	622	55.83	12088	2016
	4 blades, S, "	70,340	235	650	6.91	.302	613	55.83	12746	3186
	4 blades, S-S, "	73,150	235	650	6.94	.314	615	55.83	14175	1772
	4 blades, O-U, "	73,800	235	650	7.21	.305	564	55.83	14268	1782
	4 blades, O-U, transport	74,800	235	650	6.99	.318	557	55.83	14450	1807

Legend: S   =   One engine per blade.

S-S   =   Side by side mounting of two engines per blade.

O-U   =   Over-under mounting of two engines per blade.

Table 2b
OPTIMUM DESIGN PARAMETERS

Condition	Configuration	W_G	n	V_{TH}	C	GL_{TO}	V_{TV}	R	F_R	F_R/n_b
n = 255, Chord and hover tip speed are optimum for min. gross wt.	2 blades, S, crane	56,800	255	652	7.50	.50	=V_TH	56.3	9415	4708
	3 blades, S, "	59,800	255	598	6.82	.50	V_TH	47.3	12148	4049
	3 blades, S-S, "	62,100	255	600	7.01	.50	V_TH	47.5	13425	2235
	3 blades, O-U, "	63,200	255	600	7.14	.50	V_TH	47.5	13462	2244
	4 blades, S, "	63,800	255	565	7.04	.475	V_TH	42.2	15256	3814
	4 blades, S-S, "	67,100	255	570	7.01	.490	V_TH	43.0	16920	2116
	4 blades, O-U, "	68,600	255	565	7.18	.50	V_TH	42.2	17391	2155
	4 blades, O-U, transport	70,000	255	565	7.34	.50	V_TH	42.2	17882	2234

Legend: S = One engine per blade.

S-S = Side by side mounting of two engines per blade.

O-U = Over-under mounting of two engines per blade.

Table 2c
OPTIMUM DESIGN PARAMETERS

Condition	Configuration	W_G	n	V_{T_H}	C	$C_{L_{T_o}}$	V_{T_V}	R	P_R	P_R/n_e
n = Opt. Hover tip speed = 743 f.p.s. Chord = optimum. To g limitation	2 blades, S, crane	52,300	401	743	7.0	.50	=V_{T_H}	43.0	9498	4750
	3 blades, S, "	56,100	453	743	6.5	.40	V_{T_H}	38.1	11383	3796
	3 blades, S-S, "	58,000	453	743	7.0	.375	V_{T_H}	38.1	12736	2121
	3 blades, O-U, "	59,400	427	743	6.75	.385	740	40.4	12373	2060
	4 blades, S, "	59,800	490	743	6.55	.335	743	35.2	13346	3338
	4 blades, S-S, "	63,200	457	743	6.55	.325	743	37.5	14563	1819
	4 blades, O-U, "	64,100	463	743	6.75	.325	706	37.3	14814	1852
	4 blades, O-U, transport	65,800	436	743	6.75	.315	679	39.7	14676	1836

Legend: S   = One engine per blade.

S-S = Side by side mounting of two engines per blade.

O-U = Over-under mounting of two engines per blade.

TABLE 3. WEIGHT BREAKDOWN

Component	(a) Optimum for V_{TH} = 650, n = 235g, 3 blade, Single engine per blade	(b) Optimum for V_{TH} = 598, n = 235g, 3 blade, Single engine per blade	CONFIGURATIONS Using CAE 357-1 Engine at V_{TH} = 650, n = 235g, and c = 6.5		
			F_R = 1,700 lb/engine 4 blades, O-U		F_R = 1,900 lb/engine 3 blades, O-U
			Final Design Proposal (Model 1108) W_G = 71,680	Same Weight Basis as (a) and (b) W_G = 71,680	Same Weight Basis as Model 1108 W_G = 64,250
Rotor group	11,892	8,432	16,673***	15,840	12,620***
Pylon	1,120	703	1,731	1,558	1,207
Gear box	200	200	200	200	200
Tail rotor and drive	328	306	383	383	332
Stabilizer	230	230	257	257	230
Body group	2,972	2,876	3,203	3,203	3,020
Landing gear	2,527	2,380	2,897	2,897	2,570
Flight controls	1,286	1,226	1,434	1,434	1,310
Engines	2,205	2,444	2,920	2,920	2,190
Engine components	1,434	1,548	1,679	1,837	1,260
APU	730	730	365	730	365
Fuel systems	1,077	1,119	1,292	1,388	1,168**
Instruments	296	296	296	296	296
Electrical	937	937	750	937	750
Electronics	275	275	275	275	275
Furnishings	317	305	345	345	321
Crew and oil	600	600	480	600	460
Cargo	24,000	24,000	24,000	24,000	24,000
Fuel	10,774	12,193	12,924*	11,676	11,676***
Total (corrected for closure error)	63,200	59,800	72,104	73,079	64,250
Closure error	0	0	424	1,399	0

* Cruise with six of eight engines at optimum tip speed.

** Cruise at optimum speed.

*** Based on latest design information

2.0 CONCLUSIONS

2.1 Structural and Dynamic Limitations

2.1.1 Static Droop Limiting Blade Aspect Ratio

The optimization of the rotor system occurred at rotor radii of less than 56 feet with chords equal to or greater than 6.5 feet in all cases. This resulted in blade aspect ratios, R/c, of less than 8.62. The pseudo blade weight, W_B', which is used in determining the tip weight to blade weight ratio can be obtained from the rotor group weight by using Equation (1).

$$W_B' = \frac{W_{RG} - 500}{1.8(b)} + 400 \tag{1}$$

The tip weight, W_T, is given by Equation (2):

$$W_T = \frac{W_{EC} + W_E}{b} \tag{2}$$

where W_{EC} and W_E, the engine component weight and the engine weight, respectively, are listed in Table 3.

The maximum tip to blade weight ratio for the 56-foot radius configurations considered is 0.50. This ratio, combined with the rotor radius (56 feet) and the maximum aspect ratio (8.6), gives a maximum static droop of less than 33 inches by reference to Figure 27. No limits have been established for the maximum static droop, but this value is well within reasonable limits.

2.1.2 In-Plane and Flapping Frequency Limiting Aspect Ratio

Since the rotor group weight was determined by the in-plane frequency requirements as shown in Section 3.4.2, the aspect ratio for each solution obtained is necessarily satisfactory.

The flapping frequency can be adjusted for each blade by material redistribution in the blade section, and, therefore, is not considered to be aspect ratio limiting as is discussed in Section 3.2.2.1.

2.2 Optimum Configurations and Design Parameters

2.2.1 Optimum Helicopter with Generalized Engines

Within the scope of this study, the optimum helicopter was found to be one having the minimum number of blades and the minimum number of engines.

For the same rotor configuration and engine arrangement, the crane fuselage with external cargo was found to result in a lower gross weight

13

than the transport fuselage with internal cargo. This means that the weight of the additional fuel required by drag of the crane fuselage and the external cargo was less than the increased fuselage weight of the transport fuselage. The weights of the transport and crane fuselages are given by Equations (80) and (81); Section 1.3 lists the values of equivalent drag area. The minimum number of engines (single engine per blade) was found to have a lower gross weight than an equivalent side-by-side configuration. Reducing the number of engines reduces the inlet area (A_I) required for a given thrust and the nacelle drag. This results in reduced fuel required and a reduction in gross weight.

Since the two-blade rotor was found to be unsatisfactory because of insufficient control power, the optimum helicopter configuration is:

> Three blades
> One engine per blade
> Crane-type fuselage

The values of the design parameters for this configuration are given in Table 2 and in Section 1.4.1.

2.2.2 Optimum Parameters for Particular Configurations

A comparison of minimum gross weights for the different configurations studied is shown in Figure 2. In all cases the gross weights increase with the following ascending order of engine arrangements:

a) Single engine per blade - lowest gross weight.
b) Side-by-side engine arrangement - two engines per blade.
c) Over-under engine arrangement - two engines per blade - highest gross weight.

2.2.3 Optimum Helicopter with CAE 357-1 Engine

With the present limit on the rotor tip centrifugal force environment of 235g, a rotor having three blades, a 55.8-foot radius, over-under engines, and crane-type fuselage is the optimum configuration for use with the 11.8-percent increased thrust (1,900-pound) CAE 357-1 engine.

A complete listing of the design parameters for this helicopter is given in Section 1.4.2. The empty weight breakdown is given in Table 7.

A four-blade rotor is necessary to meet the mission fuel requirements and the 6,000-foot, 95°F. hover requirement with the 1,700-pound rated thrust CAE 357-1 engine. The method of analysis of this four-blade rotor helicopter with eight CAE 357-1 1,700-pound rated thrust engines is discussed in Section 4.2. A complete listing of the design parameters is given in Section 1.4.

14

2.3 Nonoptimum and Nonlimited Configurations

2.3.1 Weight Penalties

According to the generalized engine parametric study, the optimum configuration is three blades and three engines with a crane-type fuselage. The following penalties result from using engine arrangements other than the optimum, depending on the number of blades and the condition being considered.

Single engine per blade .... no weight penalty
Side-by-side engine arrangement .... 1,900 to 3,400 pounds
Over-under engine arrangement .... 3,080 to 4,800 pounds

The greatest percentage of the penalty is fuel weight since the primary effect of using the nonoptimum configurations is to increase the nacelle drag (see Section 2.2.1). It is also possible to observe the differences in the use of the nonoptimum number of blades (Figure 2) and to determine the range of these values from Table 2 as follows:

Two blades .... 3,000- to 6,400-pound decrease
Three blades .... No weight penalty
Four blades .... 3,700- to 7,850-pound penalty

The weight penalties for more blades than optimum are compounded from fuel weight for the additional drag of the blade profile and the nacelle and the weight of the additional blade.

Use of the transport fuselage with internal cargo results in a weight penalty (as discussed in Section 2.2.1) as follows:

Crane-type fuselage .... No weight penalty
Transport-type fuselage .... 1,000- to 1,700-pound penalty

2.3.2 Increasing the Load Factor Limitations

A plot of the weight saving versus "n", the rotor tip environment, is shown in Figure 4 for the three-blade, single-engine-per-blade crane and in Figure 5 for the four-blade over-under engine crane.

Figure 4 shows that gross weight decreases with increasing n to 460g where the advancing blade compressibility cut-off occurs. A large portion of the gross weight reduction could be obtained if the 235g limit were increased to 300g; at this point the rotor radius would be approximately 43 feet. However, this radius is somewhat below the limit set for the validity of the rotor group weight equation, Equation (93). Thus, before any decision regarding a program of increasing the load factor limit of the engine is undertaken, the blade weight equation must be verified for the smaller radius.

15

2.3.3 Changing Rotor Lift Coefficient and/or Tip Speed Ranges

It does not appear that changing the upper limit of the design rotor mean lift coefficient, $C_{L_{r_0}}$, range would be of any benefit since only small reductions in gross weight could be obtained above a $C_{L_{r_0}}$ of 0.50 which is the maximum value considered acceptable. For the three-blade configurations the optimum design rotor mean lift coefficients all occur between .375 and .50. Reducing the lower limit on the hover tip speed to 598 feet per second would realize a reduction of 3,400 pounds for the optimum three-blade, three-engine configuration. A lower limit on the tip speed of 565 feet per second would be necessary to take maximum benefit of the weight reduction indicated for the four-blade configurations at the 235g limit.

Increasing the upper limit on tip speed would not appear to be desirable since the rotor is presently limited to 743 feet per second tip speed by advancing blade compressibility at 125 miles per hour. However, increasing the hover tip speed would allow the hover requirement at 6,000 feet, 95°F. to be met with a smaller engine for a given rotor radius, but, to meet the maximum speed requirement, the tip speed would have to be reduced to 743 feet per second or less.

An increase in tip speed results in a reduction in the $C_{L_{r_0}}$ at which the minimum gross weight occurs (for a typical case, see Figure 36).

2.4 Total Fuel Weight Reduction at Optimum Design for Each Configuration Available by Tip Speed Reduction

The fuel savings obtained by the use of the cruise tip speeds and the optimum tip speeds for the outbound and inbound portions of the mission are summarized in Table 4.

The cruise tip speed is obtained by iterating the fuel flow rate equation, Equation (47), until the fuel flow is more than 150 pounds per hour greater than that obtained with the optimum tip speed for the outbound condition. The iterations are performed in increments of 25 feet per second above the optimum tip speed found with Equation (53). The optimum tip speed, as shown in Table 4, was determined for the outbound condition and for the inbound condition using the total weights at the beginning of each of these portions of the mission. No problems with any of the optimum configurations listed in Table 4, due to rotor limitations, would be encountered except possibly the two-blade configura-

tion at 743 feet per second tip speed. In this case, where the design mean lift coefficient is .5, any tip speed reduction would result in a C_{L_r} in excess of the presently accepted maximum value for $C_{L_{r_0}}$ of 0.50.

Tip speed reduction results in a negligible fuel reduction for all configurations of condition (b), Table 4. However, from 405 to 1,461 pounds of fuel can be saved by using the optimum tip speed with the three- and four-blade configurations of condition (a). Also, appreciable fuel savings can be effected for some of the three- and four-blade configurations of condition (c).

It would be desirable to use optimum tip speed instead of cruise tip speed in any future studies in order to take maximum advantage of fuel weight reduction.

2.5 Increment in Structural Weight Required by Increments in Engine Weight or Engine Mount Weight

Differentiation of the rotor group weight, Equation (93), with respect to tip weight W_T produces the following relationship:

$$\frac{\partial W_{RG}}{\partial W_T} = \frac{.648b(.059162 - .013654c + .000966c^2)R^{2.39}}{W_T^{.64}} \tag{3}$$

With W_T = 1,200 pounds, $c \approx 6.5$ feet, and R = 55.83

$$\frac{\partial W_{RG}}{\partial W_T} = 1.05b \ \frac{pounds}{pound\ of\ tip\ weight\ at\ each\ blade}$$

Differentiation of Equation (79) for the pylon weight gives

$$\frac{\partial W_{PY}}{\partial W_{RG}} = .0046(W_{RG})^{.354} \ ; \tag{4}$$

then with W_{RG} = 16,000 pounds,

$$\frac{\partial W_{PY}}{\partial W_{RG}} = .143 \ \frac{pounds}{pound\ of\ tip\ weight} \tag{5}$$

Then the structural weight added by one pound of tip weight at each blade is

$$\frac{1.22b\ pounds}{pound\ of\ tip\ weight\ at\ each\ blade}$$

2.6 Chord for Minimum Rotor Group Weight

Differentiation of Equation (93) for the rotor group weight shows that the chord for minimum rotor group weight is 7.02 feet.

2.7 In-Flight Engine Shut-Down for Reduced Fuel Consumption

Partial differentiation of the fuel flow rate (Equation 47), with respect to MRTHP$_{700}$, shows for the case of the present hardware design (eight CAE 357-1 engines) that, with no increase in the required power (no engine cold drag), a 229-pound-per-hour reduction in fuel flow rate can be obtained for each engine shut-down. Partial differentiation of/ Equation (47), with respect to Bhp and use of the cold drag of 90 pounds per engine at 592 feet per second tip speed, shows that the resultant net decrease in fuel flow rate is 133 pounds per hour. This means that a better than 3-percent reduction in fuel consumption can be obtained by engine shut-down without provisions for fairing the engine to reduce cold drag.

Although the effect of engine shut-down is not included in the parametric study as it requires provisions for in-flight light-off and must be done so as to maintain thrust balance, it is recommended that it be considered for the Model 1108 configuration where no thrust imbalance results since less than half the available power is required during the cruise portions of the mission.

Engine shut-down must be symmetrical to avoid one-per-revolution shake due to thrust imbalance; it would not be practical to shut down engines for the three-blade, single-engine-per-blade configuration unless a method of automatically balancing the rotor was incorporated (i.e., shift the c.g. of the rotor system to lead the dead engine by 90 degrees and by an amount such that the centrifugal force of the shifted c.g. cancels the thrust imbalance).

2.8 Validity of Solutions

The solutions obtained for configurations whose blade radii are less than 45 feet are too far beyond the range of the rotor group weight equation (see Section 3.4.2.3) and are considered questionable. Static droop skin buckling might determine the rotor group weight for these configurations rather than chordwise frequency, and the design gross weight would be higher than shown in Table 2.

Before any serious program to increase the load factor limitations of the engine is undertaken, it would be wise to investigate the rotor group weight with expected tip weights and for radii of 38 to 45 feet.

18

Condition	Config.	Cruise V_T	Fuel Saved (lb.)	Optimum V_T Outbound	Optimum V_T Inbound	Fuel Saved (lb.)	V_{TH}
(a) n = 235g. Hover tip speed = 650 fps (minimum allowed by Sect.1.1.3). Chord is min. for minimum gross weight.	2b, S, C	V_{TH}	0	639	625	88	652
	3b, S, C	642	49	592	571	405	650
	3b, S-S,C	641	65	591	569	484	650
	3b,O-U,C	622	245	572	555	711	650
	4b, S, C	613	311	563	533	711	650
	4b, S-S,C	615	351	565	534	885	650
	4b,O-U,C	564	968	539	513	1317	650
	4b,O-U,T	557	1073	532	500	1461	650
(b): n = 235g. Chord and hover tip speed are optimum for minimum gross weight	2b, S, C	V_{TH}	0	639	626	88	652
	3b, S, C	V_{TH}	0	V_{TH}	596	4	598
	3b,SS, C	V_{TH}	0	V_{TH}	591	24	600
	3b,O-U,C	V_{TH}	0	V_{TH}	573	88	600
	4b, S, C	V_{TH}	0	V_{TH}	V_{TH}	0	565
	4b,SS, C	V_{TH}	0	V_{TH}	567	11	570
	4b,O-U,C	V_{TH}	0	V_{TH}	553	48	565
	4b,O-U,T	V_{TH}	0	V_{TH}	535	133	565
(c): n = optimum. Hover tip speed = 743 fps. Chord = optimum. (No load factor limitation.)	2b, S, C	V_{TH}	0	735	687	88	743
	3b, S, C	V_{TH}	0	721	645	194	743
	3b,SS, C	V_{TH}	0	704	629	442	743
	3b,O-U,C	740	15	665	609	575	743
	4b, S, C	V_{TH}	0	709	611	322	743
	4b,SS, C	V_{TH}	0	680	598	583	743
	4b,O-U,C	706	343	656	580	820	743
	4b,O-U,T	679	505	629	553	1159	743

Fuel saved = fuel at V_T - fuel at V_{TH}

C = crane
T = transport

Figure 2. Configuration Optimum Gross Weight Comparison.

(a) Optimum gross wts for $n = 235g$, $V_{TH} = 650$ fps (min. allowed by Sect. 1.1.3). Chord = optimum

(b) Optimum gross wts for $n = 235g$, $V_{TH} = $ opt. Chord = optimum.

(c) Optimum gross wts for $n = $ opt., $V_{TH} = 743$ fps. Chord = opt.
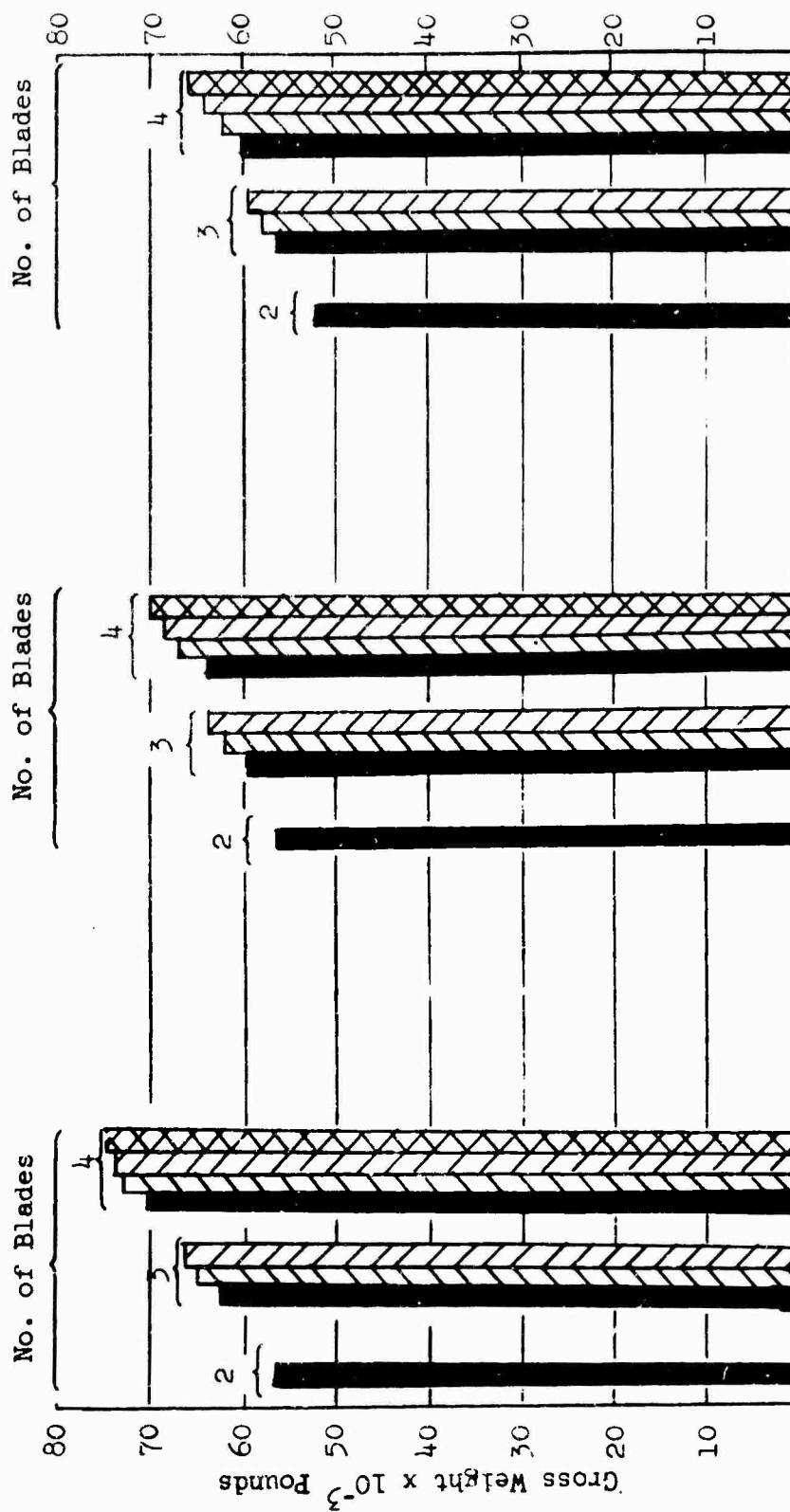
Legend: Crane with one engine/blade.

Crane with side-by-side engines.

Crane with over-under engines.

Transport with over-under engs.

20

Crane configuration
Four blades
Eight engines, over-under
Aspect ratio = 10

$W_{RG} = .00355(W_{GR})^{1.014}$

$V_{TH} = 650$

$V_{TH} = 675$

$n = 235g$ at $V_{TH} = 650$

Load factor
limit line

$n = 235g$ at $V_{TH} = 675$

$V_{TH} = 700$

$V_{TH} = 725$

$V_{TH} = 700$

$n = 235g$ at $V_{TH} = 700$

$n = 235g$ at $V_{TH} = 725$

Rated thrust V_{TH} cutoff.
$V_{TH} = 650$
$V_{TH} = 700$
$V_{TH} = 750$

235g rated
thrust cutoff

$C_{L_{r_0}}$

.57
.53
.49
.45
.41
.37
.33
.29
.25
.21

70,000   80,000   90,000

Solution Gross Weight - Pounds

Figure 3. Typical Plot of Design Mean Lift Coefficient Versus Gross Weight for the CAE Model 357-1 Engine.
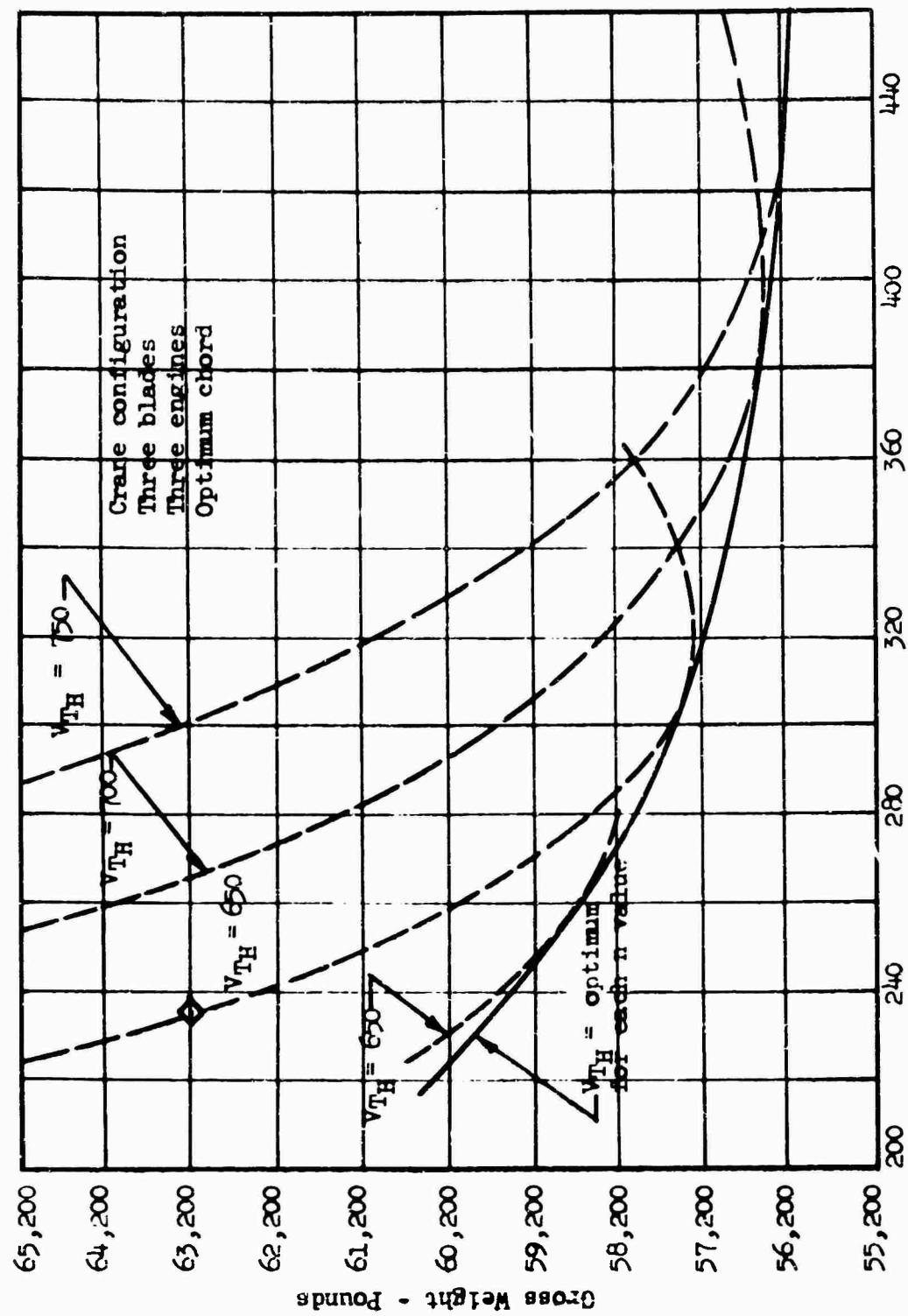
Figure 4. Solution Gross Weight Versus Tip Acceleration for Three Blades.

22
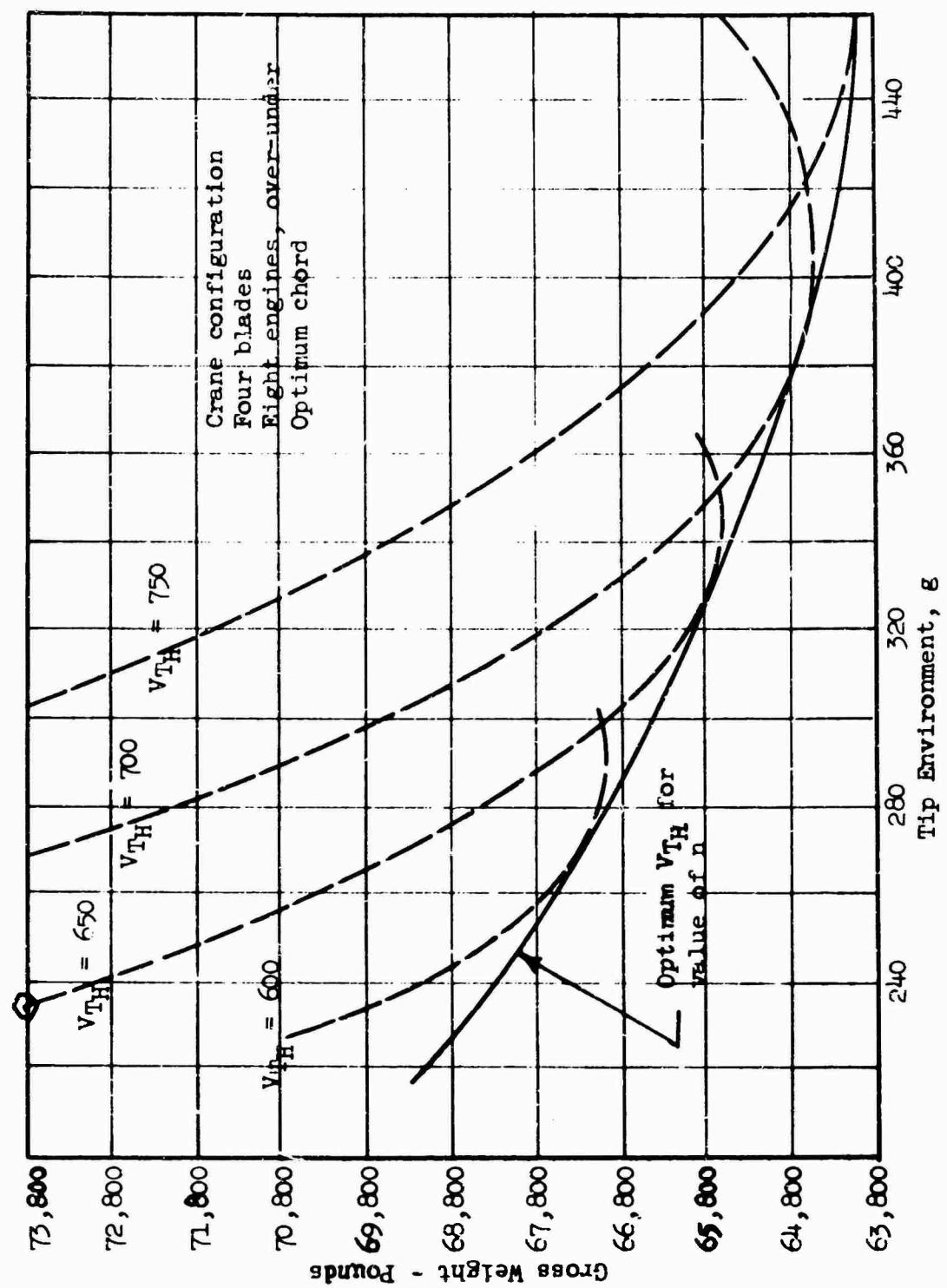
Figure 5. Solution Gross Weight Versus Tip Acceleration.

23

3.0 ANALYTICAL PROCEDURE

3.1 Introduction

It is possible to obtain an infinite number of solutions to meet a given
set of mission requirements and performance specifications. Therefore,
it is desirable to obtain these solutions in an orderly fashion that
will enable the best solution to be found (i.e., minimum gross weight
is generally accepted as the criterion for the optimum solution).

The method of obtaining solutions in the generalized engine parametric
study is known as the "R_u Method." A more conventional method of ob-
taining gross weight solutions is the R_F method, where R_F represents the
ratio of fuel weight to gross weight. The R_F method was not used be-
cause the curves did not lend themselves readily to computer solution
in the generalized engine parametric study. R_u represents the ratio of
the fuel weight and payload or the useful load to the gross weight. The
R_u method consists of determining the R_u available for a set of values
of the variable design parameters by using the weight relationships at
three or more gross weights; the R_u required is determined by using ap-
plicable performance equations and the mission requirements at these
gross weights. R_u available and R_u required are expressed as functions
of gross weight; the intersection of these two functions is the lowest
gross weight that will allow sufficient fuel for the mission requirements
with the given set of parameter values. This procedure is repeated with
different values of each of the independently variable design parameters.

For the purposes of the generalized engine study, the design mean lift
coefficient was determined at the solution gross weight for each set of
the variable design parameters. A plot was then made of these solution
design mean lift coefficients versus the solution gross weights.

By connecting points of constant hover tip speed and points of constant
load factor, lines of constant tip speed and load factor were established
(see Figure 36). Computation of the engine rated thrust to gross weight
ratio at each of these solution points and crossplotting provided lines
of constant engine rated thrust/gross weight ratio. The rotor limita-
tions (i.e., stall and compressibility) were also determined and plotted
on the same sheet. These calculations were repeated and plotted on a
different sheet for each selected chord length of a particular configur-
ation (number of blades and engine arrangement). From an overlay plot
at the different chord lengths for a particular configuration (see Fig-
ure 32) a line tangent to the lines of constant V_{TH} at a particular load
factor could be established. This envelope line determined the minimum
gross weight and chord within the rotor limitations. To find the mini-
mum gross weight obtainable in each configuration without load factor
limitations, it is noted that in each of the constant chord plots (Fig-
ure 36), increasing tip speed results in decreasing W_G minimum. However,

the advancing blade drag divergence limits the maximum allowable tip
speed. Therefore, the absolute minimum gross weight is determined using
the compressibility limit line assuming zero angle of attack for the
advancing blade. This establishes a solution limit line for each chord.
An envelope of these solution limit lines is then established on an over-
lay buildup of these lines for all the chords considered in the config-
uration (see Figure 35). It should be noted that the lines of constant
engine rated thrust/gross weight ratio (ℓ_r) can be used to establish a
solution line for a particular rated thrust engine having characteris-
tics similar to the CAE 357-1 engine (see Figures 32 and 36). Care
must be taken in interpreting the meaning of a constant rated thrust
solution line since it is predicated on the requirement that hover at
6,000 feet and 95°F. be met with no excess power. It is, of course,
possible that a particular engine being considered may have more power
than necessary to satisfy the hover requirement at the optimum solution
point for the engine. If the minimum gross weight of the rated thrust
solution line occurs at <u>less</u> than the $C_{L_{r_0}}$ for <u>minimum gross weight</u>,
then the configuration and gross weight defined by this point is the
optimum for the engine associated with this rated thrust (see the $F_R =$
14,320 line in Figure 32).

3.2 Preliminary Structural and Dynamic Analysis

3.2.1 Rotor Blade Aspect Ratio Limitation as Influenced by Static Droop

3.2.1.1 Static Droop Requirements

There are no established criteria to limit the permissible static droop
of rotor blades, but there are at least two requirements which should be
met for personnel safety and structural clearance:

a) Combining static droop and maximum rotor teetering angle, the
    lowest point on the rotor blade should be far enough above the
    ground to avoid striking a person standing upright on the ground.

b) Combining static droop and maximum rotor teetering angle, the
    rotor blade should not interfere with any other structural part
    of the helicopter (tail boom, tail rotor, etc.).

The fuselage geometry for the Hiller Model 1108 has not been established
as yet so the static droop is held variable in this study.

3.2.1.2 Idealized Airfoil Section

It is obvious that the airfoil section which gives an optimum stiffness/
weight ratio in the chordwise direction will not yield optimum stiffness/
weight ratio in the flapwise direction, and vice versa. It is also ob-
vious that the airfoil thickness ratio (depth) is very important in the

25

flapwise direction but of little consequence chordwise. Keeping these facts in mind, the airfoil thickness ratio is set at 15 percent and the following unbalanced shell airfoil will be used to determine a realistic stiffness/weight ratio in the flapwise direction.
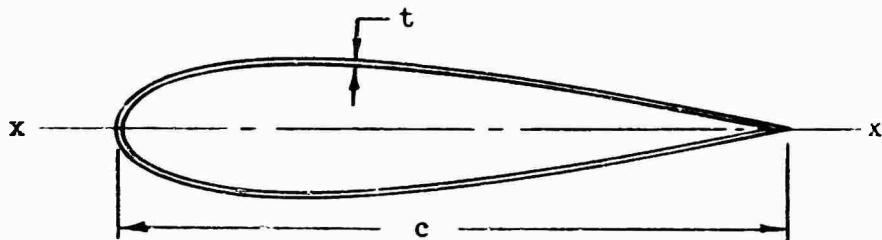

Figure 6. Idealized Airfoil Section.

$$I_{xx} = 0.00634tc^3$$

$$w = 2.055 \ tc\rho$$

$$\frac{EI}{w} = \frac{0.00634tc^3E}{2.055tc\rho} = 0.00309c^2 \left(\frac{E}{\rho} \right)$$

Most materials used in aircraft construction possess E/ρ ratios of approximately 10^8.

Therefore, $$\frac{EI}{w} \cong 309,000c^2 \qquad (6)$$

This same flapwise stiffness/weight ratio for the Hiller UH-12L rotor blade is $210,000c^2$ which shows that Equation (6) is realistic and yet can be considered a design goal.

3.2.1.3 General Static Droop Equation

Preliminary investigations of anticipated rotor blade properties reveal only slight mass and stiffness tapers are achievable for rotor blades supporting large tip weights. Therefore, the following development is done for rotor blades with uniform mass and stiffness distributions.

Consider the following cantilever beam:
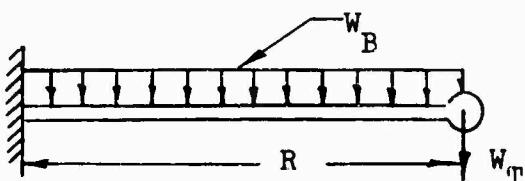
Figure 7. Static Droop Cantilever Beam.

26

$$\delta_{tip} = \frac{W_T R^3}{3EI} + \frac{W_B R^3}{8EI} = \frac{W_B R^4}{8EI}\left[1 + \frac{8}{3}\left(\frac{W_T}{W_B}\right)\right] \qquad (7)$$

Substituting Equation (6) into Equation (7) and making use of the relations aspect ratio (AR) = R/C and $w = W_B/R$ yields:

$$\delta_{tip} = \frac{R^2 (AR)^2}{2,472,000}\left[1 + \frac{8}{3}\left(\frac{W_T}{W_B}\right)\right]$$

or $\qquad AR = \frac{1,572}{R}\left[\dfrac{\delta_{tip}}{1 + \dfrac{8}{3}\left(\dfrac{W_T}{W_B}\right)}\right]^{1/2} \qquad (8)$

where: $\quad$ R $\quad$ = rotor radius, inches

$\qquad\qquad \delta_{tip}$ = tip deflection, inches

$\qquad\qquad W_T/W_B$ = tip weight/blade weight ratio

Figure 27 presents curves of allowable aspect ratio versus static droop (δ_{tip}) for two values of tip weight ratio, namely 0.4 and 0.5. These values of tip weight ratio are in the range expected for a four-bladed, rotor having two Continental 357-1 turbojet engines mounted on each tip.

3.2.2 Rotor Blade Aspect Ratio Limitation As Influenced by Blade Frequency Requirements

3.2.2.1 Rotor Blade Frequency Requirements

Flapwise (out-of-plane): - It is difficult to specify a criteria for flapwise frequencies of a teetering rotor except to require that these frequencies not coincide with those integer multiples of rotor speed which will transmit forces to the suspended mass (fuselage). It is convenient, therefore, to design the rotor blade for other criteria and then alter the flapwise design to avoid critical resonances.

Chordwise (in-plane): - In order to avoid ground resonance, the first in-plane rotating natural frequency of the rotor blades is designed to be 30 percent above nominal rotor speed. Additional benefits which are gained by this design requirement (flutter avoidance, reduced chordwise stresses, reduced deflections with engine out, etc.) overshadow the only obvious disadvantage which is additional rotor blade weight. In-plane frequencies higher than the first are designed so as not to coincide with integers of rotor speed.

27

Pitching (Torsion): - The first torsional natural frequency (including control spring) is desired to be as high as possible for avoidance of flutter. Since torsional frequency is as much a function of control system stiffness as it is blade properties, no specific requirement is set for the blade alone.

3.2.2.2 Idealized Airfoil Section

The lightest weight rotor group is obtained by designing the rotor blades to have the highest possible ratio of chordwise stiffness (EI) to running weight while maintaining chordwise frequency and mass balance requirements. One configuration which gives low weight combined with a nearly optimum stiffness/running weight ratio is the following shell airfoil balanced at the quarter chord.
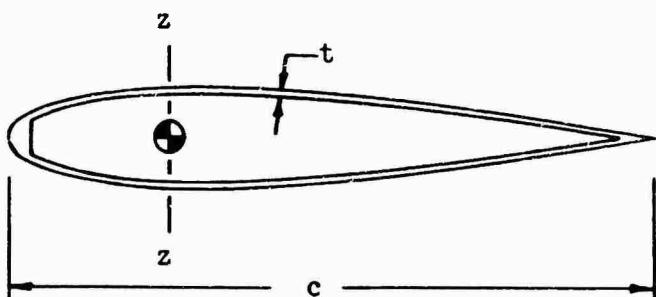
Figure 8. Idealized Airfoil Section

$$I_{zz} = .3029tc^3 + .1167tc^3 = .4196tc^3$$

$$w = 2.055tc\rho + 2.207tc\rho = 4.262tc\rho$$

$$\frac{EI}{m} = \frac{386(.4196)tc^3E}{4.262tc\rho} = 38c^2 \left(\frac{E}{\rho}\right)$$

Most materials used in aircraft construction possess E/ρ ratios of approximately 10^8.

Therefore,

$$\frac{EI}{m} \cong 3800c^2 \times 10^6 \text{ (balanced shell)} \tag{9}$$

In order to determine that Equation (9) is indeed an optimum stiffness/mass ratio in the chordwise direction, the same parameter is presented below for the Hiller UH-12L rotor blade.

$$\frac{EI}{m} \cong 2400c^2 \times 10^6 \text{ (Hiller UH-12L)} \tag{10}$$

28

3.2.2.3 General Frequency Equation

The symbols and information presented in Reference 1 are used here for the development of a general expression for the first chordwise (in-plane) rotating natural frequency of a teetering rotor blade with large tip weight/blade weight ratios.

In general,
$$\Omega_{R_1}^2 = \Omega_{NR_1}^2 + K_1 \Omega^2 \tag{11}$$

where:

Ω_{R_1} = first rotating natural frequency

Ω_{NR_1} = first nonrotating natural frequency

K_1 = Southwell coefficient

Ω = rotor angular velocity, rad/sec.

Preliminary investigations of anticipated rotor blade properties reveal only slight mass and stiffness tapers are achievable for rotor blades supporting large tip weights. The following development, therefore, is done for rotor blades with uniform mass and stiffness distributions.

From Reference 1:
$$\Omega_{NR_1}^2 = \frac{\theta_1^4}{R^4}\left(\frac{EI}{m}\right)$$

and
$$K_1 \approx 0.2 \ (\text{constant, regardless of tip weight})$$

Also, by definition,
$$\Omega = 12V_T/R$$

where:

θ_1^2 = Eigenvalue for first in-plane frequency

R = rotor radius, inches

V_T = rotor tip speed, ft/sec.

The established criteria for the first in-plane rotating natural frequency states that

$$\Omega_{R_1} \geq 1.3\Omega = 15.6 \ V_T/R$$

Rewriting Equation (11) yields

$$214.56V_T^2 = \frac{\theta_1^4}{R^2}\left(\frac{EI}{m}\right) \tag{12}$$

Substitution of Equations (9) and (10) into Equation (12) gives the following formulas for maximum allowable rotor blade aspect ratio (AR = R/C) for blades with optimum stiffness/mass ratios as well as blades which resemble the Hiller UH-12L rotor blade in stiffness/mass ratio.

29

$$AR = 4,208 \frac{\theta_1^2}{V_T} \quad \text{(balanced shell)} \tag{13}$$

$$AR = 3,345 \frac{\theta_1^2}{V_T} \quad \text{(Hiller UH-12L)} \tag{14}$$

The eigenvalues, θ_1^2, are plotted in Reference 1 as a function of tip weight/blade weight ratio. The tip speeds which are of interest for this study are 650, 700, and 750 feet per second, and so Figure 28 presents curves of allowable aspect ratio versus tip weight ratio for the tip speeds noted here.

3.3 Aerodynamic Analysis

3.3.1 Formulation of Standard Performance Equations

3.3.1.1 Hover Equations

The rotor power required to hover OGE is

$$rhp_H = ihp_H + RHP_H \tag{15}$$

Since the tail rotor power is not a function of the main rotor power and will probably be supplied by an A.P.U., it can be neglected in determining engine size. There will be accessories which will be driven from the main rotor, and they will require a fixed amount of power which is included in a fixed loss term, F.L.

The cooling air for the engines causes a thrust loss which is a function of the required thrust. This loss is included in an efficiency factor, η, which also includes the effect of engine inlet losses. Then, the total brake horsepower required to hover is written

$$Bhp_H = \frac{ihp_H + RHP_H + F.L.}{\eta} \tag{16}$$

The induced hover horsepower is written

$$ihp_H = \frac{1.13W}{550B \sqrt{2\rho_o}} \sqrt{\frac{\rho_o}{\rho}} \left(\frac{W}{\pi R^2} \right)^{1/2} \tag{17}$$

based on momentum theory and a triangular inflow distribution.

30

The rotor radius R can be written

$$R = \frac{V_{T_H}^2}{n(32.2)} \tag{18}$$

Substituting for R and letting $\rho_o = .002378$, Equation (17) becomes

$$ihp = \frac{.541n(W)^{3/2}}{BV_{T_H}^2} \sqrt{\frac{\rho_o}{\rho}} \tag{19}$$

The rotor blade profile horsepower required for hover based on blade element theory and a constant angle of attack from element to element (mean blade lift coefficient) is

$$Rhp_{b_H} = \frac{bR'c(V_{T_H}')^3}{4(550)} \frac{\rho_o}{2} \frac{\rho}{\rho_o} \left[\delta_o + \delta_2 \left(C_{L_{r_o}} \frac{\rho_o}{\rho} \right)^2 \right]$$

or

$$Rhp_{b_H} = \frac{A_b}{4,400} \rho_o \left(\frac{\rho}{\rho_o} \right) (V_{T_H}')^3 (\delta_{m_b}) \tag{20}$$

where $V_{T_H}' = \xi V_{T_H}$ and $R' = \xi R$

The engine nacelle profile horsepower in hover is

$$Rhp_{N_H} = \frac{A_I}{550} \left(\frac{\rho_o}{2} \right) \left(\frac{\rho}{\rho_o} \right) (V_{T_H}'')^3 \left[\delta_{o_I} + \delta_{2I} \left(C_{L_{r_o}} \frac{\rho_o}{\rho} \right)^2 \right] \tag{21}$$

where $V_{T_H}'' = \gamma_e V_{T_H}$

The total rotor profile horsepower in hover is

$$RHP_H = Rhp_{b_H} + Rhp_{N_H} = \frac{\rho_o (V_{T_H})^3}{1,100} \frac{\rho}{\rho_o} \left(\frac{\delta_{m_b} A_b \xi^3}{4} + \delta_{m_I} A_I \gamma_e^3 \right) \tag{22}$$

The blade area can be written

$$A_b = \sigma \pi R^2 \xi \tag{23}$$

and now

$$C_{L_{r_o}} = \frac{6C_{T_o}}{B^3 \sigma} = \frac{6W_G}{\sigma \pi R^2 \rho_o V_{T_H}^2 B^3} \tag{24}$$

See also Equation (98).

31

Combining Equations (23) and (24),

$$A_b = \frac{.2524 \times 10^4 W_G \xi}{B^3 C_{L_{ro}}(V_{T_H}^2)} \tag{25}$$

Substituting for R from Equation (18) in Equation (23),

$$A_b = \frac{.3034 \times 10^{-2} \sigma V_{T_H}^4 \xi}{n^2} \tag{26}$$

Solidity, σ, the ratio of blade area to rotor disc area, can be written for a constant chord blade,

$$\sigma = \frac{bcR}{\pi R^2} = \frac{bc}{\pi R} \tag{27}$$

3.3.1.2 **Formulation of Required Rated Thrust Equation**

$$\frac{F_R}{n_e} = 144(17.4)(D_I)^2 - 1,666 \tag{28}$$

Then,
$$A_{I_e} = \frac{A_I}{n_e} = \frac{F_R/n_e + 1,666}{3,190}$$

or
$$A_I = \frac{F_R}{3,190} + .522n \tag{29}$$

The net thrust, F_N, for a tip-mounted thrust engine is

$$F_N = \frac{Bhp\ 550}{V_{T_H}\gamma_e} \tag{30}$$

From CAE curve number 39464, Figure 12a, showing F_N versus true flight speed at 6,000 feet, 95°F., a curve of F_N as percent F_R is plotted versus tip speed, Figure 12b.

For the range of tip speeds between 600 and 850 feet per second, this can be represented by the linear relationship

$$F_N = \left(\frac{10\%\ \gamma\ V_{T_H}}{900\ \text{f.p.s.}} + 55\%\right)\left(\frac{F_R}{100\%}\right) \tag{31}$$

Substituting the right side of Equation (31) for the left side of Equation (30) and also using Equation (16) with Equation (19), Equation (22), Equation (25) and Equation (29), the following expression is obtained:

32

$$F_R \left[1 - \frac{1.57 r_e^2 (V_{T_H})^2 \delta_{m_{I_\rho}} \rho 10^{-2}}{.1112 r_e V_{T_H} 10^{-1} + 55} \right] =$$

$$\frac{\frac{550}{\eta} \left[\frac{.54 \ln(W_G)^{3/2}}{B(V_{T_H})^3 r_e} \sqrt{\frac{\rho_o}{\rho}} + \frac{.2524 \times 10^4 W_G \xi^4 \rho \delta_{m_{b_\rho}} \rho V_{T_H}}{r_e V_{T_H}^3 B^3 C_{L_{ro}} 4,400} + \frac{.522 n V_{T_H}^2 r_e^2 \rho \delta_{m_{I_\rho}}}{550 \times 2} + \frac{F.L.}{r_e V_{T_H}} \right]}{.1112 \times 10^{-3} r_e V_{T_H} + 55} \tag{32}$$

where ρ is for 6,000 feet at $95°F$.

Combining Equations (24) and (18) and solving for $V_{T_H}^3$,

$$V_{T_H}^3 = 91 \left(\frac{W_G n^2}{C_{L_{r_o}} \sigma B^3} \right)^{1/2} \tag{33}$$

$V_{T_H}^3$ and n can now be eliminated from the first term in the brackets, Equation (32), and the equation can be solved for thrust loading for $\rho = .00178$ (6,000 feet, $95°F.$).

$$\ell_F = \frac{F_R}{W_G} = \frac{\dfrac{.377 \times 10^2 \sqrt{C_{L_{r_o}} \sigma B}}{r_e} + \dfrac{.5620 \times 10^2 \xi^4 \delta_{m_{b_\rho}}}{r_e B^3 C_{L_{r_o}}}}{\eta(.1112 \times 10^{-1} r_e V_{T_H} + 55 - .2788 \times 10^{-4} r_e V_{T_H}^2 \delta_{m_{I_\rho}}} +$$

$$\frac{.464 \times 10^{-1} n V_{T_H}^2 r_e^2 \delta_{m_{I_\rho}} + \dfrac{.550 \times 10^5 F.L.}{r_e V_{T_H}}}{\eta(.1112 \times 10^{-1} r_e V_{T_H} + 55 - .2788 \times 10^{-4} r_e V_{T_H}^2 \delta_{m_{I_\rho}}} \tag{34}$$

3.3.1.3 Formulation of Forward Flight Equations

The induced horsepower in forward flight is

$$ihp_V = ihp_H K_u \tag{35}$$

where K_u is based on momentum considerations and is written

33

$$K_u = \sqrt{\frac{1}{2}\left[\sqrt{\left(\frac{V}{U_H}\right)^4 + 4} - \left(\frac{V}{U_H}\right)^2\right]} \qquad (36)$$

The hover-induced velocity, U_H, is based on momentum and energy theory and uniform inflow velocity, and is written

$$U_H = \sqrt{\frac{W}{2\pi R^2 \rho B^2}} \qquad (37)$$

Using Equation (24), this can be written

$$U_H = V_{T_H}\sqrt{\frac{C_{L_{ro}}\sigma BW}{12W_G}\left(\frac{\rho_o}{\rho}\right)} \qquad (38)$$

The rotor blade profile power in forward flight is written

$$Rhp_{b_V} = Rhp_{b_H} K_{\mu_b} \qquad (39)$$

where K_{μ_b} is a dissymmetry correction factor obtained by blade element theory, and is written

$$K_{\mu_b} = 1 + 3\left(\frac{V}{\zeta V_{T_V}}\right)^2 + 30\left(\frac{V}{\zeta V_{T_V}}\right)^4 \qquad (40)$$

The nacelle profile power in forward flight is written

$$Rhp_{N_V} = Rhp_{N_H} K_{\mu_N} \qquad (41)$$

where K_{μ_N} is a factor which includes the average induced yaw drag of the exterior of the nacelles and the dissymmetry effects on the profile power of the nacelle and is written

$$K_{\mu_N} = 1 + \left(\frac{V}{r_e V_{T_V}}\right)^2\left[1 + \left(\frac{\delta'_{2_I} + a'_I}{2\delta_{m_I}}\right)\right] + \frac{\delta'_{2_I}}{\delta_{m_I}}\left(\frac{V}{r_e V_{T_V}}\right)^4 \frac{1}{2} \qquad (42)$$

The derivation of this expression is given in Section 6.1.

3.3.2 Formulation of Fuel Flow Rate Equation

The sea level standard day performance curve (Figure 13) for the CAE 357-1 engine was used to obtain a set of constant specific fuel consumption curves with tip speed versus thrust horsepower (Figure 14). The thrust horsepower is obtained from the net thrust and tip speed by the equation,

34

$$THP = \frac{V_T F_N}{550} \qquad (43)$$

Establishing the military rated thrust at 700 feet per second tip speed as a reference and calculating the fuel flow rate as a function of military rated thrust horsepower,

$$MRTW_{f_{700}} = tsfc(F_N) = 1.30(MRTHP_{700}) \frac{550}{700} = 1.022\ MRTHP_{700}\ \text{lb. per hour} \qquad (44)$$

Fuel flows and thrust horsepower values were obtained for various engine power settings and tip speeds. These data were referenced to the $MRTW_{f_{700}}$ and $MRTHP_{700}$, respectively, to obtain the curve of Figure 15.

Each of the lines of constant tip speed in Figure 15 can be approximated very closely by a straight line. The equations of these lines are determined in the slope intercept form, i.e.,

$$\%\ MRTW_{f_{700}} = m\ \%\ MRTHP_{700} + b \qquad (45a)$$

The slopes, m, were plotted versus tip speed and a linear relationship was used to represent them. The values of the slope determined by this linear relationship are then used to determine an adjusted constant, b, which is compatible with the points at 50% $MRTHP_{700}$ in Figure 14. These constants, b, are also represented by a linear relationship with tip speed, and this relationship along with the equation for the slope, when substituted into Equation (45a), gives the expression

$$(\%MRTW_{f_{700_V}}) = -V_{T_V}(1.158 \times 10^{-3})(\%\ MRTHP_{700} + .735 \times 10^{-2})$$
$$+ 1.724(\%\ MRTHP_{700}) + C_V \qquad (45b)$$

where
$$\%\ MRTHP_{700} = \frac{BHP}{MRTHP_{700}} \times 100\% \qquad (45c)$$

and
$$C_V = 14.03\% \text{ in hover at } V = 0$$
$$C_V = 15.88\% \text{ at } V = 60 \text{ kts.}$$
$$C_V = 18.40\% \text{ at } V = 100 \text{ kts.}$$

The military rated thrust horsepower at 700 feet per second tip speed can be related to rated thrust by the following equation:

$$MRTHP_{700} = 1.168 F_R \qquad (45d)$$

The constants C_V are determined by constructing Figure 16 using Reference 2. Since the slopes remain essentially constant, it is necessary only to adjust the constant, b, for the different forward flight condi-

tions, and since the adjustment was assumed the same for all tip speeds, the difference appears only in C_V.

An integration of the fuel flow around a complete rotor cycle at 650 feet per second tip speed, 50 percent of MRT, and 125 miles per hour and an integration of the $\sin \psi \times F_N$ and the rotor ram drag showed that the net rotor horsepower specific fuel consumption <u>increase</u> above the hover horsepower specific fuel consumption was 40.8 percent <u>less</u> than that shown by Reference 2.

However, the constants, C_V, are those determined from Figure 16. This allows some margin for the non-steady-state conditions which could be expected to cause an increase in fuel consumption.

3.3.3 Formulation of Fuel Weight and R_u Required

The fuel-weight-required equations are developed on a trapezoidal elemental area basis with elemental area given by

$$W_F = W_f(\Delta t) + \frac{1}{2} \left(\frac{dW_f}{dt} \right) \Delta t (\Delta t) \tag{46}$$

where m is the slope of the top of the trapezoid which has a rectangular base (see cut).

Figure 9.
Trapezoidal
Element.
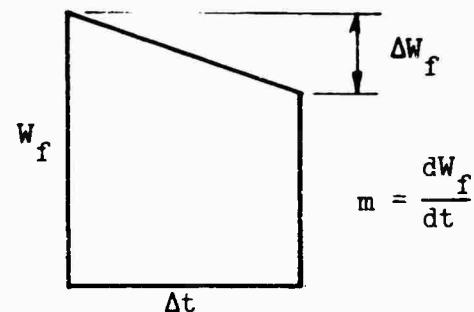
$$m = \frac{dW_f}{dt}$$

The fuel weight required for a given portion of the mission is found by employing the following equations:

$$W_f = \frac{(\% \ \text{MRTW}_{f700})}{100\%} \times 1.026 \ \text{MRTHP}_{700} \tag{47}$$

$$\frac{dW_f}{dt} = \frac{-dW_f}{d(\% \ \text{MRTHP}_{700})} \times \frac{(d)(\% \ \text{MRTHP}_{700})}{dW} \ (W_f) \tag{48}$$

for the slope, m, where

$$\frac{-dW_f}{d(\% \text{MRTHP}_{700})} = (-1.724 + .001158 \ V_{TV}) \ \frac{1.026 \ \text{MRTHP}_{700}}{100} \tag{49}$$

36

and
$$\frac{d(\% \text{ MRTHP}_{700})}{dW} = \frac{81.15 n K_u (W)^{1/2}}{B \bar{V}_{T_H}^2 \text{ MRTHP}_{700}} \tag{50}$$

Δt is the small time increment used for which dW_f/dt is assumed constant.

The term W represents the aircraft weight at the beginning of the portion of the mission. The effects of the reduction in $C_{L_{r_0}}$ and K_u with weight are neglected, which will allow a margin of conservatism to offset the slightly optimistic effect of assuming dW_f/dt to be constant when actually it increases (i.e., becomes more horizontal as fuel is burned off). If a portion of the mission was a long time interval, as for a ferry mission, an increase in accuracy would be necessary and could be obtained by breaking up the total interval into several smaller intervals. However, the intervals in the mission as described are small enough to give good accuracy in the fuel weight determinations.

The fuel weight determined for each interval is subtracted from the weight at the beginning of the next interval, i.e.,

$$W_{i+1} = W_i - W_{F_i} - \Delta W_{P.L.}$$

This weight is used in determining W_f and dW_f/dt for this next interval The weight at the beginning of the mission less the weight at the end of the mission and the total payload difference gives the fuel weight required to perform the mission, $(W_F)_{tot}$ and

$$W_{F_{req}} = \frac{(W_F)_{tot}}{1 - \frac{\% \text{ reserve}}{100\%}} = \frac{(W_F)_{tot}}{.900} \tag{51}$$

since 10 percent of the initial fuel is required for reserve.

The R_u required is written

$$R_{u_{req}} = \frac{W_{F_{req}} + \text{payload}}{W_G} \tag{52}$$

3.3.4 Cruise Tip Speed Determination

3.3.4.1 Equation for Cruise Tip Speed at Minimum Fuel Flow

A turbojet engine has a fuel consumption rate which is directly a function of the thrust output; the lower the thrust, the lower the fuel flow rate. Writing Equation (30) with Equation (16), omitting the $(V/V_T)^4$ terms and adding a rotor ram drag term, then differentiating with respect to V_T gives the following expression:

37

$$\frac{dF_N}{dV_{T_V}} = V_{T_V}{}^6(\rho_o)\,\frac{\rho}{\rho_o}\left(A_b\,\frac{\xi^3\delta_{o_b}}{4} + A_I r_e{}^3\delta_{o_I}\right) -$$

$$V_{T_V}{}^3\,550\,(\text{ihp}_V + \text{php}_V + \text{F.L.} + \text{rotor ram drag}) -$$

$$V_{T_V}{}^2\,c_{L_{r_o}}{}^2\,V_{T_H}{}^4(\rho_o)\,\frac{\rho_o}{\rho}\left(\frac{A_b\xi^3}{4}\,\delta_{2_b} + A_I r_e{}^3\delta_{2_I}\right) -$$

$$2\,c_{L_{r_o}}{}^2\,V_{T_H}{}^4\,V^2(\rho_o)\,\frac{\rho_o}{\rho}\left[\frac{3}{4}\,\xi A_b\delta_{2_b} + \left(1 + \frac{\delta_{2_I}' + a_I'}{2\delta_{m_I}}\right)A_I r_e\delta_{2_I}\right] \qquad (53)$$

The real positive root of this expression set equal to zero is the tip speed at minimum thrust or minimum fuel flow. The derivation of this expression is given in the Appendix.

It should be mentioned that the rotor ram drag is not included in the expression for Bhp since for purposes of fuel flow, it is more convenient to include it in the C_V term. The expression for rotor ram drag horsepower is

$$\text{Rotor ram drag horsepower} = \frac{1}{2}\,\frac{W_a\,V^2}{1,560(32.2)(700)}\,(\text{MRTHP}_{700}) \qquad (54)$$

and is obtained by integrating over a complete rotor cycle, the drag component of the radial force caused by the turning of the engine air through the angle of yaw.

Figure 10 shows graphically the factors involved in the optimum tip speed determination.
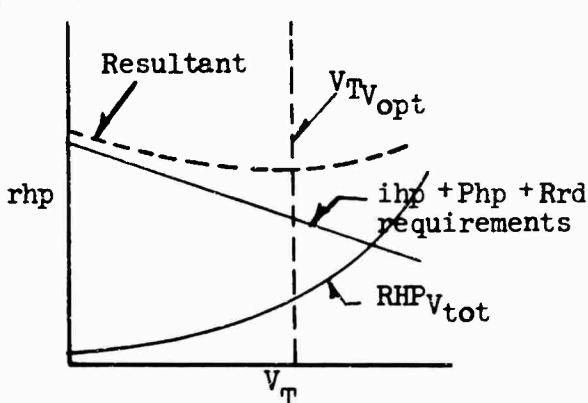
Figure 10. Optimum Tip Speed Determination.
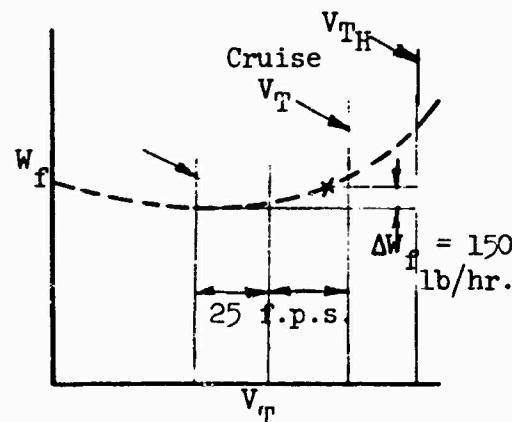
Figure 11. Cruise Tip Speed.

3.3.4.2 Selection of Cruise Tip Speed

The optimum tip speed for the 60-knot outbound mission was determined. The tip speed was then increased by increments of 25 feet per second,

until a fuel flow rate (W_f) of more than 150 pounds per hour greater than the optimum was obtained. This tip speed or the hover tip speed, whichever is lower, was then selected as the cruise tip speed. See Figure 11 for a graphical representation of the relationship between cruise tip speed, optimum tip speed, and fuel flow rate (W_f).

3.3.5 Rotor Limit Equations

The retreating blade angle of attack, α_{270}, (in radians) is written

$$\alpha_{270} = A_1 C_{L_{r_0}} + A_2\lambda' + A_3\epsilon \tag{55}$$

The retreating blade is stall limited at α_{270} = .209 radians (12°)

The advancing blade angle of attack in radians is written

$$\alpha_{90} = A_1' \, C_{L_{r_0}} + A_2'\lambda' + A_3'\epsilon \tag{56}$$

The drag divergent Mach number is given by

$$M_{DD} = .000148\,\alpha^3 - .00347\,\alpha^2 - .00825\,\alpha + .829 \tag{57}$$

where α is in degrees.

The drag divergent speed is obtained by substituting α_{90} or α_{270} in degrees into Equation (57) and multiplying the result by the speed of sound. For sea level standard temperature:

$$V_{DD} = aM_{DD} = M_{DD}(1,117) \tag{58}$$

In Equations (55) and (56), ϵ is the angle of twist in radians; for this study it was taken as ϵ = -0.1745 radians = -10° and ϵ = -.2794 radians = -16°.

The above equations for the tip angle of attack of the advancing and retreating blades are derived from blade element integrations of the elemental thrust and flapwise moment equilibrium expressions.

$$A_1 \doteq .197 + .488\mu + .986\,\mu^2 \tag{59}$$

$$A_2 \doteq .561 + .894\mu + 2.008\,\mu^2 \tag{60}$$

$$A_3 \doteq .280 - .066\mu + .824\,\mu^2 \tag{61}$$

$$A_1' \doteq .197 - .510\mu + .328\,\mu^2 \tag{62}$$

$$A_2' \doteq .561 - 1.106\mu + .488\,\mu^2 \tag{63}$$

$$A_3' \doteq .280 + .042\mu - .024\,\mu^2 \tag{64}$$

The expression for λ' is written

$$\lambda' = \frac{U_i + U_b + U_{N_1} + U_{N_2} + U_D + U_A}{V_T} \tag{65}$$

where the numerator is the total inflow. The first term U_i is written

$$U_i = U_H K_u \tag{66}$$

where U_H is given by Equation (37) and K_u by Equation (36).

Integrating for the dissymmetry drag effects on the blade and nacelle which require a certain tilting of the tip path plane, and thus an additional inflow through the rotor, yields

$$U_b = \frac{.000595 \ A_b V_T \xi \delta_{m_b} V^2}{W_G} \tag{67}$$

$$U_{N_1} = \frac{.001188 A_I V_T r_e \delta_{m_I} V^2}{W_G} \tag{68}$$

Integrating the drag component of the nacelle lifting force in the tip path plane (i.e., the radial force due to the yaw angle of the nacelle at its various azimuth positions) the expression for the average effect on the inflow is

$$U_{N_2} = \frac{.001188 \left(\dfrac{A_I}{2} a_I \dfrac{V}{V_T} \right) V^3}{W_G} \tag{69}$$

The fuselage drag causes an additional tilt of the rotor and an additional increment in the inflow which is written

$$U_D = \frac{.001188 A_\pi V^3}{W_G} \tag{70}$$

The rotor ram drag also increases the rotor tilt. This increment is written

$$U_A = \frac{1.055 F_R V}{2(1,700) W_G} \tag{71}$$

After calculating a drag divergent speed, it is checked against the speed existing at the blade tip which is written

$$V_{270} = V_T - V \tag{72a}$$

or $$V_{90} = V_T + V \tag{72b}$$

3.4 Weight Equations

3.4.1 Statistical Weight Study

3.4.1.1 Introduction

The equations utilized in this section are purely statistical in origin and have been derived as a result of research into group weight break-downs of as many types and members of helicopters as were readily available.

The spectrum of gross weights involved ranges from 1,080 pounds to 84,000 pounds and presents a wide and liberal picture of helicopter component weights. The method of derivation used was to correlate pertinent component weights with some exponential function of a major parameter such as gross weight, horsepower, etc. and present the basic equation in the form of: $W_c = C(x)^n$. The parameter "x" was then expanded into its own variables; e.g., assuming that "R" is the selected parameter, then

$$R = \sqrt{\frac{W_G}{\pi w}} \quad \text{or} \quad \frac{V_{TH}}{ng} \quad .$$

This method enabled a parameter to be sensitive to design or philosophy changes over and above that of the basic parameter itself, and resulted in a useful "tool" that could be used in "sizing" the concept.

For the purpose of the subject helicopter it may be seen that the upper ranges of the resultant curves are largely extrapolated to follow the general trend. Inconsistencies do occur when considering a helicopter of the current configuration; however, the sum of the values derived from the curves will prognosticate a close and reasonably reliable empty weight.

To determine the reliability of the methods used in this study, actual component weights of several helicopters were selected at random and compared with the statistical weights derived from the equations. It was found that the statistical weights varied within 5 percent of the actual weights. It is postulated, therefore, that the extrapolation of lower gross weight helicopter components will yield reasonably realistic weight predictions when applied to the tip powered concept.

3.4.1.2 Sources and Curve Fitting Methods

The weight breakdowns considered as a basis for the equations used in this study are taken from the following aircraft:

Manufacturer	Designation
Hiller	H32
Hughes	269

Manufacturer	Designation
Gyrodyne	54a
De Havilland	Skeeter
Bell	H-13H
Bell	47G
Hiller	OH-5A
Hiller	UH-12E
Kaman	HTK-1
Cessna	CH-1
Republic	Allouette
McDonnell	120
Vertol	H25A
Hiller	1042
Hiller	1040
Sikorsky	H19
Vertol	H21
Sikorsky	H34
Sikorsky	H37
Vertol	YH16A
Sikorsky	S-64A
Hughes	XH-17
Vertol	YH16B
Hughes	XH28

The component weights, taken from the above helicopter weight breakdowns, were plotted against a selected major parameter; the resultant scatter was then represented by a relationship or a line which satisfied the requirements of the method of least squares. Higher ranges above the area where the scatter terminated were assumed to follow the trend, and the line was therefore extrapolated to include the gross weight range under consideration.

3.4.1.3 Equations

Rotor Group - (W_{RG})

Blade and hub weights were plotted against one or a combination of parameters in an attempt to satisfy a basic relationship. However, this could not be achieved with sufficient definity to permit an extrapolation to the higher gross weight ranges; therefore, it was considered feasible to consider the entire rotor group as a single weight function and plot the available information against one or a combination of parameters.

The most acceptable parameter that resulted from the scatter pattern was the gross weight (W_{G}) times rotor radius (R).

The relationship resulting from this combination of parameters versus rotor group weight is as follows:

$$W_{RG} = .00214(W_G \times R)^{1.0414} \tag{73}$$

R may be expanded to give greater flexibility of usage in two ways.

1) $R = \sqrt{W_G/\pi w}$

This value substituted into Equation (73) gives

$$W_{RG} = .00118\left(\frac{W_G^{1.56}}{w^{.52}}\right) \tag{74}$$

2) $R = \dfrac{V_{T_H}^2}{ng}$

Therefore $\quad W_{RG} = 5.75 \times 10^{-5}\left(\dfrac{W_G}{n}\right)^{1.0414}(V_{T_H})^{2.0828} \tag{75}$

Stabilizer Weights - (W_{STA})

Stabilizer weights for conventional helicopters are not easily identified with basic parameters such as gross weight or rotor radius. In order to present a scatter pattern that could be considered representative, it was decided to utilize two determining parameters such as V_{max} and L_F (fuselage length).

The stabilizer weights available were then plotted against L_F times V_{max} for existing helicopters; the resulting equation was:

$$W_{STA} = 1.032 \times 10^{-15} (L_F \times V_{max})^{3.523} \tag{76}$$

Assuming that $L_F = 14.4R$, as appears to be reasonable when tip-driven helicopters are considered, the equation can be written as:

$$W_{STA} = 12.4 \times 10^{-12} (R \times V_{max})^{3.523}$$

But $\qquad R = \sqrt{W_G/\pi w}$.

Therefore, $W_{STA} = 1.65 \times 10^{-12}\left[\dfrac{(W_G)^{1.761} \times (V_{max})^{3.523}}{w^{1.761}}\right] \tag{77}$

A third variation may be occasioned by using the relationship $R = \dfrac{V_{T_H}^2}{ng}$

Substituting

$$W_{STA} + 7.45 \times 10^{-7}\left[\dfrac{(V_{T_H})^{7.05} \times (V_{max})^{3.523}}{n^{3.523}}\right] \tag{78}$$

43

Pylon - (W_{PY})

The pylon is the basic structure provided for rotor support, although in most cases this component is integral with the fuselage structure.

Available examples of identified pylon weights were best shown when plotted against rotor group weight, and the relationship established indicates:

$$W_{PY} = .0034(W_{RG})^{1.354} \tag{79}$$

Body Group Weights

Deriving an equation for body group weights involved making three categories:

1) Helicopter fuselages designed for maximum utility, i.e., covered cabin, maximum protection for crew and cargo, heavy all-weather protection.
2) The average fuselage.
3) The skeletal or austerity fuselage, open-frame type, minimum cabin protection, little or no cargo protection.

The fuselage weights considered represent all three of the above categories; therefore, fuselage weights were plotted against gross weight only to result in an inconclusive scatter from which no relationship could be satisfactorily deduced; therefore, it was decided to incorporate fuselage length with the gross weight.

The combination of these two parameters enabled an average relationship to be established that appeared to be a dividing line between categories 1) and 3).

The equations resulting from this combination of parameters is:

$$\begin{aligned}
&\text{Category 1) Passenger-Cargo.} && W_{BG} = .1268(L_F W_G)^{.594} \\
&\text{Category 2) Average Type.} && W_{BG} = .1071(L_F W_G)^{.594} && (80) \\
&\text{Category 3) Crane Type.} && W_{BG} = .0944(L_F W_G)^{.594}
\end{aligned}$$

In order to present as optimistic a prediction as the state of the art would allow, the three relationships established were reexamined. It was found that the fuselage of the S-64a, which is a crane-type vehicle, fell below the crane-type average weight on the curve. The curve was therefore shifted so as to pass through the S-64a fuselage point. The resulting equation is:

$$W_{BG} = .0875(L_F W_G)^{.594} \tag{81}$$

44

where $L_F = 14.4R$.

The fuselage length is taken as 1.2 times the rotor radius, but because L_F must be in inches whereas R is given in feet, the substitution of $L_F = 14.4R$ is used.

A fuselage length of 1.2 times the radius is considered appropriate for tip-driven helicopters.

Landing Gear - (W_{LG})

This function was plotted against gross weight.

$$W_{LG} = .0158(W_G)^{1.084} \tag{82}$$

Flight Controls - (W_{FC})

Flight controls were plotted against gross weight resulting in the relationship:

$$W_{FC} = .1205(W_G)^{.867}$$

However, using the philosophy as outlined in the body group weight, a low point on the curve was established and the following equation was calculated to pass through the point:

$$W_{FC} = .0885(W_G)^{.867} \tag{83}$$

Engine Components - (W_{EC})

The engine components considered in this study are as follows:

a) Inlet and exhaust
b) Engine fuel and oil supply components located in the nacelle
c) Engine controls
d) Engine nacelle
e) Engine mount and installation

It was determined that the statistical correlation of these points when plotted separately as either engine weight or engine thrust against component weight had little or no consistency to establish a trend; therefore, the components were added together and plotted against maximum rated thrust. This relationship is expressed as follows:

$$W_{EC} = 1.73b\left(\frac{F_R}{b}\right)^{.686} \tag{84}$$

Engine Weights - (W_{ENG})

Gas turbine engines of thrust ratings from 350 pounds to 17,000 pounds were plotted using dry engine weights against maximum thrust ratings. The relationship of this combination resulted in an expression relating engine weight to maximum thrust as follows:

$$W_{ENG} = .6309(F_R)^{.926}$$

The engine under consideration is the CAE Model 357-1 and weighs approximately 360 pounds. If this weight is inserted into the graph and a line drawn parallel to the curve established by the above equation a weight for a generalized engine is established and is expressed as follows:

$$W_{ENG} = .372n\left(\frac{F_R}{n_e}\right)^{.926} \tag{85}$$

The following components were evaluated by the relevant design groups, and a list of required items for each group was detailed.

Instruments,	$W_I =$	296 lb.
Electrical system,	$W_{EL} =$	937 lb.
Auxiliary power units,	$W_{APU} =$	730 lb.
Electronics system,	$W_{COM} =$	275 lb.
Accessory gearbox,	$W_{AGB} =$	200 lb.
Combined total weight,	$C =$	2,438 lb.

Furnishings - (W_{FU})

Furnishings weight was considered as a function of gross weight and is related as follows:

$$W_{FU} = .2145(W_G)^{.660} \tag{86}$$

Tail Rotor - (W_{TR})

The weight origin of the equation for this function is comprised of two helicopters, namely, the Hughes XH15 and XH28, as these represent tail rotors for tip-driven helicopters.

Gear-driven tail rotors cannot be used as they are designed for torque compensation and therefore represent a greater percent of the gross weight. The plot of weight of the two examples against their respective gross weights, resulted in a relationship as follows:

$$W_{TR} = .00039(W_G)^{1.234} \tag{87}$$

3.4.2 Rotor System Analytical Weight Study

It is difficult to correlate data specifically relating to the main
rotor system of the Hiller Model 1108 tip turbojet helicopter since
there is an insufficient number of existing helicopters using teeter-
ing rotors with tip weight/blade weight ratios approaching 0.5. Rotor
blade design considerations for conventional helicopters place equal
importance on static strength, fatigue strength, and location of natural
frequencies. For teetering rotors with very large tip weight ratios,
the blade strength required to insure proper natural frequency values,
as well as acceptable static droop, renders bending, centrifugal and
fatigue stresses relatively unimportant.

Unable to draw on existing data, it is necessary to formulate a rotor
group weight equation which includes the same parameters which affect
design frequencies and static droop, namely rotor radius, blade chord
and tip weight. It is of particular interest to note that such a rotor
group can be designed with no reference to helicopter gross weight.

3.4.2.1 Rotor Blade Weight

The most important design criterion for the rotor blades is that they
possess chordwise (in-plane) bending stiffness sufficient to result in
a first chordwise rotating natural frequency of at least 1.3 times
rotor angular speed (Ω). Preliminary design shows the specific rotor
blade weight decreases with increasing blade chord for a given chordwise
stiffness requirement. Figure 29 presents the results of this weight
study for two chordwise stiffnesses and two structural materials, steel
and titanium. The blades represented by these curves are NACA 0015 air-
foils which have sufficiently high flapwise stiffnesses to give accept-
able static droop.

It is immediately obvious that unlimited use of titanium in the rotor
blades can reduce the weight of one blade by more than 500 pounds for
rotor radii in the 50- to 70-foot range. For this study, the rotor
blade is assumed to be made of titanium so that the state of the art
in rotor blade design must be equalled or improved to meet target
weights.

Using the data presented in Figure 29 as running weight at the blade
root and considering a mild mass taper with radius, the following esti-
mates are made:

$$W_{c=5.5}/W_{c=6.5} = 1.183$$

$$W_{c=6.0}/W_{c=6.5} = 1.070$$

$$W = \left[5.263 - 7.896\left(\frac{c}{6.5}\right) + 3.633\left(\frac{c}{6.5}\right)^2\right]W_{c=6.5} \qquad (88)$$

It can be seen that Equation (88) does not predict the trends of the titanium curves of Figure 29 accurately due to the mass taper assumed.

It is necessary at this point to establish a basic blade weight through which the final weight equation will pass. Preliminary design work indicates that a rotor blade having the following properties can be built which will satisfy frequency requirements.

$$W_B = 2,175 \text{ pounds per blade}$$
$$R = 56 \text{ feet}$$
$$c = 6.5 \text{ feet}$$
$$W_T = 1,200 \text{ pounds (tip weight)}$$

For $R = 56$ feet and $W_T = 1,200$ pounds, then Equation (88) can be expanded as follows:

$$W_B = \left[5.263 - 7.896 \left(\frac{c}{6.5} \right) + 3.633 \left(\frac{c}{6.5} \right)^2 \right] 2,175$$

or $\qquad W_B = 11,447 - 2,642c + 187c^2 \text{ pounds per blade} \qquad (89)$

Equation (89) can be used to determine blade weight as long as $R = 56$ feet and $W_T = 1,200$ pounds but must be altered further to include varying radius and tip weight.

If tip weight and blade chord are held constant, the methods of Reference 1 can be used to predict chordwise stiffness changes required for various radii. Inspection of Figure 29 indicates distributed weight changes which must be reintroduced into the frequency equations until blade weight and chordwise stiffness are compatible. Upon increasing rotor radius the combination of increased distributed weight coupled with more radius over which this weight is distributed leads to rapidly increasing blade weight with radius for constant chord and tip weight. An analysis of this type results in the following data:

$$\text{for } R = 56 \text{ feet, } W_B = 2,175 \text{ pounds per blade}$$
$$\text{for } R = 65 \text{ feet, } W_B = 3,105 \text{ pounds per blade}$$

assuming that blade weight varies as some power 'x' of rotor radius

$$\left(\frac{65}{56} \right)^x = \frac{3,105}{2,175} = 1.428$$

where $x = 2.39$.

Multiplying Equation (89) by $(R/56)^{2.39}$ results in the following blade weight equation which still assumes $W_T = 1,200$ pounds:

$$W_B = (11,447 - 2,642c + 187c^2) \left(\frac{R}{56} \right)^{2.39}$$

48

or $\qquad W_B = (.05916 - .01365c + .000966c^2)R^{2.39}W_T^{0.36}$ pounds per blade $\qquad$ (91)

Limitations: $\qquad 5.0 \le c \le 7.0$ feet

$\qquad\qquad\qquad 50.0 \le R \le 70$ feet

$\qquad\qquad 1,000 \le W_T \le 2,000$ pounds per blade

3.4.2.2 Rotor Hub and Blade Retention Weight

The rotor blade retention system and the hub which completes the rotor group unit are more difficult to analyze concerning weight than is a rotor blade, since there are several concepts of blade retention, each of which might bear no resemblance to any other. Preliminary design indicates that the blade retention design is governed by the same criteria which is used for the blades as well as centrifugal force and bending stress, namely first chordwise rotating natural frequency. Other components in the hub/retention area, on the other hand, seem to be designed to be independent of those parameters which influence blade weight. These components are functions of general rotor size and remain unchanged for the variation limitations of the parameters in Equation (91).

Weight analysis of two vastly different hub/retention designs has shown that both result in blade retention weights which are approximately 80 percent as heavy as the blades which they retain (less tip weight). These two designs also have in common about 500 pounds of material which is indicative solely of the huge bearings, gimbal rings, etc., which must be used. These findings, in fact, suggest the following weight assumptions for the hub and blade retention systems.

$$W_H = 500 \text{ lb. (total} \qquad\qquad (92)$$
$$W_R = 0.8W_B \quad \text{(lb. per blade)}$$

W_B in this equation is defined by Equation (91).

3.4.2.3 Total Rotor Group Weight

The total weight of the rotor group is obtained by adding Equations (91) and (92). The blade weight and blade retention weight are presented per blade in these equations and so are multiplied by the number of blades, b.

$$W_{RG} = W_H + bW_R + bW_B = W_H + b(1.8W_B)$$

Expanding: $\qquad W_{RG} = 500 + 1.8b(.05916 - .01365c + .000966c^2R^{2.39}W_T^{0.36}$

$$(93)$$

where: $\qquad$ b $\;=$ number of blades

$\qquad\qquad$ c $\;=$ blade chord, feet

$\qquad\qquad$ R $\;=$ rotor radius, feet

$\qquad\qquad W_T =$ tip weight per blade, lb. (W_T is calculated using Equation (2) making sure that the result gives tip weight <u>per blade</u>.)

49

Limitations:
$$5.0 \leq c \leq 7.0 \text{ feet}$$
$$50 \leq R \leq 70 \text{ feet}$$
$$1,000 \leq W_T \leq 2,000 \text{ pounds}$$

The rotor group weight predicted by Equation (93) does not include tip turbojet engines, engine fairings (nacelles), engine mounts, or engine control components, but is intended to include blade tip buildup to which the engine mounts and nacelles are attached and all fuel and engine control lines which pass through the blades.

Calculating a check point, using Equation (93), for b = 4, c = 6.5 feet, R = 56 feet, and W_T = 1,200 pounds gives

$$W_{RG} = 500 + 15,670 = 16,170 \text{ pounds}$$

3.4.3 Formulation of Fuel Weight Available and R_u Available

The weight equations for the helicopter components were determined by statistical studies (Section 3.4.1) and actual design studies (Section 3.4.2). For the purposes of speed in calculation, these equations are divided into two groups:

a) Components with constant weight or weight which is only a function of gross weight.

b) Components whose weights are a function of other parameters besides, but possibly including, gross weight.

The group a) weights are calculated for each of the three gross weights used and stored permanently; it is then necessary to calculate only the items in group b) when executing the program.

The sum of the component weights (excepting fuel tanks) plus the crew and the payload, subtracted from the gross weight, gives the weight available for fuel and tanks. Since the fuel tank weights are a direct linear function of the fuel weight,

$$W_{F_{avail}} = \frac{W_G - \left[\Sigma W_i + W_{P.L.} + W_c\right]}{(1 + K_{F.T.})} \tag{94}$$

Then

$$\frac{W_F + W_{P.L.}}{W_G} = R_{u_{avail}}$$
$$= \frac{W_G \left[\Sigma W_i + W_c - K_{F.T.} W_{P.L.}\right]}{(1 + K_{F.T.}) W_G} \tag{95}$$

3.5 Determination of R_u Solutions and Final Plots

After determination of R_u available and required for the three succes-
sive gross weights, all other parameters remaining fixed, the minimum
gross weight or R_u solution gross weight for this set of parameters is
determined by fitting parabolic expressions to the two sets of three
points.

These parabolas are of the general form

$$x = Ay^2 + By + C \tag{96}$$

The gross weight, W_G, is substituted for x, and R_u is substituted for y.
The coefficients A, B, and C can be determined by simultaneous solution
of the three equations obtained by substituting the three R_u's and
their corresponding gross weights into Equation (96). Two equations of
$W_G = f(R_u)$ are obtained, one for R_u available and one for R_u required.
Subtraction of the expressions for R_u available and R_u required results
in a quadratic expression which can be solved for y or R_u solution.

$$R_u \text{ solution} = y = \frac{-B \pm \sqrt{(B')^2 - 4A'C'}}{2A'} \tag{97}$$

The choice of sign for use with the radical in this expression can be
made by picking the smallest positive root given by Equation (97).

After determination of the R_u solution, the W_G solution is obtained by
substituting the value of R_u solution for y in Equation (96).

This value of W_G solution is used in the expression

$$C_{L_{r_0}} = \frac{.833 \times 10^6 W_G n^2}{B^3 V_{T_H}^6} \tag{98}$$

To determine $C_{L_{r_0}}$ solution, Equation (98) is obtained from Equation (24)
using Equation (18).

Then the engine thrust to weight ratio, Λ_F solution, at this W_G solu-
tion is determined from Equation (34).

The solution point is plotted on a curve of $C_{L_{r_0}}$ versus W_G as discussed
in the Introduction, Section 4.1 (see Figures 30 and 34).

51

Altitude 6000 feet; ambient temperature, 95°F.;
military rated compressor tip speed, 22,000 rpm.
(From CAE Curve No. 39464)
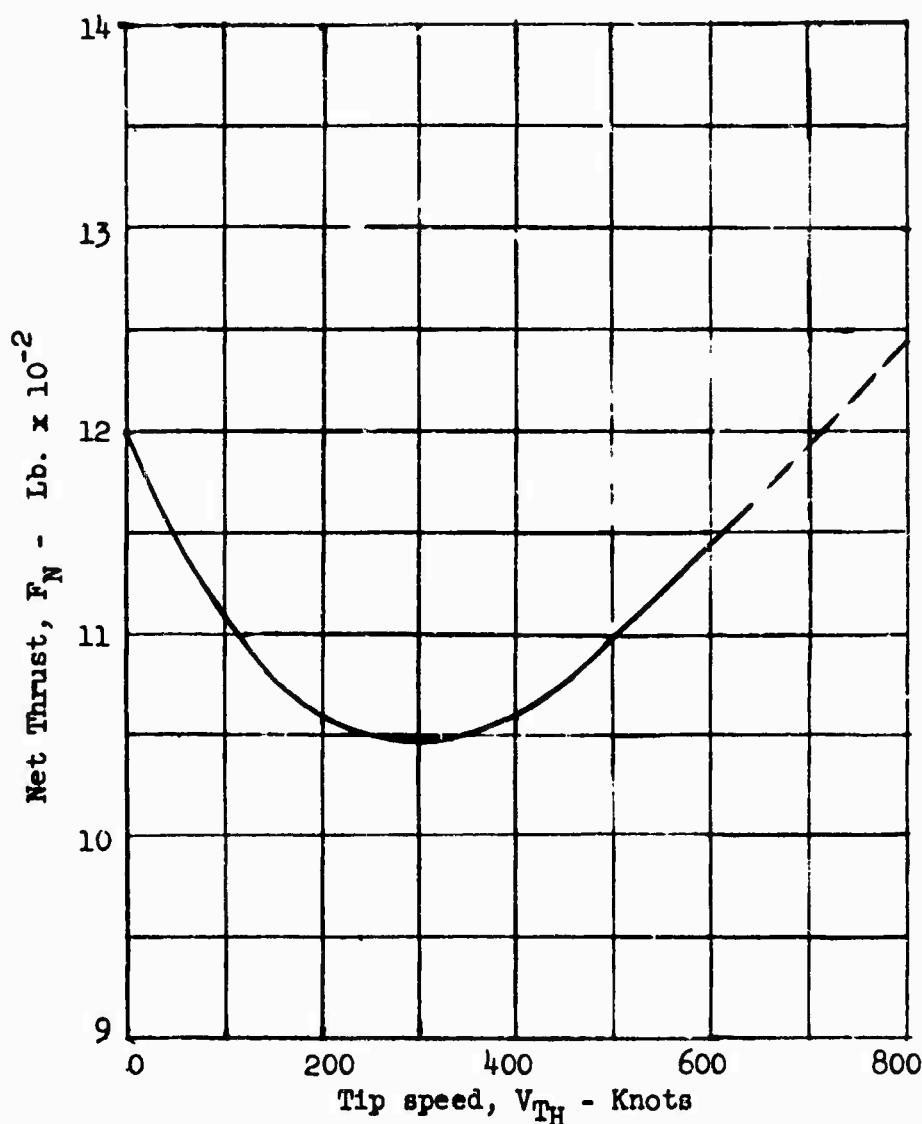
Figure 12a. Estimated Performance Characteristics.
CAE Model 357-1 Turbojet Engine.
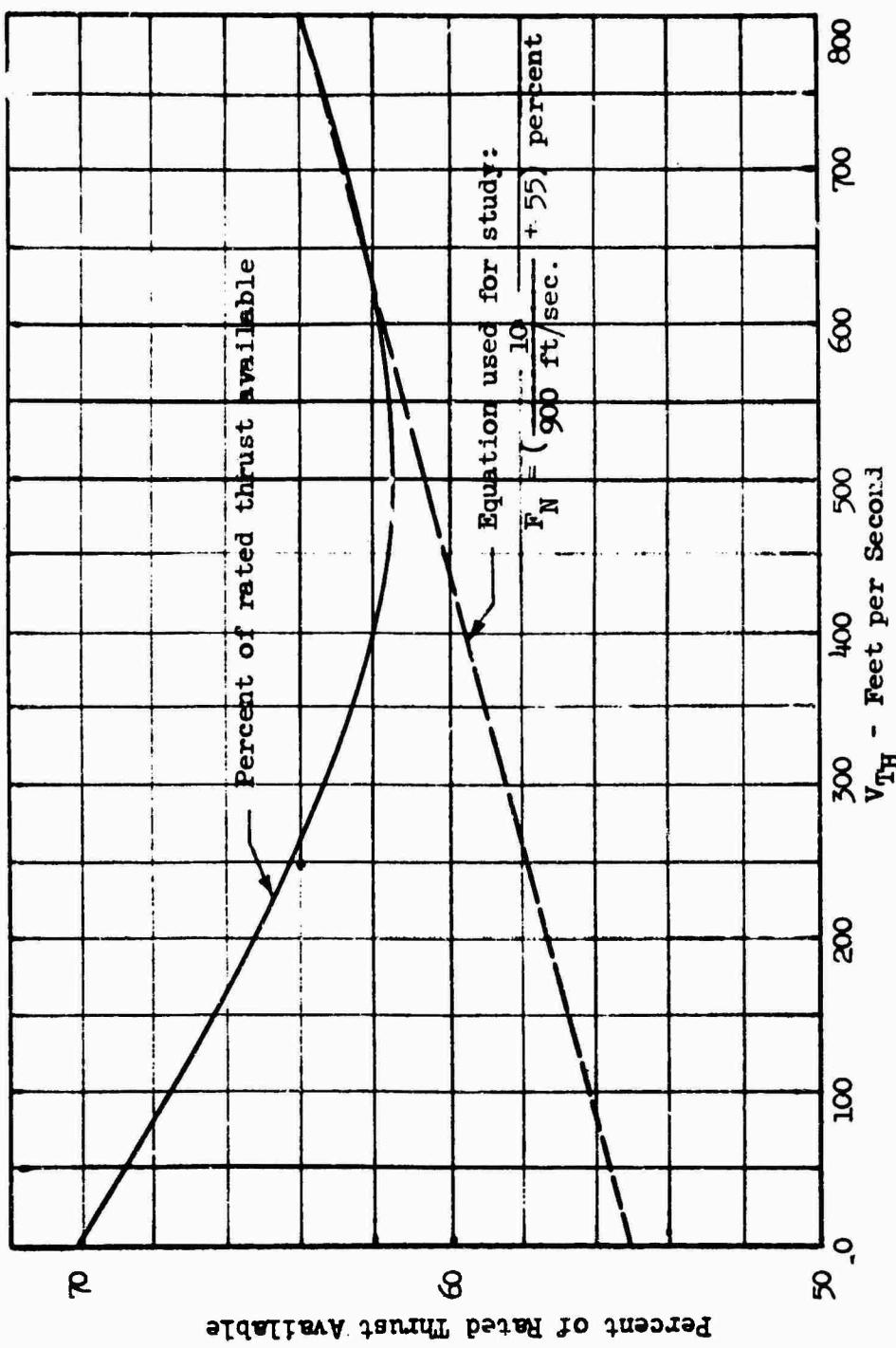
Figure 12b. Available Rated Thrust Versus Tip Speed.

The graph is labeled:
- Vertical axis: Percent of Rated Thrust Available (values 50, 80, 70)
- Horizontal axis: V_{TH} - Feet per Second (values 0, 100, 200, 300, 400, 500, 600, 700, 800)
- Curve label: Percent of rated thrust available
- Equation label: Equation used for study:

$$F_N = \left(\frac{10}{900 \text{ ft/sec.}} + 55\right) \text{ percent}$$

53
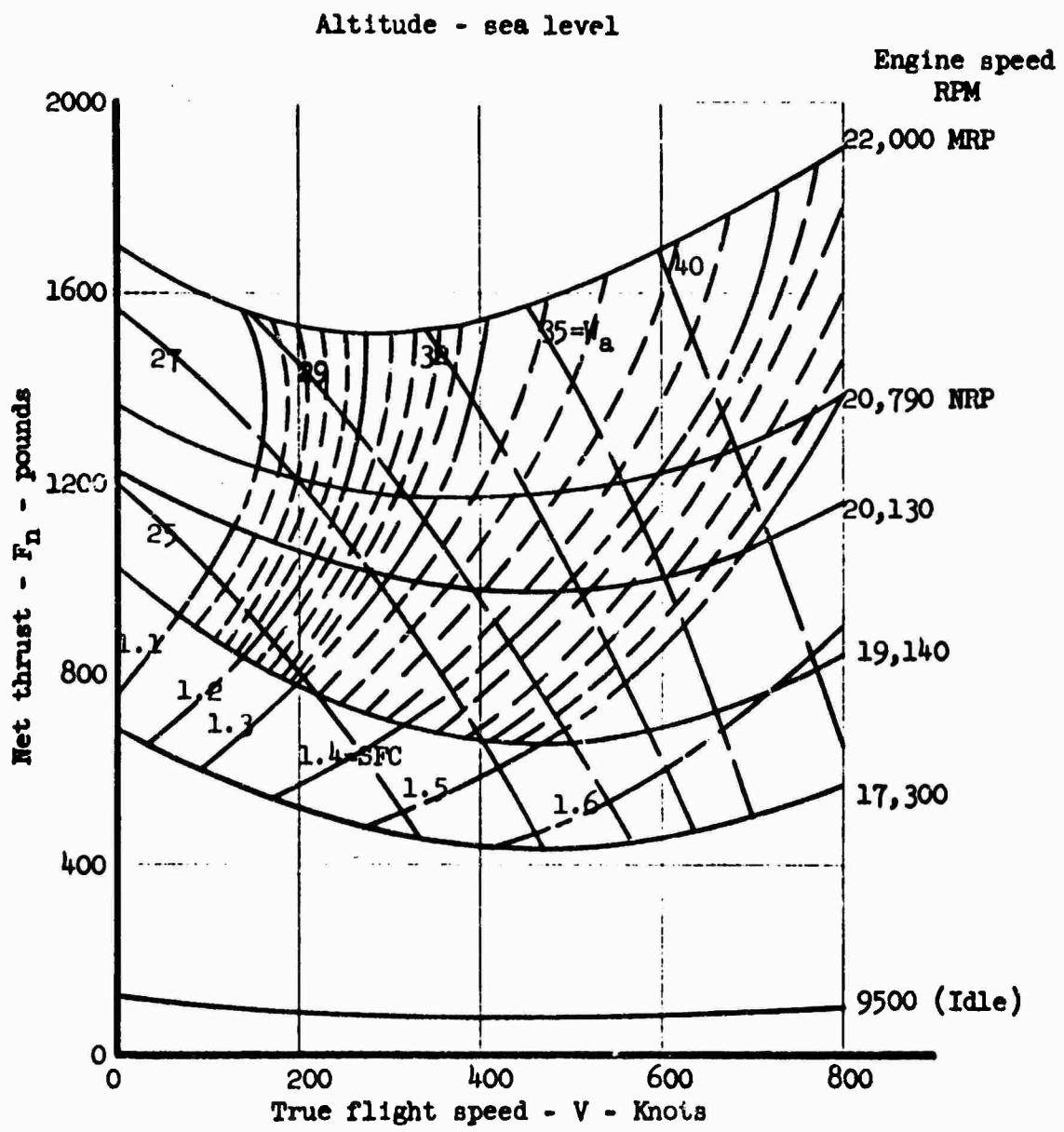
Figure 13. 357-1 Estimated Performance Net Thrust
Versus Flight Speed

54
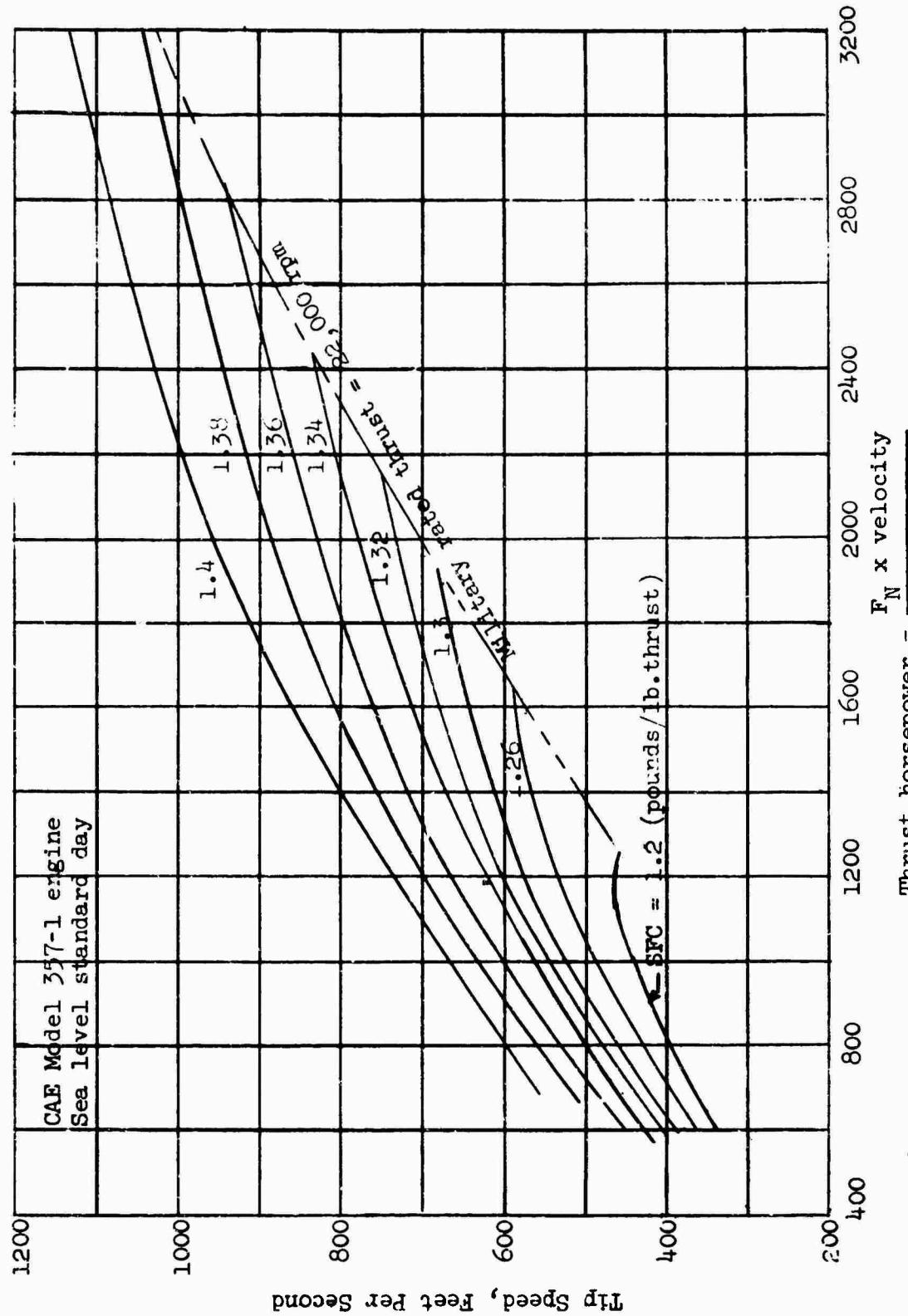
Figure 14. Engine Flight Velocity Versus Engine Thrust Horsepower.

55
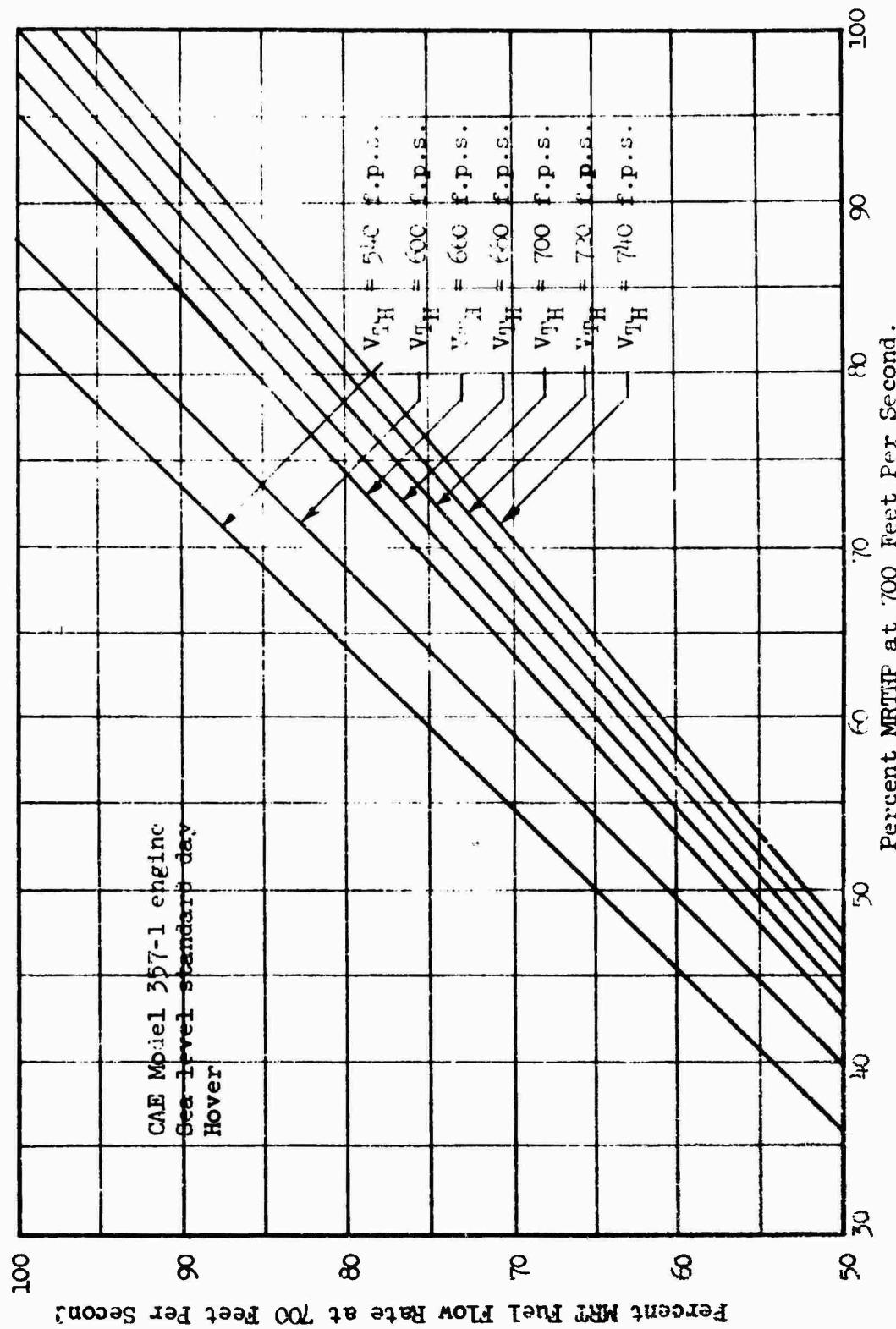
Figure 15. Fuel Flow Versus Horsepower Referred to Hover at $V_I = 700$ Feet Per Second.
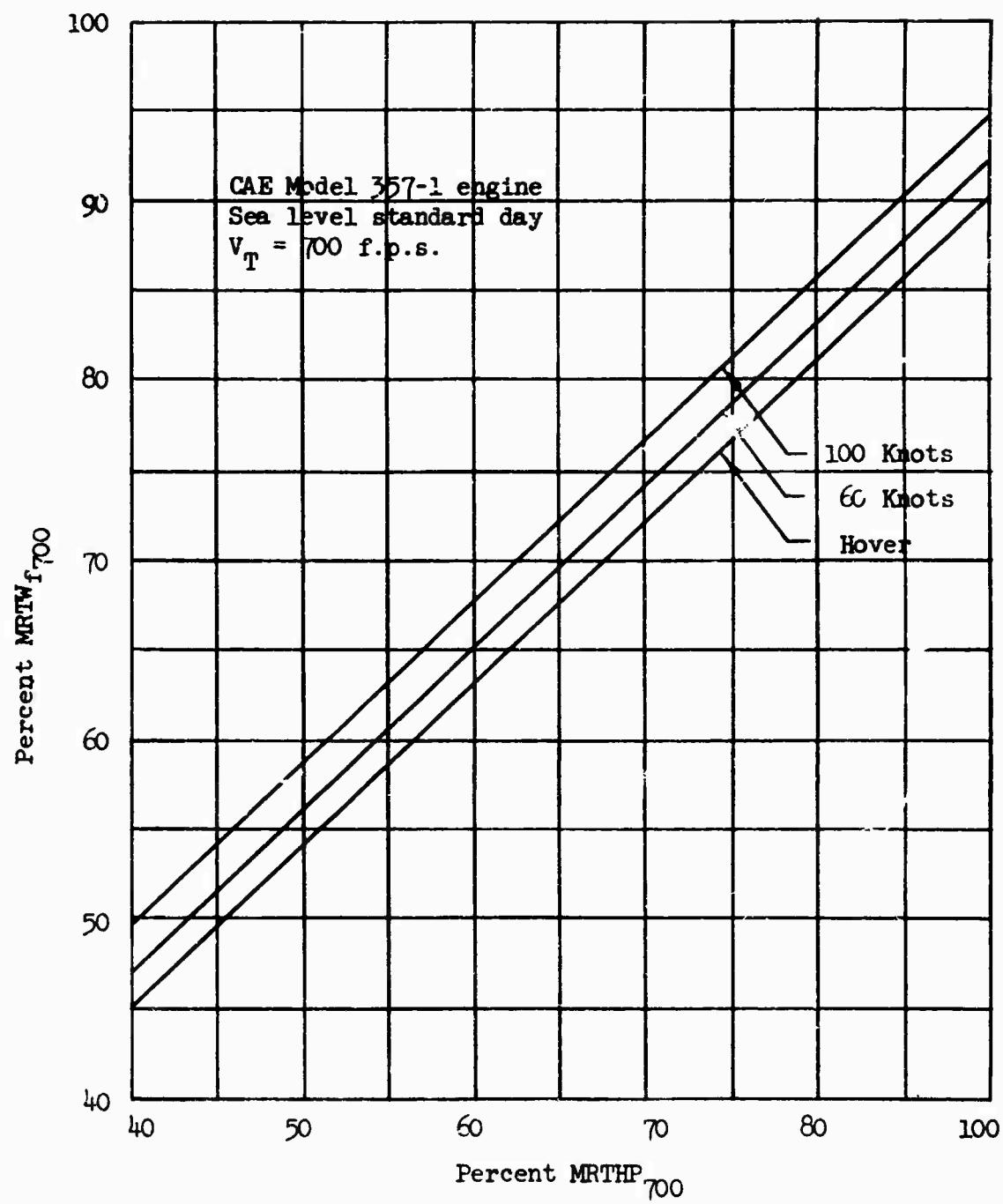
Figure 16. Fuel Flow Versus Horsepower Expressed in Percent of Hover Values.

57
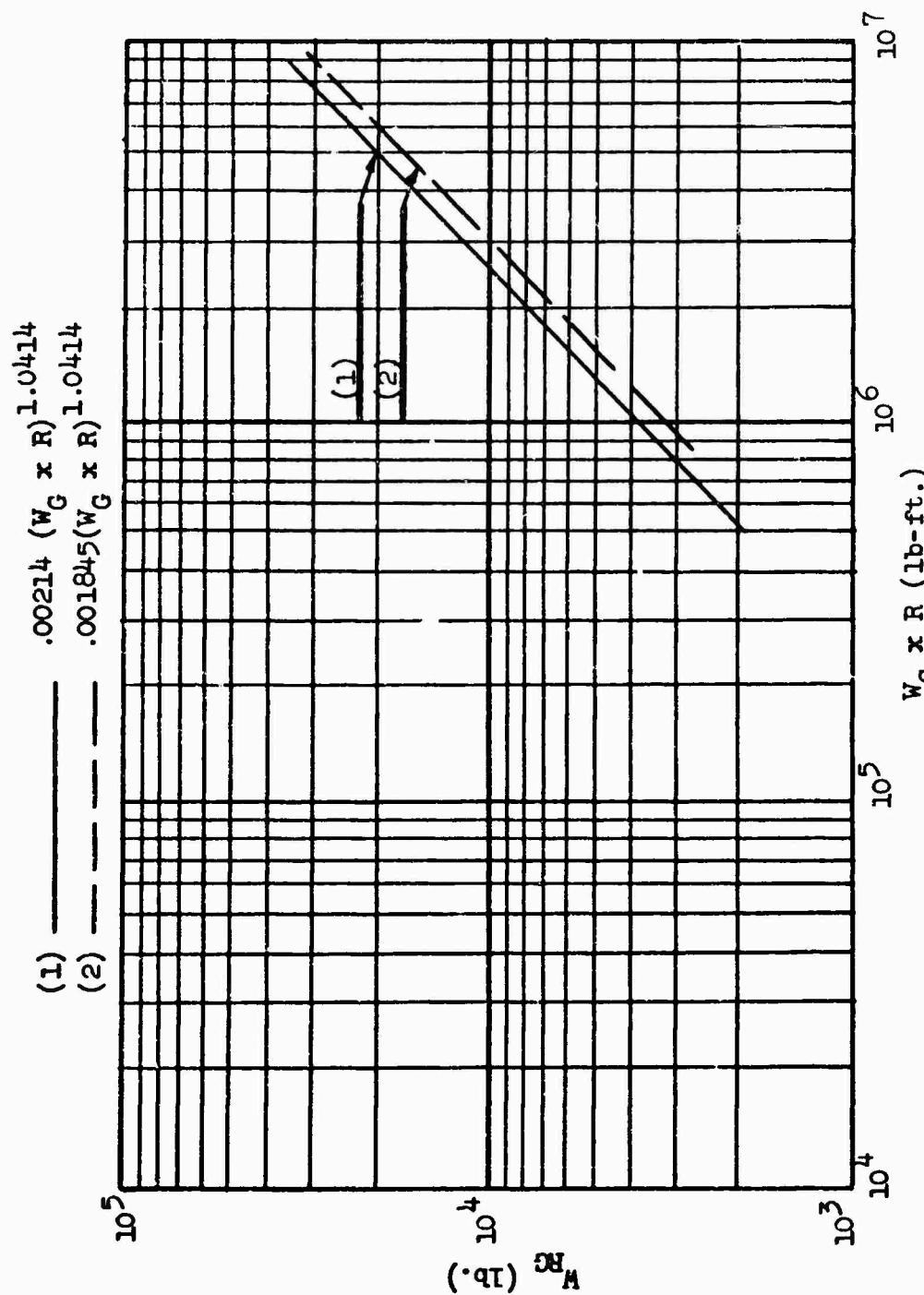
Figure 17. Rotor Group Weight Trend.

58

$$(1) \quad \text{------} \quad 1.052 \times 10^{-15}(L_F \times V_{max})^{3.523}$$
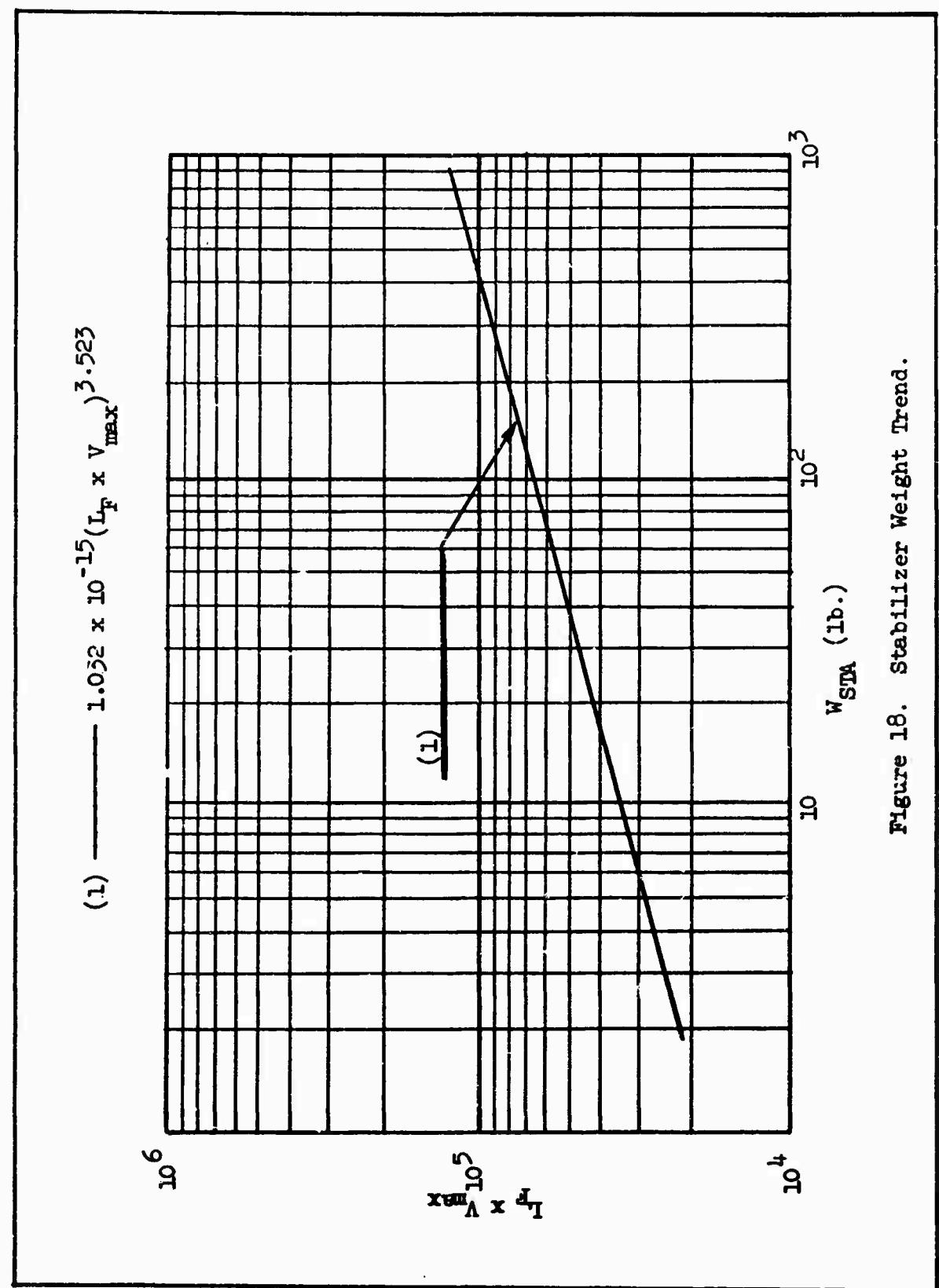
Figure 18. Stabilizer Weight Trend.

59
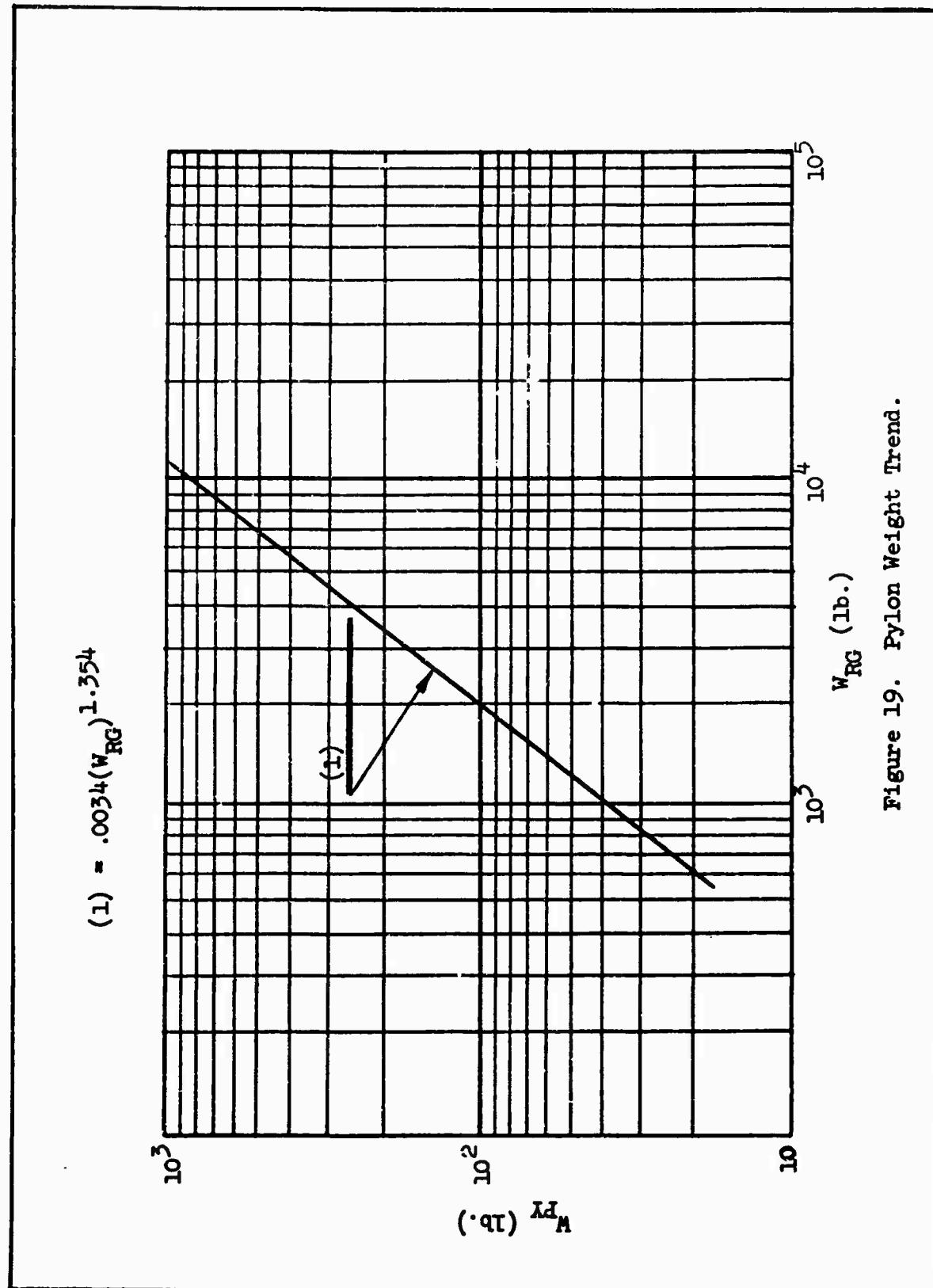
Figure 19. Pylon Weight Trend.

$$(1) = .0034(W_{RG})^{1.354}$$

W_{RG} (lb.)

W_{PY} (lb.)

60

Figure 20. Body Group Weight Trend.

$(1) = .1268(L_F \times W_G)^{.594}$

$(2) = .1071(L_F \times W_G)^{.594}$

$(3) = .0944(L_F \times W_G)^{.594}$

$(4) = .0875(L_F \times W_G)^{.594}$

W_{BG} (lb.)

$(L_F \times W_G)$ (lb-in.)

61
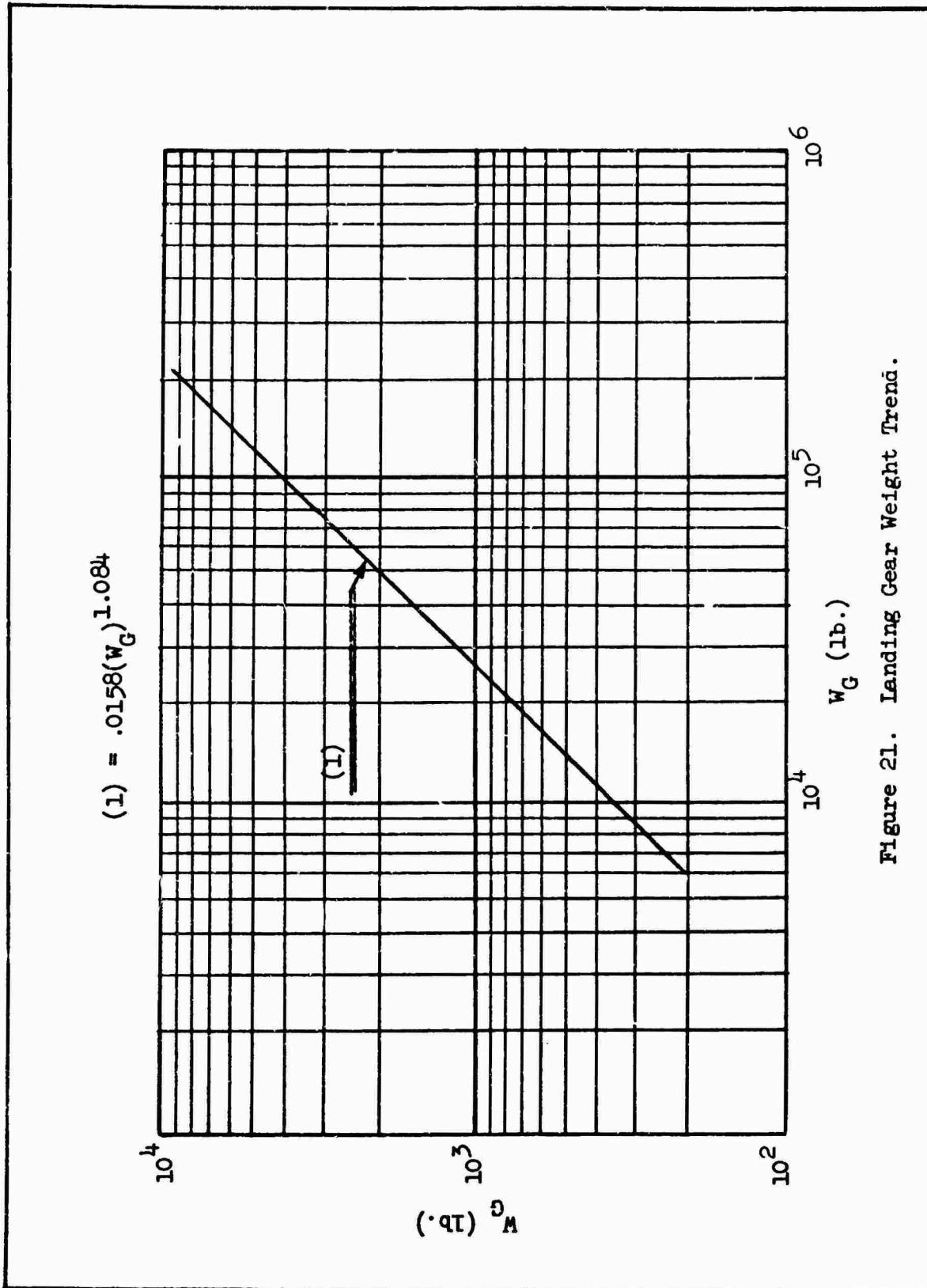
Figure 21. Landing Gear Weight Trend.

$$(1) = .0158(W_G)^{1.084}$$

W_G (lb.)

W_G (lb.)

$(1) = .1205(W_G)^{.867}$

$(2) = .0885(W_G)^{.867}$
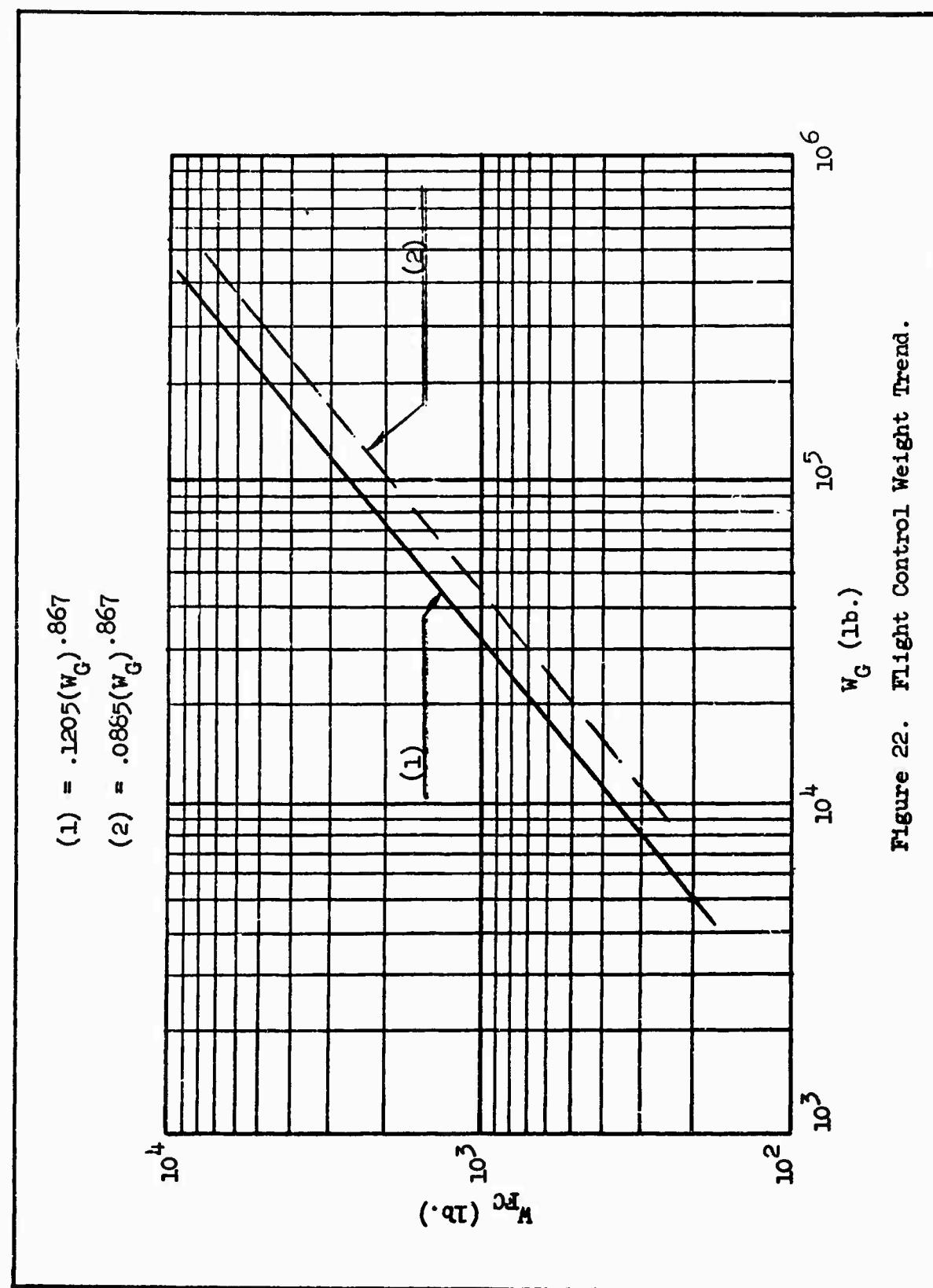
Figure 22. Flight Control Weight Trend.

63

$$(1) = 1.73b(F_R/b)^{.686}$$
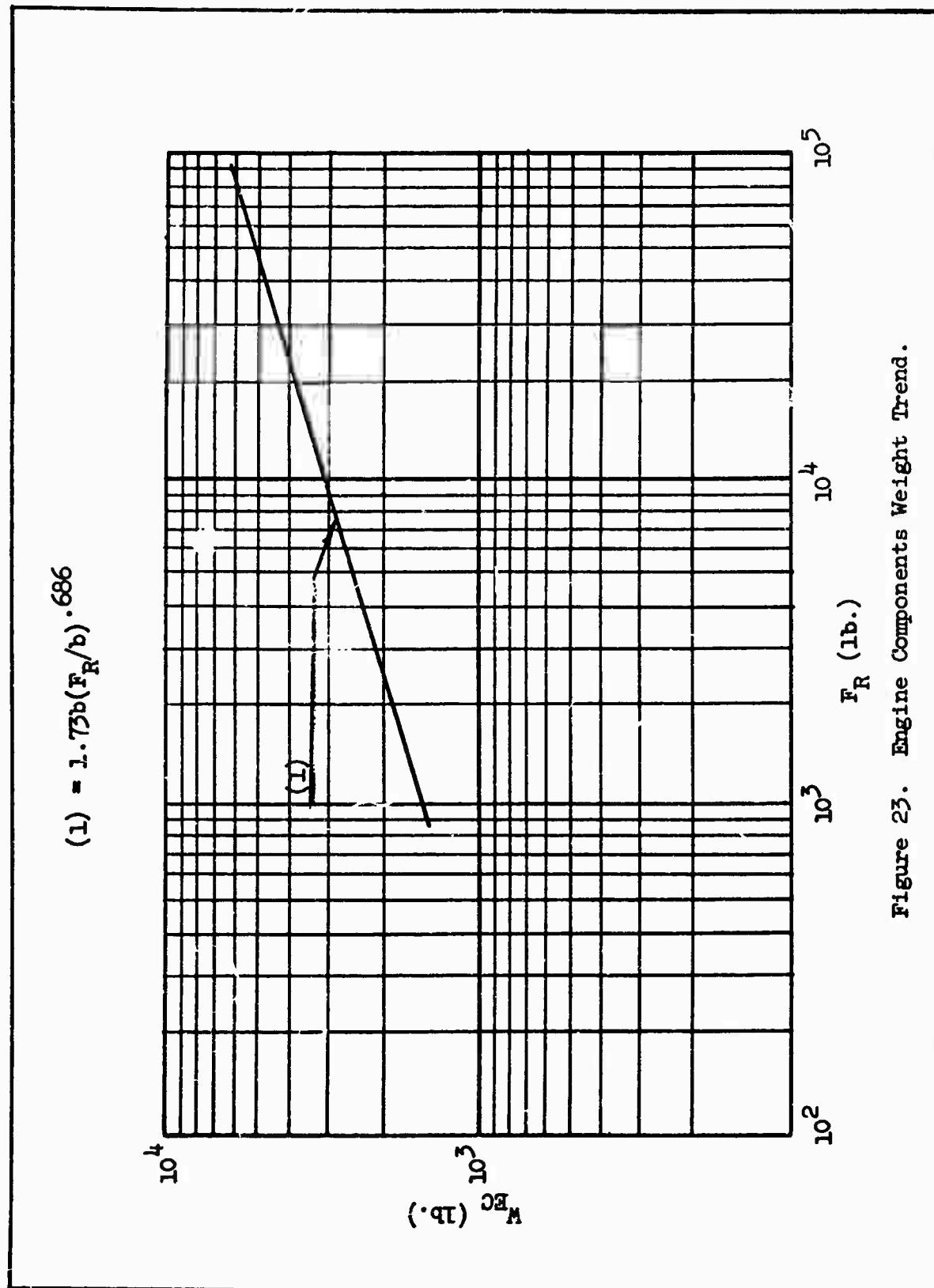
Figure 23. Engine Components Weight Trend.

Figure 24. Engine Weight Trend.

$(1) = .6309(F_R)^{.926}$

$(2) = .372(F_R)^{.926}$

F_R (lb.)

W_{ENG} (lb.)

$$(1) = .2145(W_G)^{.66}$$

W_G (lb.)

W_{FU} (lb.)
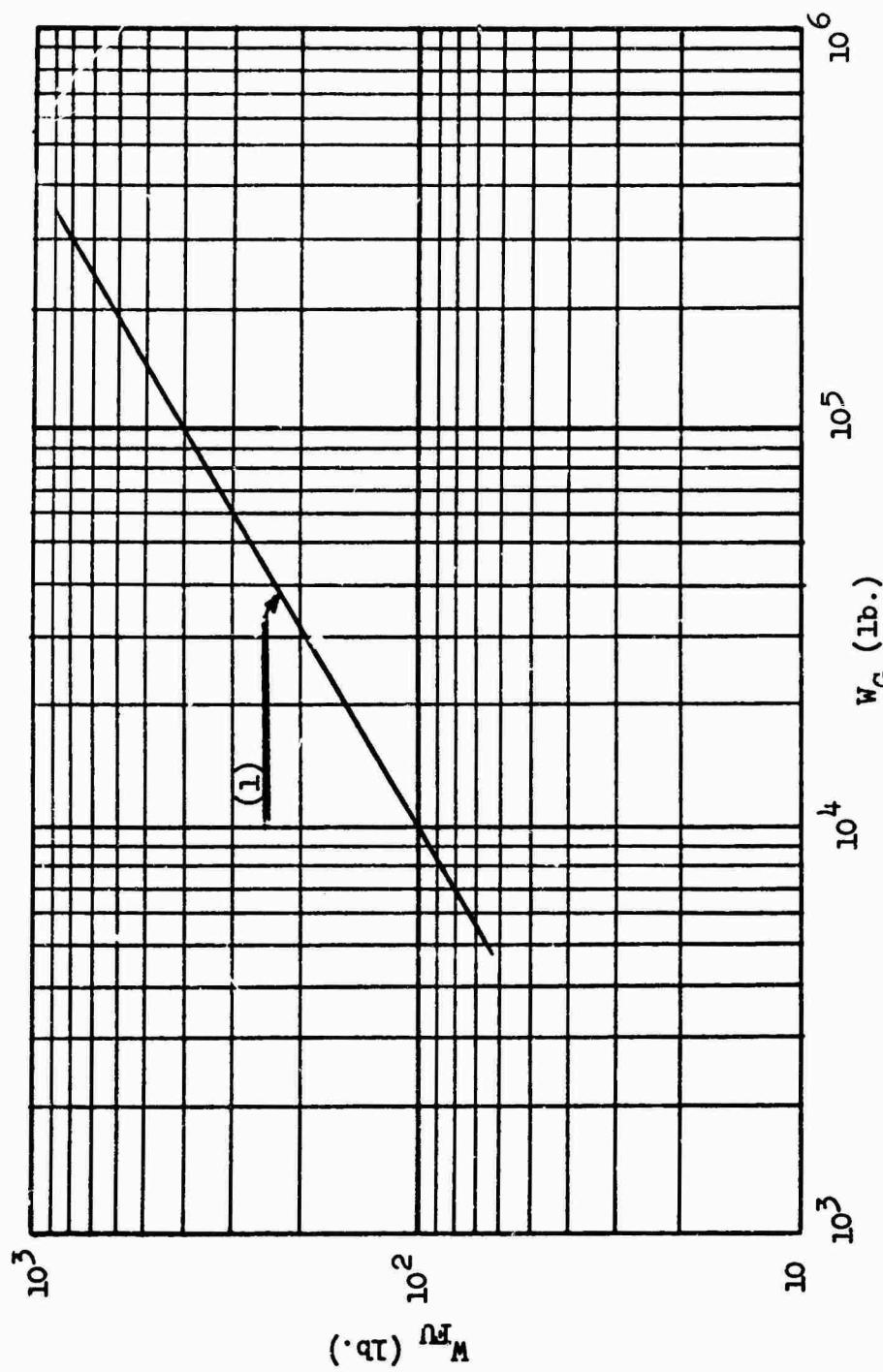
Figure 25. Furnishings Weight Trend.

Figure 26. Tail Rotor Group Weight Trend.

$(1) = .00039(W_G)^{1.234}$

W_G (lb.)

W_{TR} (lb.)

Uniform Blade Mass Distribution
Uniform Blade Stiffness Distribution
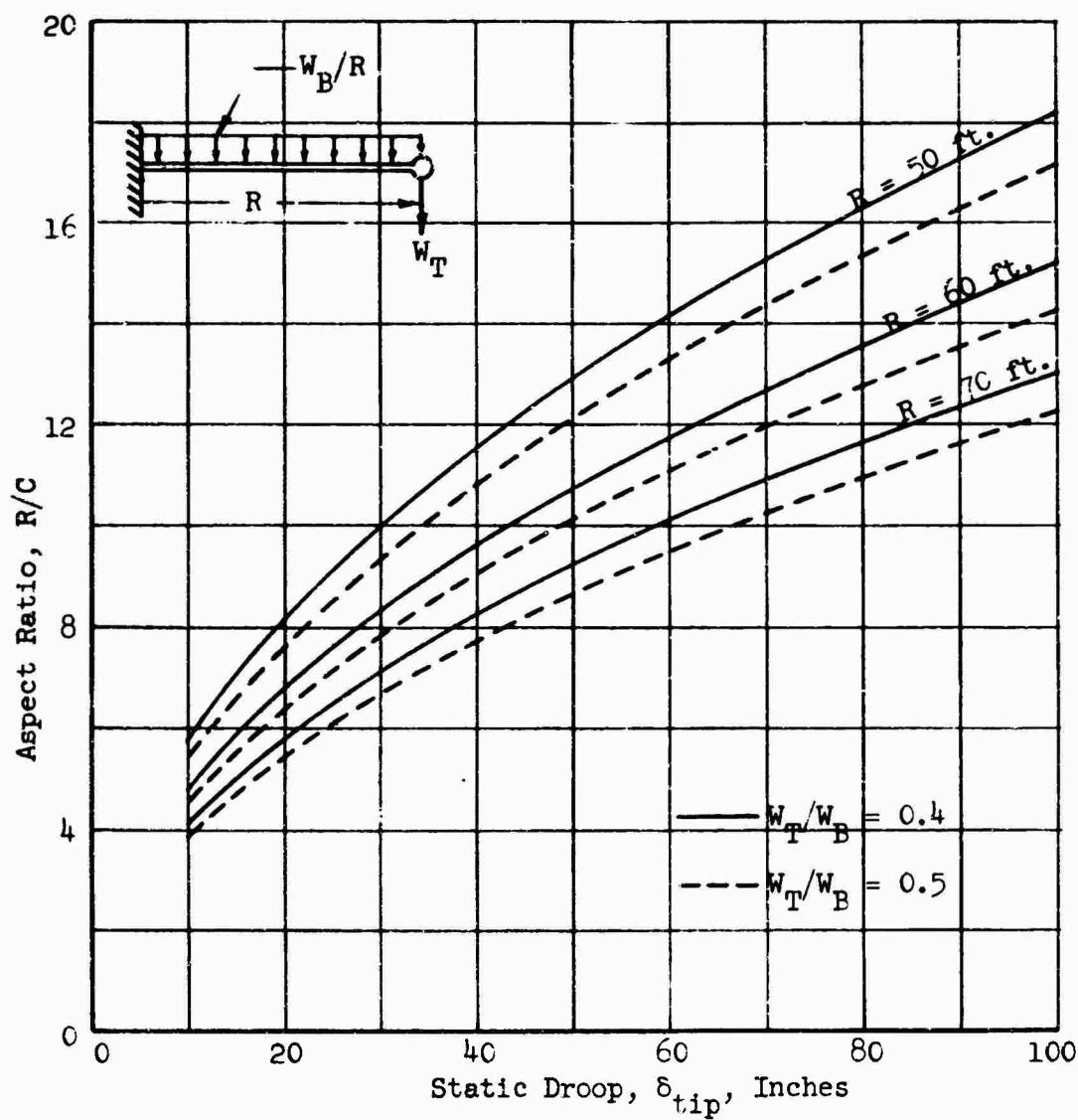
Figure 27. Allowable Blade Aspect Ratio Versus Static Droop.
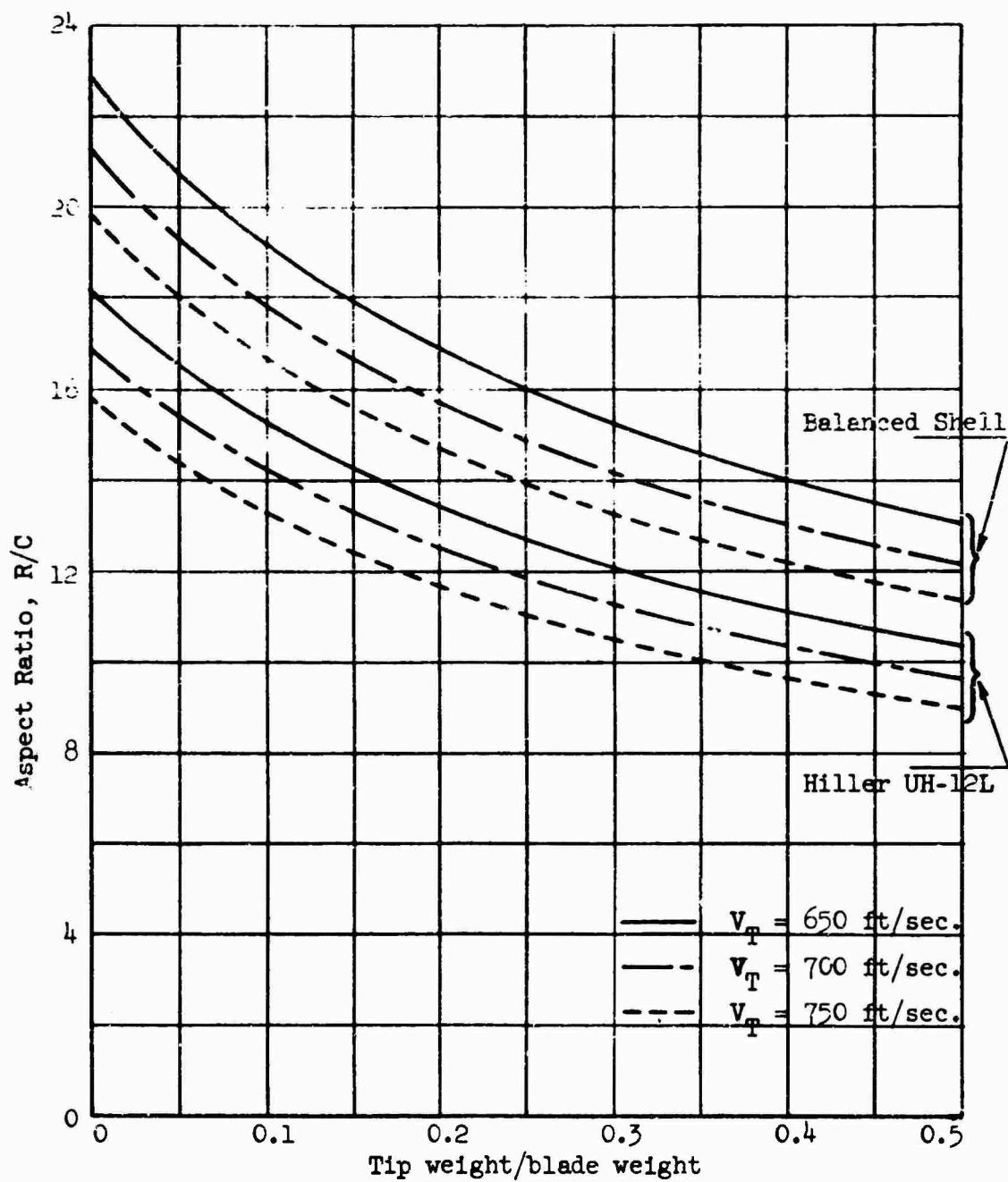
Figure 28. Allowable Blade Aspect Ratio Versus Tip Weight Ratio.
Criteria: First In-Plane Rotating Natural Frequency = 1.3Ω.

69
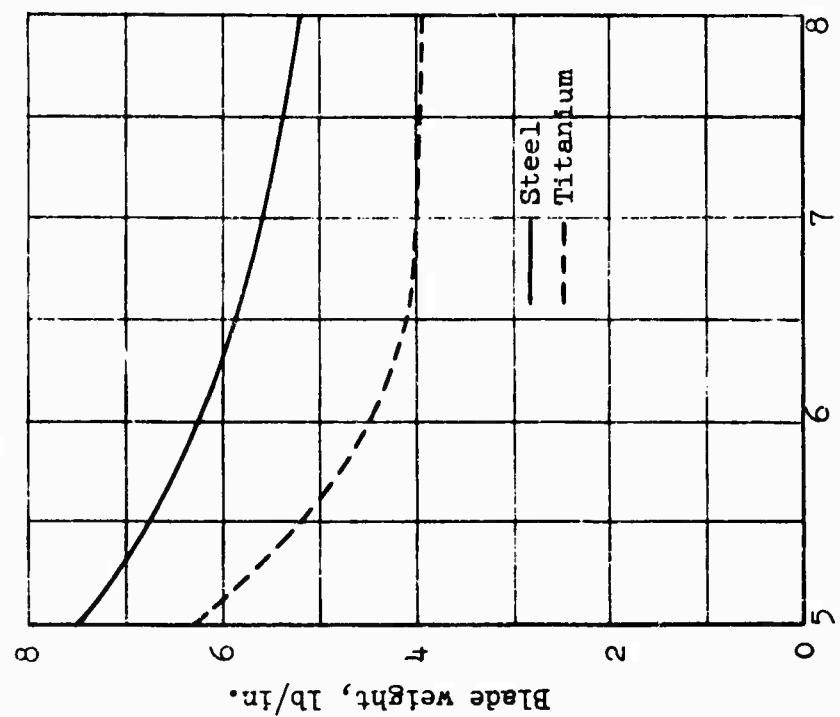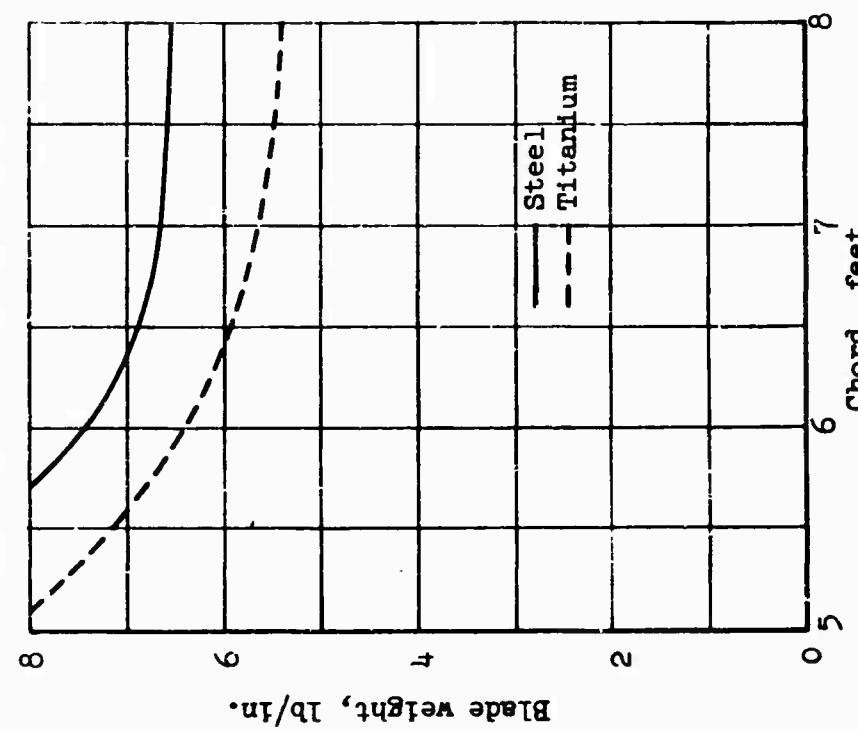
Figure 29. Rotor Blade Weight/Inch Versus Blade Chord.

4.0   COMPUTATION PROCEDURE

4.1 Generalized Engine Parametric Study

4.1.1 Outline of Method

Solution gross weights are determined for each value of n and hover tip speed using the R_u method as described in Sections 3.1 and 3.5. The fuel required at a selected value of n for a tip speed was determined at each of three gross weights by the following procedure:

a) Determine radius - Equation (18)

b) Determine solidity - Equation (27)

c) Determine $C_{L_{r_o}}$ - Equation (98)

d) Determine ℓ_F and F_R - Equation (34)

e) Determine $MRTHP_{700}$ and $MRTW_{f700}$ - Equations (44) and (45d)

f) Calculate weight of fuel for the hover at start of mission - Section 3.3.3.

g) Calculate cruise tip speed - Section 3.3.4

h) Calculate weight of fuel for each of the remaining portions of the mission and the total weight of fuel required - Section 3.3.3

The cruise tip speed is calculated as described in Section 3.3.4 for use in determining the fuel weight required at each of the three gross weights used to define the R_u functions.

The value of the design mean lift coefficient, $C_{L_{r_o}}$, and the rated thrust to gross weight ratio was calculated for each solution gross weight. After all the solution gross weights for the design variables have been calculated, these values are used to calculate points of constant thrust to weight ratio as described in Section 4.1.3.

After each solution gross weight was determined, the A_π limit, $A_{\pi_{E.L.}}$, was calculated as explained in Section 4.4, and the rotor blade limits were determined by the procedure as explained in Section 4.3.

The advancing blade rotor limits were established at 743-foot-per-second tip speed by assuming that the blade twist "ϵ" necessary for zero angle of attack of the advancing blade at the 125-mile-per-hour design maximum speed is used.

71

4.1.2 Tip Acceleration Limits

In order that all values of $C_{L_{r_o}}$ in the range specified in Section 1.1.4 are obtained within the gross weight range given in that section, it is necessary to consider the expression for n in terms of $C_{L_{r_o}}$ and W_G. By rewriting Equation (98) with (27) and (18), the following equation is obtained:

$$n = \frac{C_{L_{r_o}}(B^3)V_{T_H}^4 \, cb}{.818 \times 10^5 W_G} \tag{99}$$

Then, by appropriate substitutions of W_G and $C_{L_{r_o}}$ maximum and minimum, the maximum and minimum values of n are determined. These values are rounded in such a way that each value is an integer multiple of 25 plus 10 so that a point of 235g is obtained for each hover tip speed if 235 lies in the range.

The values of n maximum and n minimum must be determined each time the tip speed is changed.

4.1.3 Establishment of Points of Constant Rated Thrust Loading, A_F

The solution values of A_F and n were of a random nature; to obtain even integers for plotting, the computer program used a parabolic curve for interpolating to provide solutions for selected values of A_F and n. This is graphically illustrated by Figure 30.
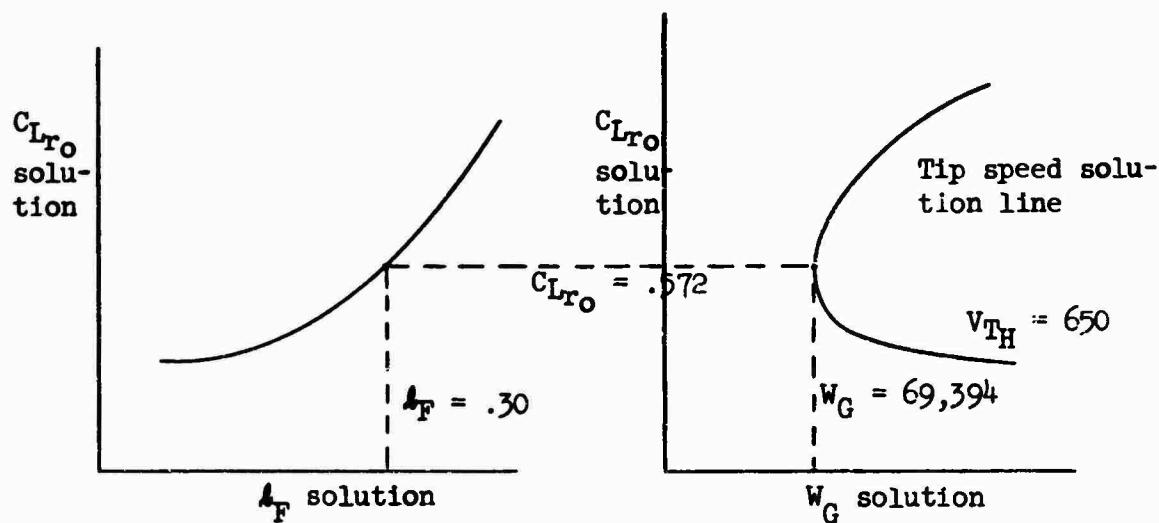

Figure 30. Solution A_F, $C_{L_{r_o}}$ and W_G Relationships.

72

Final plots are then constructed to determine the influence of design parameters upon gross weight (see Figure 32). Figures 33 and 34 are crossplots derived from Figure 32 to clearly define the relationships between tip speed, chord, and gross weight.

4.2 Method Used to Determine the Optimum Configuration for Use With the CAE 357-1 Engine

The method used to determine the design parameters and configuration for use with the CAE 357-1 engine was somewhat different from that followed for the generalized engine parametric study. The primary difference was that the rated thrust was constant for all solutions and a cutoff line was used to eliminate those solutions which did not have adequate thrust to satisfy the 6,000-foot pressure altitude, 95°F. hover requirement.

Lines of constant tip acceleration (235g) were then constructed using Equation (98) and the above values of tip speed. A tip acceleration limit line could then be plotted by connecting intersection points for each tip speed. Thus, any point on the n limit line ($C_{L_{r_o}}$ = .42, W_G = 78,850 pounds) will meet the cruise-mission requirements. Equation (98) shows that increasing the tip acceleration limit would move the n limit line to lower gross weights and vice versa.

By equating the power required to hover at 6,000 feet, 95°F. to the power available with eight (four blades with over-under engines) CAE 357-1 engines, lines of $C_{L_{r_o}}$ versus W_G were obtained for different values of hover tip speed. These lines intersect the constant tip acceleration lines previously established, and connecting the common tip speed points provides a rated thrust cutoff line. An intersection or overlapping of the n limit line and the rated thrust cutoff line provides complete mission capability with the thrust rating used to construct the rated thrust cutoff line. Figure 3 shows that the particular configuration will not meet the complete mission requirement. At the time Figure 3 was constructed, the rotor group weight equation which had been used in the parametric analysis was under suspicion, and preliminary layout work indicated an increase in rotor group weight would be required. Figure 3 was therefore constructed using a large increase in rotor group weight to determine the effect on the choice of design variables. Rotor group weight was found to have little effect on the choice of design variables which confirmed the validity of the parametric study. The 5-percent increase in rotor group weight determined to be required from detailed design layout studies was found to be within the excess thrust capability of the configuration used in Figure 3 when Equation (73) was used for rotor group weight.

Increasing the blade chord to 6.5 feet was found to decrease the rotor weight by 1,200 pounds; the increase in chord increased power required, thereby decreasing thrust at 6,000 feet, 95°F. and increasing fuel flow.

The net effect is a 600-pound decrease in weight. The configuration selected for the Model 1108 is one with a chord of 6.5 feet, a hover tip speed of 650 feet per second, a rotor radius of 55.83 feet, four blades, and two CAE 357-1 engines, one placed above the other at each blade tip.

The Model 1108 was then checked for mission compliance. The fuel required for the mission was computed using the method outlined in Section 3.3.3 with the design parameters stated in the previous paragraph. The empty weight was computed using the design layout rotor group weight; other weights were determined from the equations in Sections 3.4.1 and the then current status of the fixed weight items.

4.3 Aerodynamic Rotor Limitations

The solutions obtained in this study have been checked for rotor limitations at 125 miles per hour design maximum speed. Limitations applied are as follows:

a) Retreating blade stall at $\alpha = 12^{\circ}$.

b) The retreating blade drag divergent Mach number versus angle of attack is a straight line ($M_D = .9 - .0346\alpha$).

c) Advancing blade tip Mach number = .829.

Condition c) is based on the assumption that the blade is twisted to provide zero angle of attack on the advancing blade at the design maximum speed.

A tip speed of 743 feet per second for sea level standard conditions is obtained from Equation (57).

The retreating blade limits, conditions a) and b), are determined for a selected configuration at each of three gross weights by using a set of three values of $C_{L_{r_O}}$ separated by .10 in the equations of Section 3.3.5. The set is incremented by .10 until at least one of the limit conditions are exceeded; parabolic expressions are fitted, and the intersection with the limit is determined as in Figure (31). The intersection points at each of the three gross weights are used to plot limit lines.

Two values for blade twist ϵ were used, -10° and -16°. The limiting values of $C_{L_{r_O}}$ for $\epsilon = -10^{\circ}$ were less than .50 $C_{L_{r_O}}$ at retreating blade stall and in some cases for retreating blade drag divergence. The values of $C_{L_{r_O}}$ for drag divergence and stall were greater than .5 for $\epsilon = -16^{\circ}$. Since $C_{L_{r_O}} = .5$ was set as the maximum allowable, retreating blade conditions are not a factor in determining any of the optimum solutions.
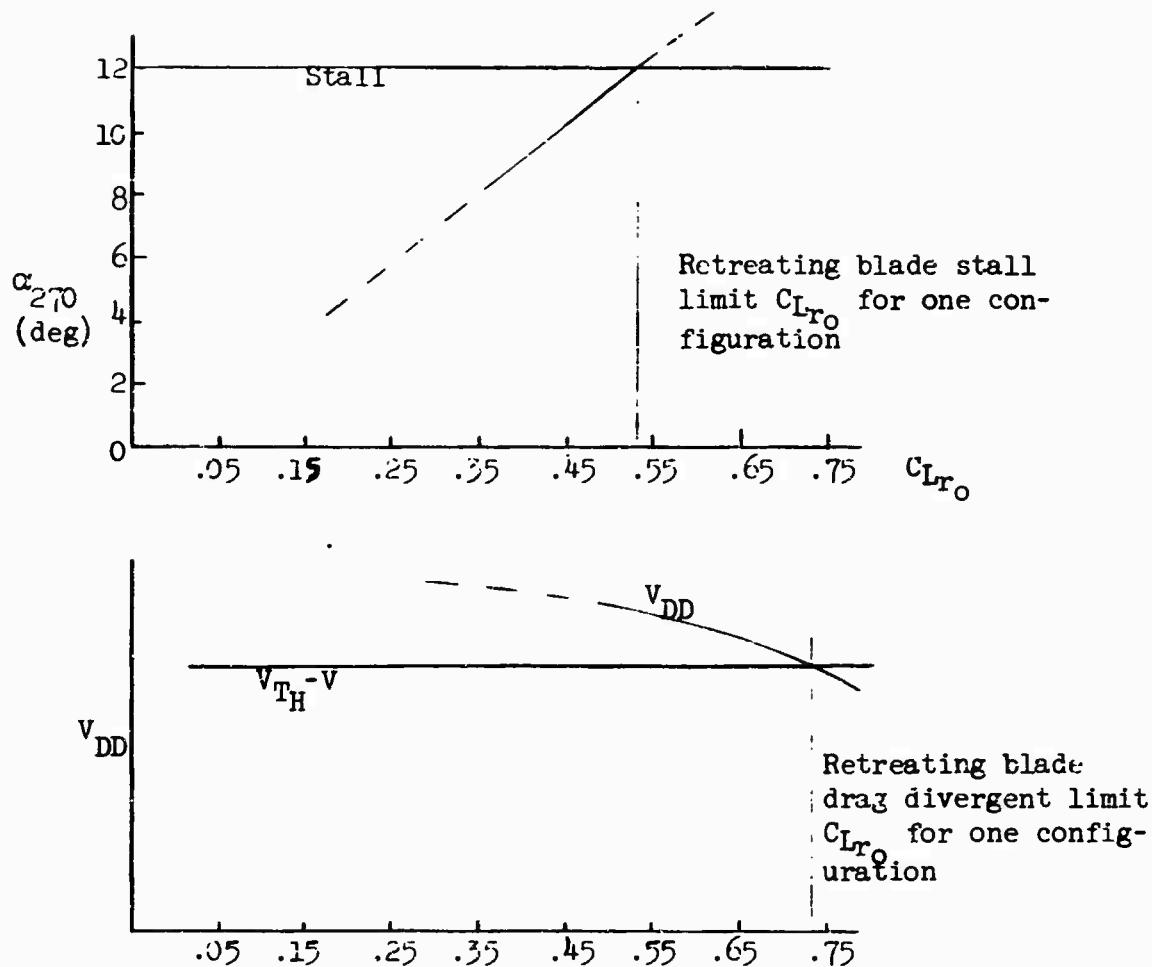
Figure 31. Typical Retreating Blade Limit $C_{L_{r_0}}$ Relationships.

4.4 Power Limits

The power limit for each configuration in the main parametric study is determined by solving for a limiting value of $A_{\pi_{E.L.}}$ using the military rated thrust.

$$A_{\pi_{E.L.}} = \frac{\eta MRTHPv_{T_H} - (ihpv_{max} + Rhpv_{max} + F.L.)550}{\frac{1}{2} \rho_0 \, v_{max}^3 \, \frac{\rho}{\rho_0} \, (1.467)^3} \tag{100}$$

where

$$MRTHP_{v_{T_H}} = MRTHP_{700} \left[\left[1 + (v_{T_H} - 700) \frac{2}{1,560} \right] - \frac{1.055 \, v_{max}^2 (1.467)^2}{2(700)1,560} \right] \frac{v_{T_H}}{700} \tag{101}$$

Solutions will be valid if the value of $A_{\pi_{E.L.}}$ is larger than A_{π}. The study shows that there are no solutions which are power limited at sea level because of the large amount of power available as a result of the 6,000-foot, 95°F. hover requirement.

75
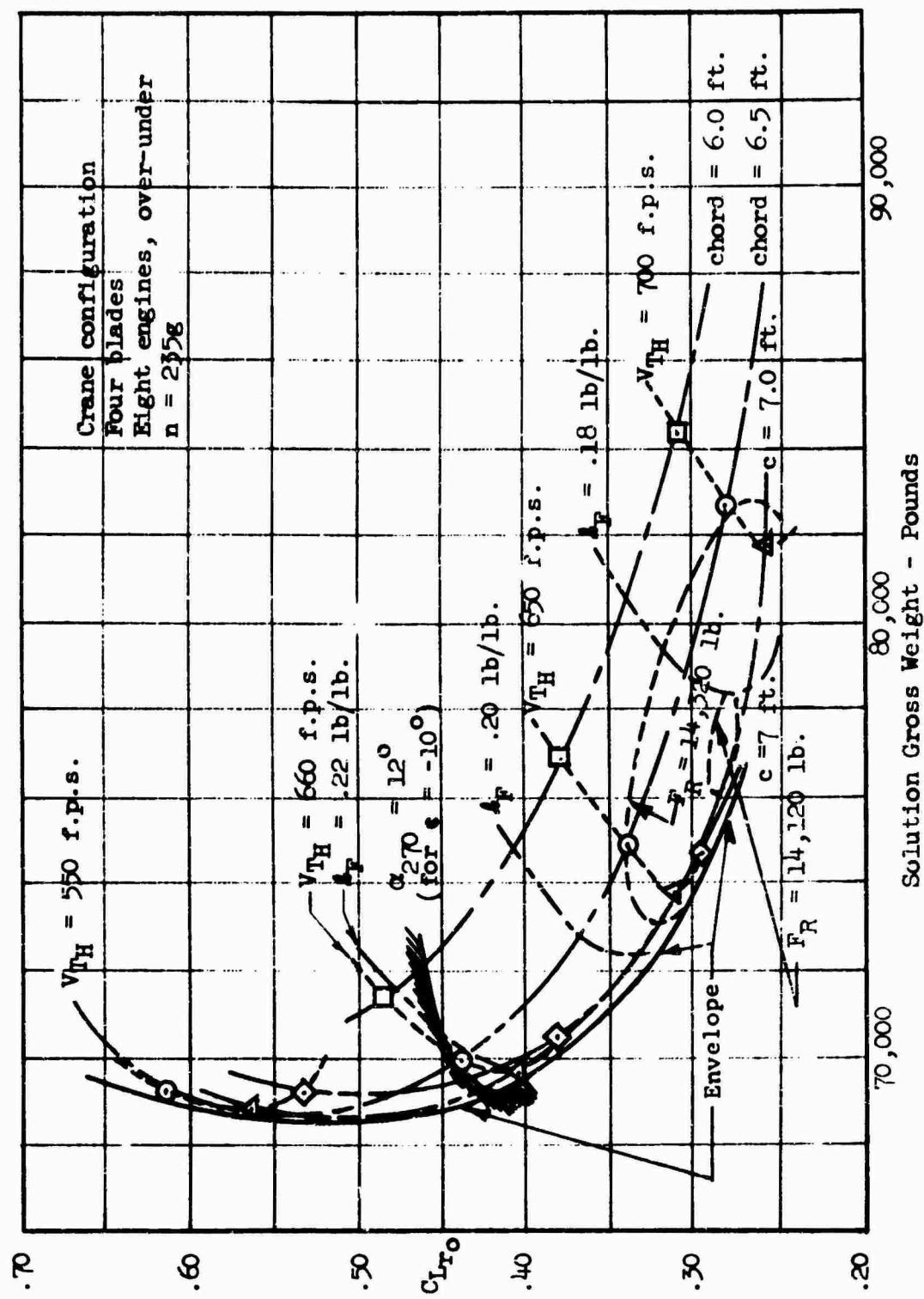
Figure 32. Typical Constant Load Factor Overlay Plot Used in
Generalized Engine Parametric Study.
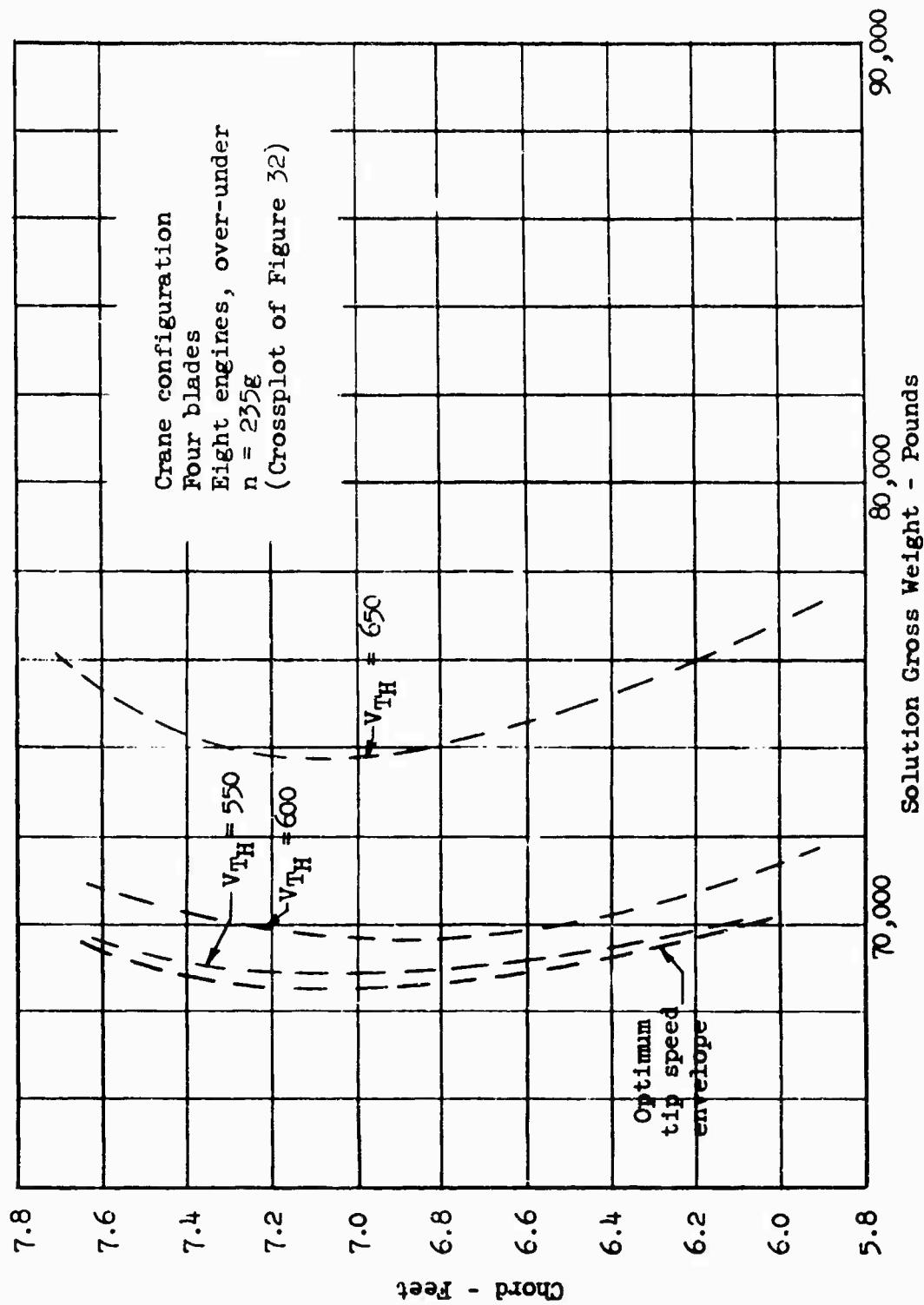
Figure 33. Typical Chord Versus Solution Gross Weight.

77
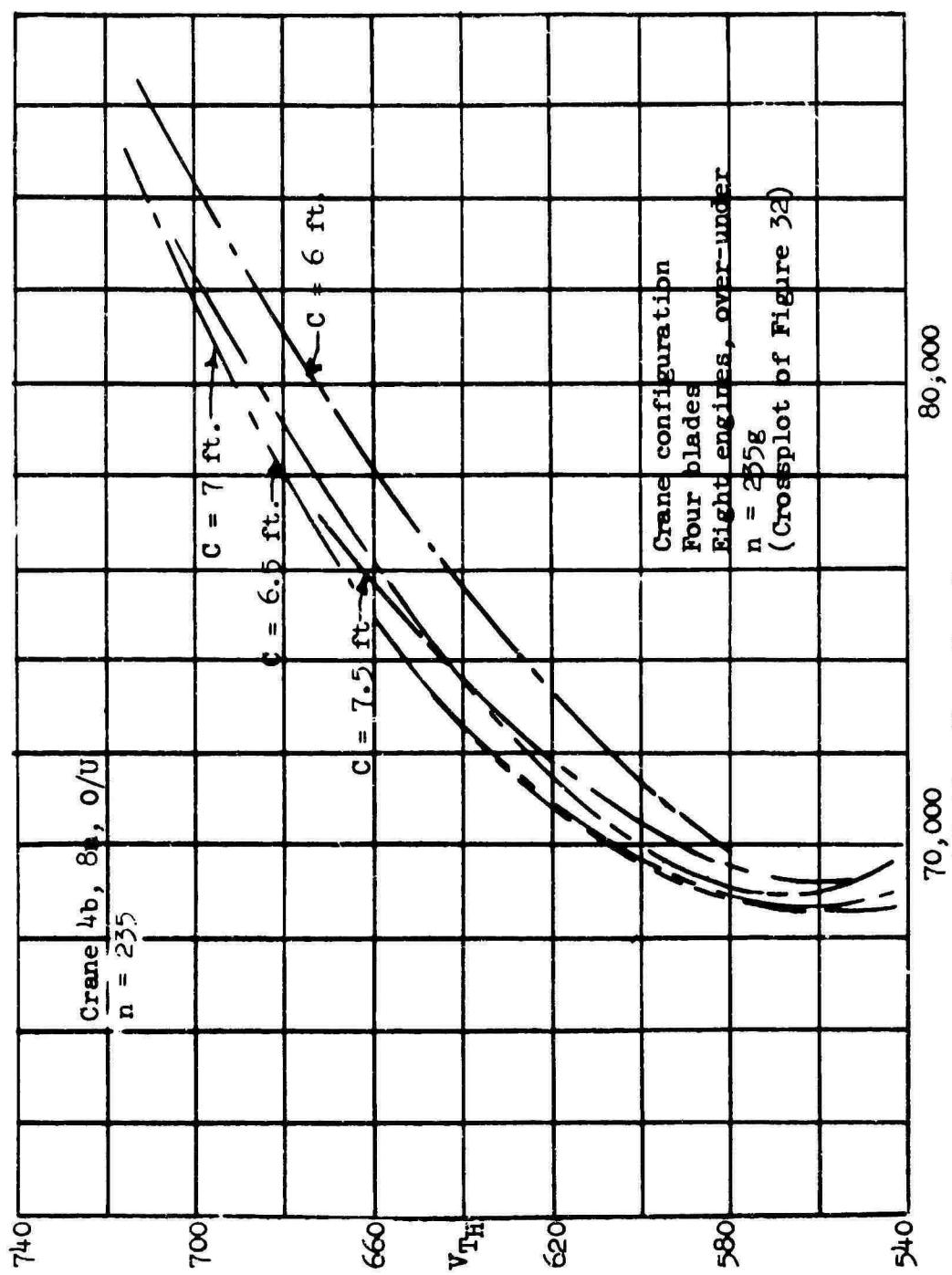
Figure 34. Typical Hover Tip Speed Versus Solution Gross Weight.
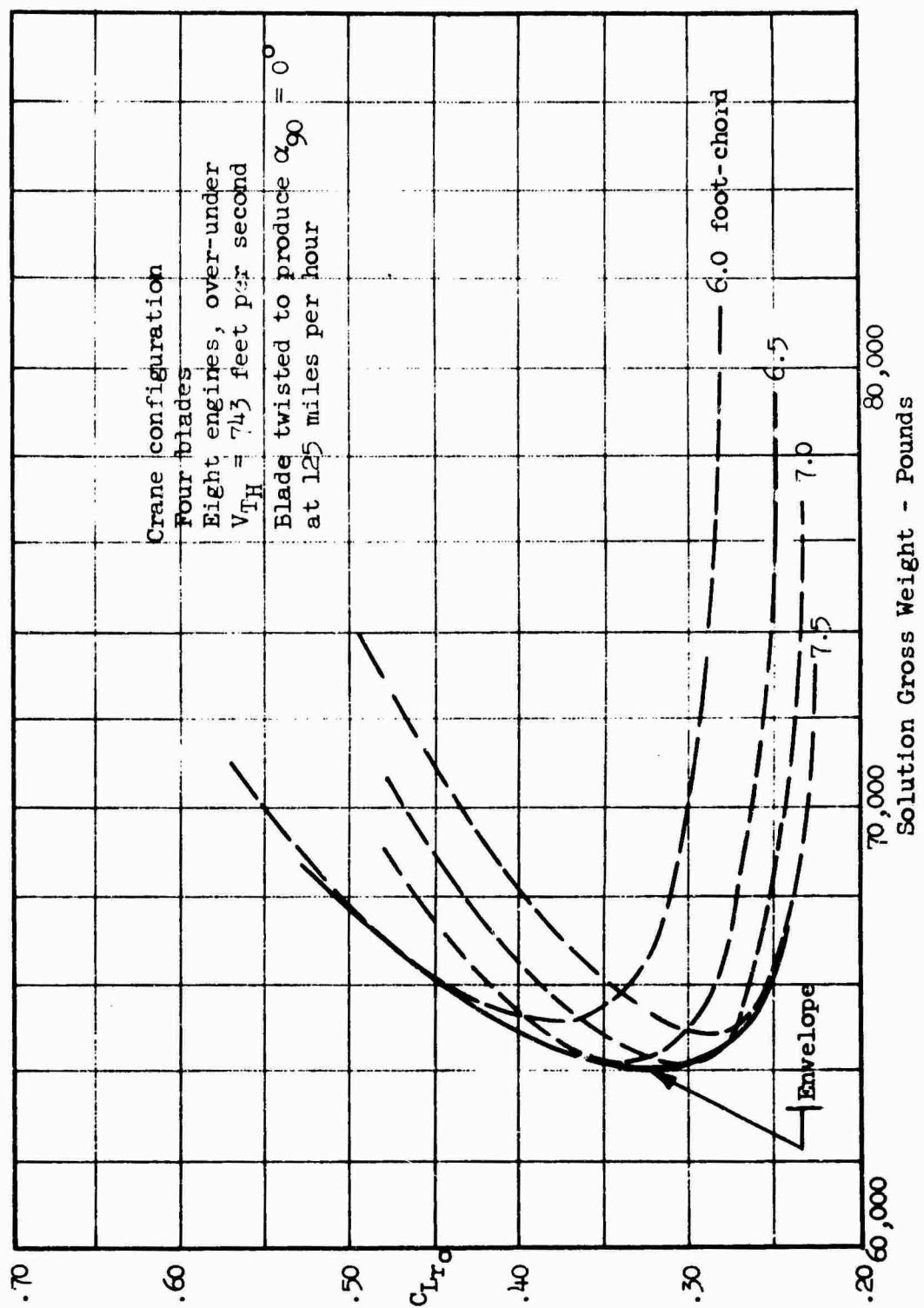
Figure 35. Typical Advancing Blade Drag Divergence Limited Design Mean Lift Coefficient, C_{Lr_o}, Versus Gross Weight.

79
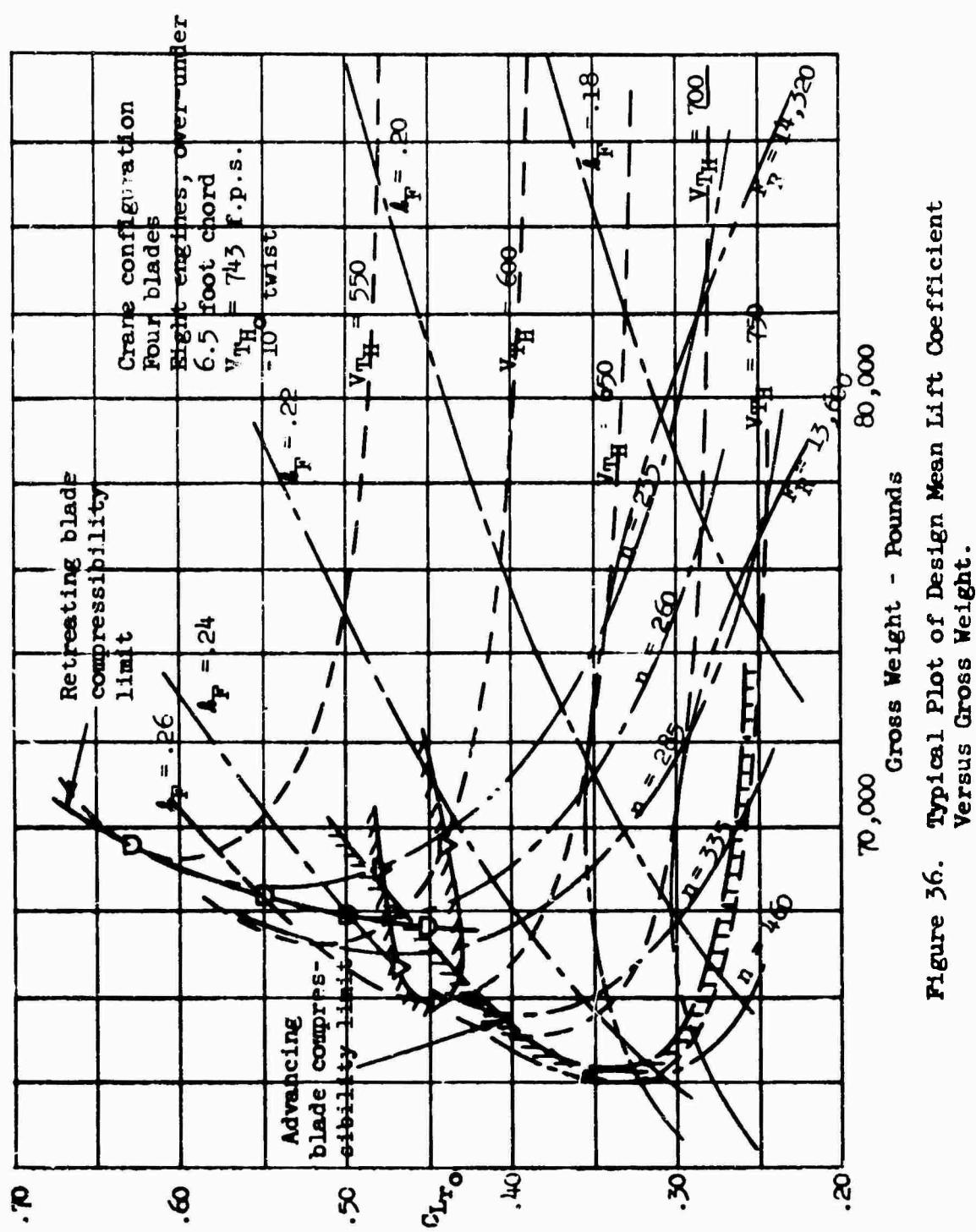
Figure 36. Typical Plot of Design Mean Lift Coefficient Versus Gross Weight.
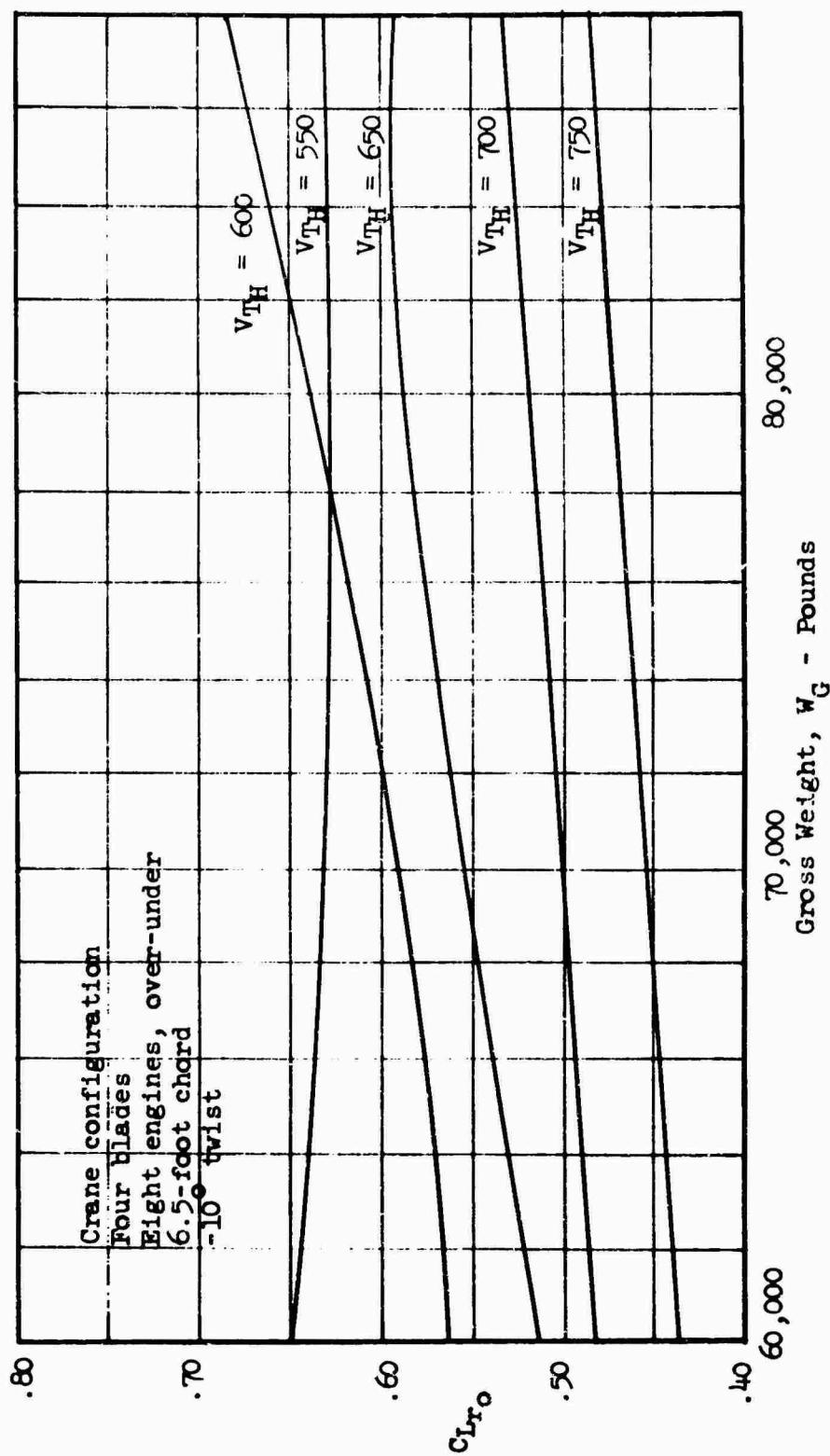
Figure 37. Typical Retreating Blade Drag Divergence Limited $C_{L_{ro}}$ Versus Gross Weight.
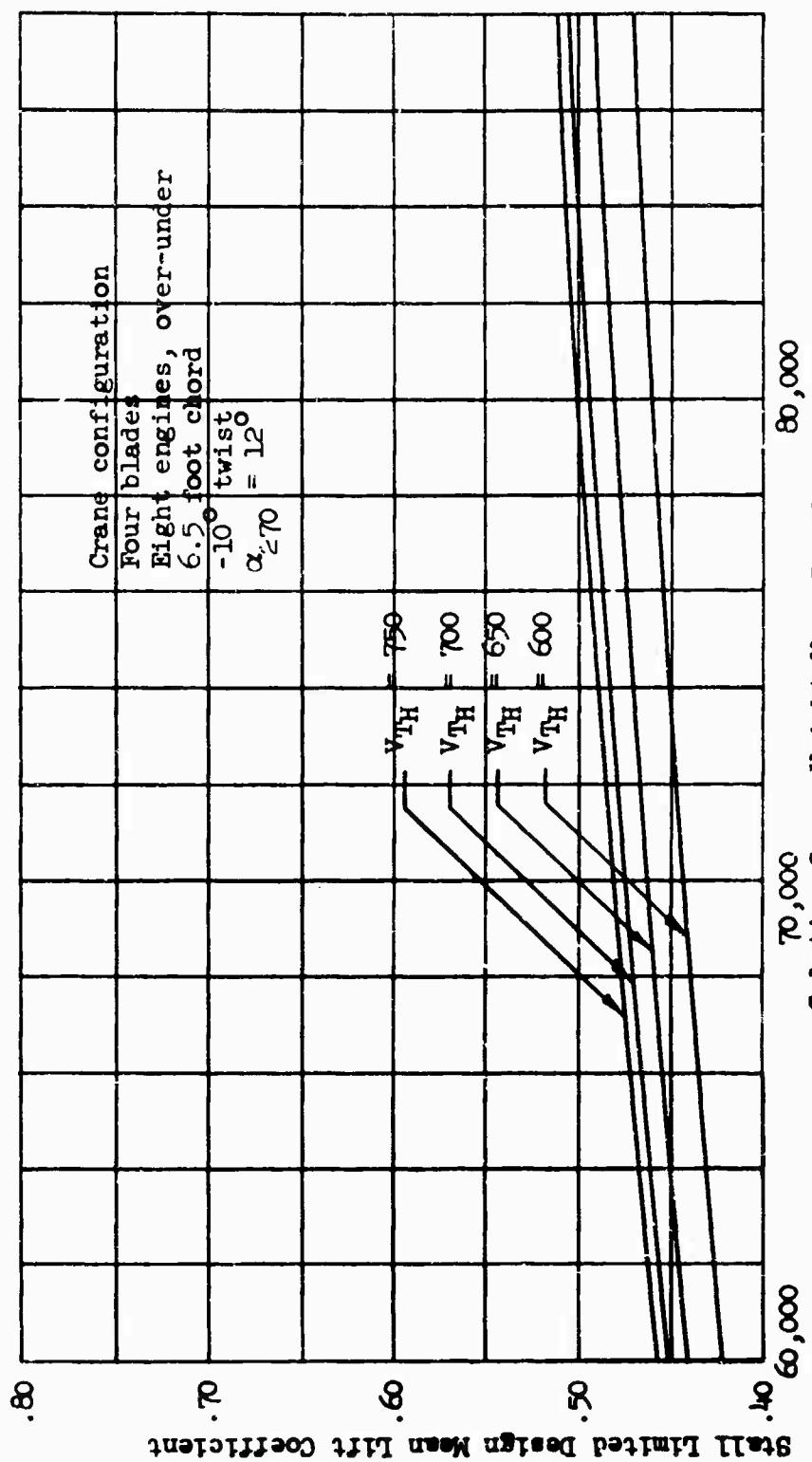
Figure 38. Typical Retreating Blade Stall Limited Design Mean Lift Coefficient Versus Gross Weight.

n	LF	CLRO	WG	APEL	RR
160.0	.16082	.32794	105837.3	626.50	82.01
185.0	.17097	.32579	90936.1	570.22	70.92
210.0	.18112	.32936	80987.3	539.96	62.48
235.0	.19182	.34072	74869.0	535.87	55.83
260.0	.20290	.35634	70771.6	544.38	50.47
285.0	.21465	.37671	68255.0	565.06	46.04
310.0	.22711	.40096	66789.4	594.41	42.33
335.0	.24026	.42838	66031.9	630.02	39.17
360.0	.25446	.46039	66037.6	674.66	36.45
385.0	.26988	.49735	66706.8	728.60	34.08
410.0	.28677	.54014	68028.3	793.26	32.00
435.0	.30552	.59010	70049.8	871.14	30.16

LF	CLRO	WG
.14000	.35021	151922.7
.16000	.32836	107257.0
.18000	.32868	81843.2
.20000	.35187	71623.5
.22000	.38679	67474.3
.24000	.42782	66039.1
.26000	.47340	66198.6
.28000	.52270	67424.6
.30000	.57513	69394.2
.32000	.63052	72012.3

Legend: n   - Centrifugal force field at tip.

LF   - A_T solution - Total engine rated thrust to weight ratio at solution point.

CLRO - $C_{L_{ro}}$ solution - Design mean lift coefficient at solution point.

WG   - W_G solution.

APEL - $A_{\pi E.L.}$ - A_π engine limit.

RR   - R - Rotor radius.

Figure 39. Typical Computer Output Data - Model 1108.

# 5.0 REFERENCES

1. Yntema, R. T., "Simplified Procedures and Charts for the Rapid
    Estimation of Bending Frequencies of Rotating Beams," NACA TN
    3459, June 1955.

2. "A Design Study of Helicopters Powered by Rotor Tip-Mounted Turbo-
    jet Engines," Hiller Aircraft Company Engineering Report No. 58-139,
    Appendix C, Figure C11, page C.25, Palo Alto, California, October
    1958.

6.0 APPENDIX

6.1 K_{μ_N} Derivation

6.1.1 Tangential Force Effects from Forward Velocity

Nacelle Yaw Drag
Relationships
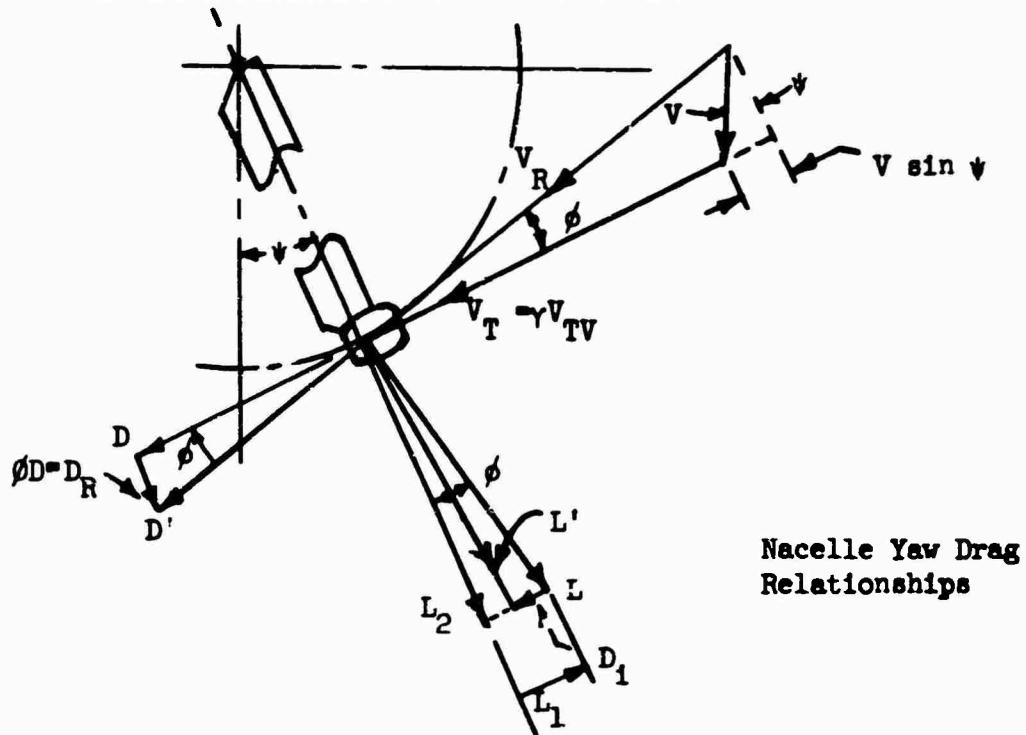
where:

D   Nacelle profile drag

D_1 Nacelle induced drag

L   Lift on nacelle due to yaw angle ϕ

L_1 Leading tangential force with $D_1 = 0$

L_2 Radial force due to yaw lift of the nacelle

V_R Resultant velocity

Remaining symbols defined in list of symbols.

$$D' = D'\cos\phi = D \qquad \text{(for small } \phi) \tag{102}$$

$$D = \frac{\rho}{2} V_R^2 \left(\delta_{0I} + \delta_{2I} C_{L_T}^2 + \delta_{2I}' \phi^2\right) A_1 \tag{103}$$

$$P_D = \frac{V_T D}{550} \tag{104}$$

$$\phi = \frac{V \cos \psi}{V_T + V \sin \psi} \tag{105}$$

For small values of ϕ, $V_R = V_T + V \sin \psi$ $\tag{106}$

Average power for one revolution is written:

$$(P_D)_{avg} = \frac{1}{2\pi} \int_0^{2\pi} \frac{V_T D}{550} \, d\psi \tag{107}$$

Substituting Equations (105) and (106) into Equation (103) and the resultant in Equation (107), we obtain:

$$(P_D)_{avg} = \frac{1}{2\pi} \frac{\rho}{2} \frac{A_I V_T}{550} \int_0^{2\pi} (V_T + V \sin \psi)^2 \left[\delta_{mI} + \delta'_{2I} \frac{V^2 \cos^2 \psi}{(V_T + V \sin \psi)^2} \right] d\psi$$

$$= \frac{1}{2\pi(1100)} V_T \rho A_I \int_0^{2\pi} \left[(V_T^2 + 2V_T V \sin\psi + V^2 \sin^2 \psi)\delta_{m_I} + \delta'_{2I} V^2 \cos^2 \psi \right] d\psi$$

$$= \frac{1}{2\pi(1100)} V_T \rho A_I \left[\left\{ V_T^2 \psi - 2V_T V \cos \psi + V^2 (-\tfrac{1}{4} \sin 2\psi + \tfrac{\psi}{2}) \right\} \delta_{m_I} + \right.$$
$$\left. \delta'_{2I} V^2 (\tfrac{1}{4} \sin 2\psi + \tfrac{\psi}{2}) \right]_0^{2\pi}$$

$$= \frac{1}{2\pi(1100)} V_T \rho A_I \left\{ \left[(V_T^2 2\pi - 2V_T V + V^2 \pi)\delta_{m_I} + \delta'_{2I} V^2 \pi \right] + (2V_T V \delta_{m_I}) \right\}$$

$$= \frac{\rho V_T^3 A_I}{1100} \left[\delta_{m_I} + \frac{V^2}{V_T^2} \frac{1}{2} (\delta_{m_I} + \delta'_{2I}) \right] \tag{108}$$

The small leading component of tangential force due to the difference between the induced drag, D_i, of the nacelle and the leading force given by

$$L_i = \phi L$$

can be neglected because of the relatively high induced drag and because neglecting it is conservative.

The power required due to the forces tangential to the rotor acting on the nacelle is written

$$P_{N_i} = R h p_{N_H} \left[1 + \frac{1}{2}\left(\frac{V}{V_T}\right)^2 \left(1 + \frac{\delta'_{2I}}{\delta_{m_I}} \right) \right] \tag{109}$$

Drag Force Effects from Radial Force

The radial force due to the angle ϕ and the resultant "lift" force of the nacelle is written:

$$L_2 \doteq L' \doteq L \doteq \frac{1}{2} \rho V_R^2 \, A_I a_I' \phi \tag{110}$$

The component of this force in the V direction is then written:

$$D_L = \cos \psi \, \frac{\rho V_R^2 \, A_I a_I \phi}{2} \tag{111}$$

Substituting equations (104), (105) and (106) into equation (111) and rewriting

$$D_L = \cos \psi \, \frac{\rho}{2} \, A_i a_I' \, (V_T + V \sin \psi)^2 \, \frac{V \cos \psi}{(V_T + V \sin \psi)}$$

or

$$D_L = \cos \psi \, \frac{\rho}{2} \, A_I a_I' (V_T V \cos \psi + V^2 \cos \psi \sin \psi) \tag{112}$$

The power required at any instant or ψ angle to overcome this drag force is:

$$P_{D_L} = \frac{V}{550} \, D_L \tag{113}$$

The average power required during one revolution of the nacelle is:

$$\begin{aligned}
(P_{D_L})_{avg} &= \frac{V}{550} \, A_I a_I' \, \frac{\rho}{2} \, \frac{1}{2\pi} \int_0^{2\pi} (V_T V \cos^2 \psi + V^2 \cos^2 \psi \sin \psi) d\psi \\
&= \frac{V}{550} \, A_I a_I' \, \frac{\rho}{2} \, \frac{1}{2\pi} \left[V_T V \left(\frac{1}{4} \sin 2\psi + \frac{\psi}{2} \right) - \frac{V^2 \cos^3 \psi}{3} \right]_0^{2\pi} \\
&= \frac{A_I a_I' (\rho/2)}{550} \left(\frac{V^2 V_T}{2} \right)
\end{aligned} \tag{114}$$

Equation (114) can also be written:

$$(P_{D_L})_{avg} = \frac{A_I \delta_{m_I}}{550} \, \frac{\rho}{2} \, V_T^3 \left[\frac{V^2}{V_T^2} \quad \frac{1}{2} \frac{a_I'}{\delta_{m_I}} \right] = Rhp_{N_H} \left(\frac{V}{V_T} \right)^2 \left(\frac{a_I'}{2\delta_{m_I}} \right) \tag{115}$$

This accounts for the power required to overcome "external" drag of the rotor system due to the radial component of the nacelle drag due to "lift" developed by the yaw angle ϕ.

Still to be accounted for is the radial component of the profile drag force which contributes to the "external" drag.

The radial component of the profile drag is written

$$D_R = \phi A_I \, \frac{1}{2} \, \rho V_R^2 \, (\delta_{m_I} + \delta_{2_I}' \phi^2) \tag{116}$$

Its average power then becomes:

87

$$(P_{D_R})_{avg} = \frac{A_I}{550} \frac{\rho}{2} \frac{1}{2\pi} V \int_0^{2\pi} (\phi\, \delta_{m_I} + \phi^3 \delta_{2_I}')(V_T + V \sin \psi)^2 \cos \psi \; d\psi$$

$$= \frac{A_I}{550} \frac{\rho}{2} \frac{1}{2\pi} V \int_0^{2\pi} \left[V \cos^2\psi \, \delta_{m_I} + \frac{V^3 \cos^4\psi \, \delta_{2_I}'}{(V_T + V \sin \psi)^2} \right](V_T + V \sin \psi) d\psi$$

$$= \frac{A_I}{550} \frac{\rho}{2} \frac{1}{2\pi} V \left[V V_T \pi \, \delta_{m_I} + V^3 \delta_{2_I}' \int_0^{2\pi} \frac{\cos^4 \psi \; d\psi}{V_T + V \sin \psi} \right] \quad (117)$$

To simplify the integration, since if $\delta_{2_I}' = 0$, the drag would be a function of $\cos^2\psi + V \cos^2\psi \sin \psi$, the average value of which would integrate to $1/2$ the maximum value of the drag (i.e., that value at $\psi = 0°$ and $\psi = 180°$), assume that the mean value of the drag equals the average value. The maximum value of D_R is also the maximum value of the radial drag component in the direction of the velocity and occurs at ϕ maximum or $\psi = 0$, $180°$.

$$\phi_{max} \doteq \frac{V}{V_T} \quad (118)$$

$$V_R \doteq V_T \quad (119)$$

Then:
$$(P_{D_R})_{avg} = \left(\frac{V}{V_T}\right) \frac{A_I}{550} \frac{V}{2} \quad \frac{1}{2} \rho V_T^2 \left[\delta_{m_I} + \delta_{2_I}' \left(\frac{V}{V_T}\right)^2 \right]$$

$$= \frac{A_I}{550} \quad \frac{1}{2} \rho V_T^3 \, \delta_{m_I} \frac{1}{2} \left[\left(\frac{V}{V_T}\right)^2 + \frac{\delta_{2_I}'}{\delta_{m_I}} \left(\frac{V}{V_T}\right)^4 \right] \quad (120)$$

From equations (115) and (120),

$$P_{N_2} = Rhp_{N_H} \left[\frac{1}{2}\left(\frac{V}{V_T}\right)^2 + \frac{1}{2} \frac{a_I'}{\delta_{m_I}} \left(\frac{V}{V_T}\right)^2 + \frac{\delta_{2_I}'}{2\delta_{m_I}} \left(\frac{V}{V_T}\right)^4 \right] \quad (121)$$

Also, the total nacelle power required is:

$$P_N = P_{N_1} + P_{N_2} = Rhp_{N_H}(K_{\mu_N}) \quad (122)$$

Then from equations (109), (121), and (122)

$$K_{\mu_N} = 1 + \left(\frac{V}{V_T}\right)^2 \left[1 + \frac{1}{2} \frac{1}{\delta_{m_I}} (\delta_{2_I}' + a_I') + \frac{1\delta_{2_I}'}{2\delta_{m_I}} \left(\frac{V}{V_T}\right)^4 \right] \quad (123)$$

where a_I' does not include the radial force effects due to the flow of air through the nacelle. That is, the momentum change of the air flowing

through the nacelle in the radial direction is not included in the K_{μ_N} term. It is, however, used in determining the net rotor horsepower and hence in the fuel flow determination through the C_V term of equation (45).

6.2 Derivation of Equation for Optimum Tip Speed

Since the optimum tip speed is that which requires minimum engine thrust for a given flight condition, we need an expression for F_n which is

$$F_n = \frac{(Bhp + \frac{\text{rotor ram drag hp}}{\eta})\,550}{\gamma\,V_{T_V}} \tag{124}$$

where: Rotor ram drag hp $= MRTHP_{700}\,(\frac{1}{2})\,\frac{1.055V^2}{1560(700)}$ (125)

and where:
$$Bhp = \frac{ihp_V + Rhp_{bV} + Rhp_{NV} + Php_V + F.L.}{\eta} \tag{126}$$

Differentiating the expression for F_n, equation (124), with respect to V_{T_V}, the expression

$$\frac{+dF_n}{dV_{T_V}} = \frac{-(ihp_V + F.L. + Php_V + \text{Rotor ram drag})\,(550/\eta)}{\gamma\,V_{T_V}^2} +$$

$$\frac{d}{dV_{T_V}}\left\{ \rho V_{T_V}^3\,\frac{\frac{A_b\xi^3}{4}\delta_{o_b} + A_I\gamma^3\delta_{o_I} + C_{L_{r_o}}^2\left(\frac{V_{T_H}}{V_{T_V}}\right)^4\left(\frac{\rho_o}{\rho}\right)^2\left[\frac{A_b\xi^3}{4}\delta_{2_b} + \gamma^3 A_I\delta_{2_I}\right] +}{} \right.$$

$$\frac{\left(\frac{V}{V_{T_V}}\right)^2\left\{\frac{3}{4}A_b\xi\left[\delta_{o_b} + \delta_{2_b}C_{L_{r_o}}^2\left(\frac{\rho_o}{\rho}\right)^2\left(\frac{V_{T_H}}{V_{T_V}}\right)^4\right] +}{}$$

$$\left. \frac{\left[1 + \frac{1}{2}\frac{(\delta_{2_I}' + a_I')}{\delta_{m_I}}\right]A_I\gamma\left[\delta_{o_I} + C_{L_{r_o}}^2\left(\frac{\rho_o}{\rho}\right)^2\left(\frac{V_{T_H}}{V_{T_V}}\right)^4\delta_{2_I}\right]\right\}}{1100\gamma V_{T_V}} \right\}\frac{550}{\eta} \tag{127}$$

results if the coefficients for the $(V/V_T)^4$ terms in the expressions for K_{μ_b} and K_{μ_N} are taken to be zero for purposes of simplification. The second term becomes:

$$\frac{d}{dV_{T_V}}\left\{ \right\} = \frac{d}{dV_{T_V}}\left\{ \frac{\rho_o V_{T_V}^2}{1100\gamma}\left(\underset{4}{A_b\xi^3\delta_{o_b}} + A_I\gamma^3\delta_{o_I}\right)\left(\frac{\rho}{\rho_o}\right) + \right.$$

$$\frac{\rho_o}{1100\gamma}\left(\frac{\rho_o}{\rho}\right)\frac{C_{L_{r_o}}(V_{TH})^4}{V_{T_V}^2}\left(\frac{A_b\xi^3}{4}\delta_{2_b} + A_I\gamma^3\delta_{2_I}\right) +$$

$$\frac{\rho_o V^2}{1100\gamma}\left(\frac{\rho}{\rho_o}\right)^2\left\{\frac{3}{4}A_b\xi\delta_{o_b} + \left[1 + \frac{1}{2}\frac{(\delta_{2_I}' + a_I')}{\delta_{m_I}}\right]A_I\gamma\delta_{o_I}\right\} +$$

$$\left.\frac{C_{L_{r_o}}^2 V_{TH}^4 V^2\rho_o(\rho_o/\rho)}{V_{T_V}^4 \; 1100\gamma}\left\{\frac{3}{4}A_b\xi\delta_{2_b} + \left[1 + \frac{(\delta_{2_I}' + a_I')}{2\delta_{m_I}}\right]A_I\gamma\delta_{2_I}\right\}\right\}\frac{550}{\eta}$$

$$= \left\{\frac{2V_{T_V}\rho_o(\rho/\rho_o)}{1100\gamma}\left(\frac{A_b\xi^3}{4}\delta_{o_b} + A_I\gamma^3\delta_{o_I}\right) - \right.$$

$$\frac{2}{V_{T_V}^3}\frac{C_{L_{r_o}}^2 V_{TH}^4\rho_o(\rho_o/\rho)}{1100\gamma}\left(\frac{A_b\xi^3}{4}\delta_{2_b} + A_I\delta_{2_I}\gamma^3\right) + 0 -$$

$$\left.\frac{4}{V_{T_V}^5}\frac{C_{L_{r_o}}^2 V_{TH}^4 V^2\rho_o(\rho_o/\rho)}{1100\gamma}\left\{\frac{3}{4}A_b\delta_{2_b}\xi + \left[1 + \frac{(\delta_{2_I}' + a_I')}{2\delta_{m_I}}\right]A_I\delta_{2_I}\gamma\right\}\right\}\frac{550}{\eta}$$

(128)

Combining equations (127) and (128) and setting the result equal to zero multiplying by $V_{T_V}^5$ to eliminate negative powers of V_{T_V} and simplifying gives:

$$0 = V_{T_V}^6(\rho_o)\left(\frac{\rho}{\rho_o}\right)\underset{4}{(A_b\xi^3\delta_{o_b} + A_I\gamma^3\delta_{o_I})} -$$

$$V_{T_V}^3 \; 550 \; (\text{ihp}_V + \text{Php}_V + \text{F.L.} + \text{rotor ram drag HP}) -$$

$$V_{T_V}^2 C_{L_{r_o}}^2 V_{TH}^4\rho_o\left(\frac{\rho_o}{\rho}\right)\left(\frac{A_b}{4}\xi^3\delta_{2_b} + A_I\gamma^3\delta_{2_I}\right) -$$

$$2C_{L_{r_o}}^2 V_{TH}^4 V^2\rho_o\left(\frac{\rho_o}{\rho}\right)\left\{\frac{3}{4}\xi A_b\delta_{2_b} + \left[1 + \frac{(\delta_{2_I}' + a_I')}{2\delta_{m_I}}\right]A_I\gamma\delta_{2_I}\right\} \quad (129)$$

The real positive root of Equation (129) is the optimum tip speed, $V_{T_{V_{opt}}}$.

DOCUMENT CONTROL DATA - R&D		
(Security classification of title, body of abstract and indexing annotation must be entered when the overall report is classified)		

1. ORIGINATING ACTIVITY (Corporate author)	2a. REPORT SECURITY CLASSIFICATION
Hiller Aircraft Company, Inc.	Unclassified
Palo Alto, California	2b. GROUP

3. REPORT TITLE

Heavy-Lift Tip Turbojet Rotor System, "Parametric Design Study", Volume II

4. DESCRIPTIVE NOTES *(Type of report and inclusive dates)*

5. AUTHOR(S) *(Last name, first name, initial)*

6. REPORT DATE	7a. TOTAL NO. OF PAGES	7b. NO. OF REFS
October 1965	91	2

8a. CONTRACT OR GRANT NO.	9a. ORIGINATOR'S REPORT NUMBER(S)
DA 44-177-AMC-25(T)	
b. PROJECT NO.	USAAVLABS Technical Report 64-68B
c. Task 1M121401D14412	9b. OTHER REPORT NO(S) (Any other numbers that may be assigned this report)
d.	Hiller Engineering Report No. 64-42

10. AVAILABILITY/LIMITATION NOTICES
Qualified requesters may obtain copies of this report from DDC.
This report has been furnished to the Department of Commerce for sale to the public.

11. SUPPLEMENTARY NOTES	12. SPONSORING MILITARY ACTIVITY
	US Army Aviation Materiel Laboratories
	Fort Eustis, Virginia

13. ABSTRACT

In Volume II on the heavy-lift tip turbojet rotor system, the parametric analysis determines the optimum design parameters of a 24,000-lb.-payload helicopter powered by turbojet engines installed at the rotor blade tips. The method used determined a gross weight which would satisfy statistical component weight equations and aerodynamic equations simultaneously. The optimizing criterion was the minimum gross weight required to perform a specific mission.

The results of the analysis indicate that the optimum configuration using the Continental Model 357-1 engine is a helicopter with a) four blades, b) two engines per blade, and c) a crane-type fuselage.

The optimum configuration with a generalized or "rubber" engine is a helicopter with a) three blades, b) one engine per blade, and c) a crane-type fuselage.

DD FORM 1 JAN 64 **1473**

14. KEY WORDS	LINK A		LINK B		LINK C	
	ROLE	WT	ROLE	WT	ROLE	WT
Tip Turbojet Rotor System Parametric Design Study						

INSTRUCTIONS

1. ORIGINATING ACTIVITY: Enter the name and address of the contractor, subcontractor, grantee, Department of Defense activity or other organization (*corporate author*) issuing the report.

2a. REPORT SECURITY CLASSIFICATION: Enter the overall security classification of the report. Indicate whether "Restricted Data" is included. Marking is to be in accordance with appropriate security regulations.

2b. GROUP: Automatic downgrading is specified in DoD Directive 5200.10 and Armed Forces Industrial Manual. Enter the group number. Also, when applicable, show that optional markings have been used for Group 3 and Group 4 as authorized.

3. REPORT TITLE: Enter the complete report title in all capital letters. Titles in all cases should be unclassified. If a meaningful title cannot be selected without classification, show title classification in all capitals in parenthesis immediately following the title.

4. DESCRIPTIVE NOTES: If appropriate, enter the type of report, e.g., interim, progress, summary, annual, or final. Give the inclusive dates when a specific reporting period is covered.

5. AUTHOR(S): Enter the name(s) of author(s) as shown on or in the report. Enter last name, first name, middle initial. If military, show rank and branch of service. The name of the principal author is an absolute minimum requirement.

6. REPORT DATE: Enter the date of the report as day, month, year; or month, year. If more than one date appears on the report, use date of publication.

7a. TOTAL NUMBER OF PAGES: The total page count should follow normal pagination procedures, i.e., enter the number of pages containing information.

7b. NUMBER OF REFERENCES: Enter the total number of references cited in the report.

8a. CONTRACT OR GRANT NUMBER: If appropriate, enter the applicable number of the contract or grant under which the report was written.

8b, 8c, & 8d. PROJECT NUMBER: Enter the appropriate military department identification, such as project number, subproject number, system numbers, task number, etc.

9a. ORIGINATOR'S REPORT NUMBER(S): Enter the official report number by which the document will be identified and controlled by the originating activity. This number must be unique to this report.

9b. OTHER REPORT NUMBER(S): If the report has been assigned any other report numbers (*either by the originator or by the sponsor*), also enter this number(s).

10. AVAILABILITY/LIMITATION NOTICES: Enter any limitations on further dissemination of the report, other than those imposed by security classification, using standard statements such as:

(1) "Qualified requesters may obtain copies of this report from DDC."

(2) "Foreign announcement and dissemination of this report by DDC is not authorized."

(3) "U. S. Government agencies may obtain copies of this report directly from DDC. Other qualified DDC users shall request through
_____ ."

(4) "U. S. military agencies may obtain copies of this report directly from DDC. Other qualified users shall request through
_____ ."

(5) "All distribution of this report is controlled. Qualified DDC users shall request through
_____ ."

If the report has been furnished to the Office of Technical Services, Department of Commerce, for sale to the public, indicate this fact and enter the price, if known.

11. SUPPLEMENTARY NOTES: Use for additional explanatory notes.

12. SPONSORING MILITARY ACTIVITY: Enter the name of the departmental project office or laboratory sponsoring (*paying for*) the research and development. Include address.

13. ABSTRACT: Enter an abstract giving a brief and factual summary of the document indicative of the report, even though it may also appear elsewhere in the body of the technical report. If additional space is required, a continuation sheet shall be attached.

It is highly desirable that the abstract of classified reports be unclassified. Each paragraph of the abstract shall end with an indication of the military security classification of the information in the paragraph, represented as (TS), (S), (C), or (U).

There is no limitation on the length of the abstract. However, the suggested length is from 150 to 225 words.

14. KEY WORDS: Key words are technically meaningful terms or short phrases that characterize a report and may be used as index entries for cataloging the report. Key words must be selected so that no security classification is required. Identifiers, such as equipment model designation, trade name, military project code name, geographic location, may be used as key words but will be followed by an indication of technical context. The assignment of links, rules, and weights is optional.

6511-65